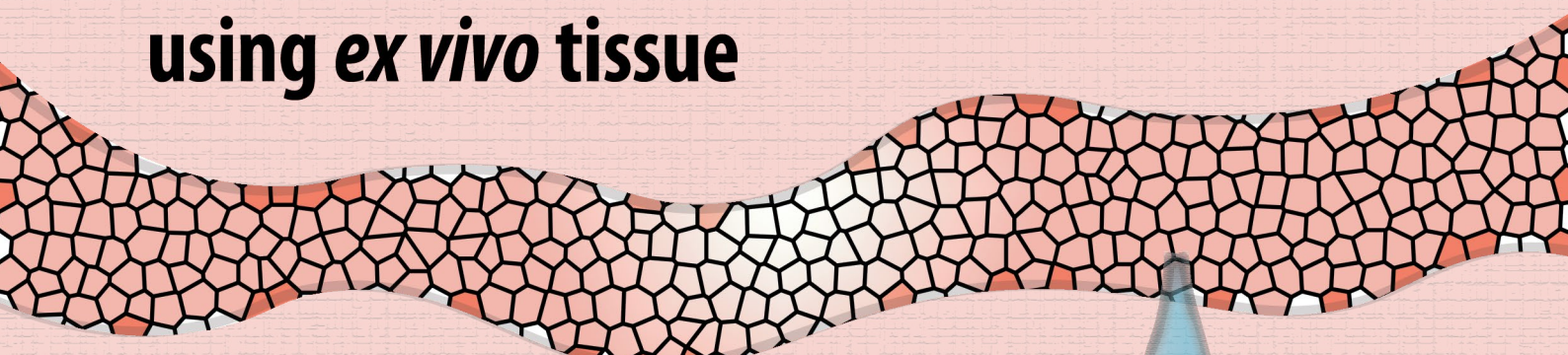


# Epididymis-on-a-chip device a unique approach to study tight barriers in the human male reproductive system using *ex vivo* tissue



## Author

BSc. Thomas Burgers  
Student number: s1455591  
Double degree in Nanotechnology and  
Biomedical engineering (imaging & diagnostics)

## Master thesis committee

Supervisor: Prof. dr. ir. Séverine Le Gac  
Daily Supervisor: Dr. Bastien Venzac  
External collaborator: Univ. Prof. Dr. rer. nat. Stefan Schlatt  
External committee member: Dr. Ruchi Bansal

November, 22, 2019

UNIVERSITY OF TWENTE.

## FOREWORD

Before you lies the master thesis "epididymis-on-a-chip: a unique approach to study a tight barriers in the male reproductive system using *ex vivo* tissue". This research was performed as a final project to conclude my double degree in biomedical engineering and nanotechnology.

The project was conducted in the group of Séverine Le Gac, Applied Microfluidics for BioEngineering Research (AMBER). I would like to thank Bastien Venzac as my daily supervisor for his guidance, support and suggestions throughout my project as well as Séverine Le Gac for the scientific discussions and the extensive feedback.

During this project I collaborated with the center of reproductive medicine in Münster (CeRA). I would like to thank Stefan Schlatt en Swati Sharma for educating me on the biological side of the project and for providing them with the required samples for the project. Furthermore I would like to thank Gerco Hassink from the biomedical signals and systems group for letting me borrow their glass puller and Armagan Kocer for using her glass puller.

Lastly, I would like to thank my other colleagues, friends and family for listening, commenting and discussing about the project with me and for being supportive and keeping me motivated throughout the course of this project.

I hope you enjoy your reading.

Thomas Burgers

Enschede, November 11, 2019

# TABLE OF CONTENT

<b>Table of Content</b>	<b>3</b>
<b>1 Summary (Dutch)</b>	<b>5</b>
<b>2 Summary (english)</b>	<b>6</b>
<b>3 List of symbols and abbreviations</b>	<b>7</b>
<b>4 Introduction</b>	<b>9</b>
4.1 Anatomy reproductive system	9
4.1.1 Seminiferous tubules	10
4.1.2 Epididymis	10
4.2 Reproductive medicine: pathology	13
4.3 Current methods of studying the epididymis	14
4.4 An introduction to organ-on-a-chip technology	15
4.5 Epididymis-on-a-chip	17
<b>5 Material and Methods</b>	<b>18</b>
5.1 Fabrication techniques	18
5.1.1 3D printing theory	18
5.1.2 3D printing: setup	18
5.1.3 Soft lithography	19
5.1.4 Glass pulling theory	19
5.1.5 Glass pulling setup	20
5.2 Tissue handling and staining	21
5.2.1 Human epididymis sample retrieval	21
5.2.2 Tissue preparation	22
5.2.3 Enhanced survival of epididymis on chip	22
5.2.4 Tissue fixation protocol	23
5.2.5 Experiment tissue variability assessment	24
5.3 Barrier penetration and permeability setup	24
<b>6 Results: materials &amp; methods</b>	<b>25</b>
6.1 Setup adaptations and analysis	25
6.2 Tissue variability	26
6.3 Tissue survival when stored for prolonged time on ice	27
6.4 Live dead staining control experiments	28
6.5 ZO-1 immunostaining of the epididymis	29
<b>7 Designing the epididymis-on-a-chip</b>	<b>30</b>
<b>8 Design iteration 1: Culturing the epididymis on a microfluidic chip</b>	<b>31</b>
8.1 Introduction	31
8.2 Results & discussion	32
<b>9 Design iteration 2: epididymis-on-a-chip using PDMS-PCR tape chip and printed clamping structure</b>	<b>3D 34</b>
9.1 Introduction	34
9.2 Results & discussion	35

<b>10</b>	<b>Design iteration 3: Epididymis-on-a-chip, a PDMS-PDMS bonded chip, with side connect to insert tissue loaded 3D-printed cartridge</b>	<b>37</b>
10.1	Introduction	37
10.2	Results & discussion	39
<b>11</b>	<b>discussion</b>	<b>43</b>
11.1	Objective 1: culturing the epididymis	43
11.1.1	Tissue quality	43
11.1.2	Cell culture media and culturing conditions	43
11.1.3	Tissue loading, 3D-print toxicity and fungal infections	43
11.1.4	Autofluorescence and live-dead staining	43
11.2	Objective 2: Clamping the epididymal lumen	44
11.3	Objective 3: access the lumen of the epididymal tubules	44
<b>12</b>	<b>Conclusion</b>	<b>46</b>
<b>13</b>	<b>Recommendation</b>	<b>47</b>
13.1	Tissue treatment and handling	47
13.1.1	Culturing the tissue: media type	47
13.1.2	Dissecting the tissue: collagenase	48
13.2	Imaging of the epididymis	48
13.2.1	Immunolabeling the epididymis	48
13.3	Adapting the design	48
13.3.1	COMSOL simulations	48
13.3.2	Permeability and inflammation induction	49
13.3.3	TEER measurements	49
13.3.4	Adapt the design to allow perfuse the epididymis at physiological rates	49
13.4	Effect of administration to microplastics / testosterone / androgens etc.	49
13.5	Future perspective of the device	50
13.5.1	Drug development in reproductive toxicology	50
13.5.2	Seminiferous-tubules-on-a-chip	51
<b>14</b>	<b>Acknowledgements</b>	<b>52</b>
<b>15</b>	<b>References</b>	<b>53</b>
<b>16</b>	<b>Appendix</b>	<b>57</b>
	Appendix A. Recipe for Flashforge Hunter printer using the DLPrint software	57
	Appendix B. Operating the glass puller	57
	Appendix C. Loading epididymal tubules onto a chip and precondition of the chip	57
	Appendix D. Time-lapse setup and fluorescence microscopy setup	57
	Appendix E. Extended permeability experiment	58
	Appendix F. USB camera, backlight and chip holder	59
	Appendix G. 3D printing, post-treatment and biocompatibility	60
	Appendix H. P-87 Sutter Instruments glass puller recipes	61
	Appendix I. P-87 Sutter Instruments glass puller recipes	62
	Appendix J. Table indicating the age of the patients undergoing sex reassignment surgery, body height, weight and the corresponding hormonal data.	62
	Appendix K. COMSOL Multiphysics simulations microchannel barrier	63
	Appendix L. PCR tape detachment	67
	Appendix M. Glass-syringe connector design	68
<b>17</b>	<b>CV output</b>	<b>70</b>

# 1 SUMMARY (DUTCH)

Het mannelijk geslachtsorgaan is opgebouwd als een netwerk van buizen. Spermatozoa differentieren van kiemcellen tot spermatozoa in de seminiferous tubules en reizen daarna door naar de epididymis waar ze volwassen worden. Door dit proces in de epididymis is de kans op het bevruchten van een eicel bevorderd.

Spermatozoa worden niet herkend door het lichaam als lichaamseigen. Dit zorgt ervoor dat er immuunreacties worden ontketend als het immuunsysteem antigenen van de spermatozoa tegenkomt. Om dit te voorkomen is er een sterke fysiologische barriere tussen het bloed en het orgaan, bloed-testes barriere en bloed-epididymis barriere (BEB) voor de seminifereuze buizen en epididymis respectievelijk. Een afwijking of breuk in deze barriere kan leiden tot onvruchtbaarheid. Over de hele wereld leiden 30 miljoen mannen aan onvruchtbaarheid (5-10% prevalentie) en in de helft van deze gevallen is de oorzaak onbekend. Onvruchtbaarheid is gedefinieerd als 'niet in staat zijn om zwanger te worden voor sexueel actieve koppels die geen contraceptie gebruiken binnen jaar.' (World Health Organization). In deze master thesis presenteren we een platform dat de BEB kan bestuderen, waarbij we gebruik maken van humaan weefsel afkomstig van patienten met gender dysphorie die geslachtverandering operaties ondergaan.

Voor het design and fabricatie van deze microfluidische chip hebben wij een orgaan-op-chip model gemaakt. In het onderzoeksveld van orgaan-op-een-chip wordt microfluidische chip technologie gebruikt om micro-omgevingen te creëren die fysiologisch relevant zijn. Conventionele *in vitro* modellen voor het groeien van cellen zijn te simplistisch en resulteren in 2D cell-lagen, wat niet correleert met de 3D situatie in het lichaam. Een andere optie die niet optimaal is, is het gebruik van diermodellen, aangezien dit ethische zorgen met zich meebrengt, tijdsintensief is en er een groot verschil is tussen de geslachtsorgaan anatomie tussen mens en diersoorten. Met ons model is het mogelijk om een verklaring te vinden voor de huidig niet verklaarbare oorzaken van onvruchtbaarheid doordat de BEB bestudeerd kan worden.

Microfluidische chips werden ontworpen in SOLIDWORKS en gefabriceerd gebruikmakend van polydimethylsiloxane (PDMS) softlithografie met 3D-geprinte mallen. Het platform bestaat uit een 3D-geprint platform waar een epididymis buis van 5-10 millimeter gespannen en afgesloten kan worden tussen twee structuren. Dit zorgt ervoor dat de vloeistof in de epididymis alleen met de omgeving kan communiceren via de BEB. Deze 3D-geprinte cartridge wordt vervolgens in een PDMS behuizing chip gestopt (2-laags PDMS). Het resultaat is een epididymis buis in een cultuurkamer met een volume van 15  $\mu$ L. De voedingsstoffen werden verversd via diffusie door micrometerschaal grootte kanalen die de cultuurkamer verbinden met 1.5 mL celcultuurmedium (DMEM, 10% FBS, 1% pen/strep). Chemicaliën of fluorescente kleurstoffen kunnen geïnjecteerd worden in de lumen van de epididymis via een uit glas getrokken naald die via de 3D-geprinte diskette geleid wordt naar de juiste positie.

Het ontworpen epididymis-op-een-chip platform kon 5-10 millimeter buizen van de epididymis in leven houden voor minstens 11 dagen. Hierbij bleef de buisstructuur intact. Ter vergelijking een epididymis buis met dezelfde grootte was gekweekt in een *in vitro* situatie (1.5mL vloeistof). Hieruit bleek dat cel overleving verminderde en de buisstructuur verdween. De toevoeging van 10% FBS aan het celkweekmedium verhoogde de cel overleving.

Dit unieke platform is het eerste platform dat de mogelijkheid biedt om de omgeving in de lumen te bestuderen en te bestuderen hoe verstoringen in de omgeving van het weefsel de BEB integriteit beïnvloeden. Door de kleine hoeveelheid benodigd weefsel voor een experiment is het mogelijk om minstens 150 experimenten uit te voeren met één sample. Een ander voordeel is dat dit platform de mogelijkheid biedt om na het kweken van het weefsel dit te analyseren of in beeld te brengen zowel op de chip als daarbuiten. Het bestuderen van de BEB helpt een beter begrip te krijgen van de functie van de barriere en hoe een disfunctie van de BEB tot onvruchtbaarheid kan leiden. Als de oorzaak van de onvruchtbaarheid duidelijk is, kan dit leiden tot de ontwikkeling van een behandeling.

## 2 SUMMARY (ENGLISH)

The male reproductive organ is composed of a convoluted network of tubules. Spermatozoa differentiate from germ cells into spermatozoa in the seminiferous tubules and consecutively travel through the epididymis where the spermatozoa mature. Upon maturation the ability to fertilize an oocyte (egg) is enhanced.

Spermatozoa are not labeled as body-self, the body identifies them as antigens and hence triggers an auto-immune response towards them. To prevent this, spermatozoa in the male reproductive organ are protected by a strong physiological barrier with the blood, testes-blood and blood-epididymis barrier respectively (BTB and BEB). Dysfunction of this barrier can lead to infertility, globally affecting 30 million men with a prevalence estimated between 5 and 10 percent depending on the continent. Infertility is defined as “the inability of a sexually active, non-contracepting couple to achieve pregnancy in one year” (World Health Organization). The cause for infertility is not understood for half of the cases (15 million men). In this report we propose a real-time BEB study tool using human *ex vivo* tissue originating from patients with gender dysphoria undergoing sex reassignment surgery.

In this work we designed and fabricated a microfluidic chip to construct an organ-on-a-chip device for the epididymis. The research field of organ-on-a-chip utilizes microfluidic chip technology to construct physiological relevant microenvironments. Conventional *in vitro* cell culture are too simplistic since it results in non-physiological 2D cell layers. An alternative physiological relevant technique is the use of animal models but is time consuming and raises ethical concerns. Research on the male reproductive organs translates poorly to the human situation. We focused on creating a platform to gain more knowledge on the BEB to find an explanation for the unexplained infertility cases.

Microfluidic devices were designed in SOLIDWORKS and fabricated by softlithography of polydimethylsiloxane (PDMS) using 3D-printed molds. The final platform was composed of a 3D-printed cartridge on which an epididymal tubule of about 5-10 millimeter could be placed. The tubule was kept in place by trapping pillars that seal the lumen at the endings. This ensures that the BEB is the only way luminal fluids interact with the surrounding media. This 3D-printed cartridge can be inserted in a two layer PDMS chip (PDMS housing) that is bonded through plasma activation. As a result the epididymal tubule is confined in a chamber of about 15 $\mu$ L. The nutrients in this chamber get replenished by diffusion through an array of micrometer sized channels that are connected to 1.5mL cell culturing medium (DMEM, 10% FBS, 1% pen/strep). Chemicals or fluorescent dyes can be inserted into the luminal environment by injecting the epididymal tubule with a dye filled glass-pulled needle through a needle entry designed into the 3D-printed cartridge.

Our epididymis-on-a-chip platform is able to maintain small epididymal tubules of 5-10 millimeter *ex vivo* viable for at least 11 days with in-tact tubule structure. As a comparison when epididymal tissue (5-10 mm tubule) was cultured in a *in vitro* dish (1.5mL) cell survival was lower and tubule structure disappears. Adding 10% fetal bovine serum to the cell culture media (Dulbecco's Modified Eagle's Medium, 1% penicillin/streptomycin) increased the cell survival.

This unique epididymis-on-a-chip platform is the first platform to provide luminal access of human epididymal tubules, with the ability to measure the effect of perturbations in their micro- and luminal environment. The low quantity of sample needed for testing allows to do at least 150 experiments with one sample. Another advantage of the platform is that the tubules can be extracted for off-chip analysis or imaging. Studying the BEB using this platform it can be discovered what can disturb the barrier, how it functions. A better understanding of the BEB might also lead to a better understanding is can lead to a better understanding

### 3 LIST OF SYMBOLS AND ABBREVIATIONS

OoC	Organ-on-a-chip
FBS	Fetal Bovine Serum
DMEM	Dulbecco's Modified
PBS	Phosphate buffered saline
Pen-strep	Penicillin Streptomycin
CO <sub>2</sub>	Carbondioxide
PCR tape	Polymer chain reaction tape
PSA	Pressure sensitive adhesive
PDMS	Polydimethylsiloxane
ZO-1	Zona occludin-1
SRS	Sex reassignment surgery
A	Ampere [A]
V	Volt [V]
µm	Micrometer
kHz	Kilo herz
mW/cm <sup>2</sup>	Milli watt per square centimeter
h	Hours
min	Minutes
DLP	Digital light projector
Acr-GFP	Green fluorescent protein
ART	Assistive reproductive technologies
CFTR	Cystic fibrosis transmembrane conductance regulator
OA	Obstructive azoospermia
OAT syndrome	Oligoozoospermia, asthenozoospermia, teratozoospermia syndrome
BEB	Blood-epididymis barrier
BTB	Blood-testes barrier
ATP	Adenosine triphosphate
CLDN	Cadherins
RNA	Ribonucleinacid
DI	Deionized water
RFP	Red fluorescent protein
FITC	Fluorescein isethionate
FTD resin	Fun to do
UV	Ultraviolet
TNF-alpha	Tumor necrosis factor – alpha
TEER	Transendothelial resistance
FDA	Federal drug agency
LH	Luteinizing hormone
FSH	Folicle stimulating hormone
SBHG	Sex hormone binding globulin
DHT	Dihydrotestosterone
rho	Density [kg/m <sup>3</sup> ]
c	Speed of sound [m/s]
mu	Viscosity [Pa*s] or [kg/(m*s)]
Re	Reynolds number [-]
Ma	Mach number [-]

m	Meter
s	Seconds
kg	Kilogram
NAD	nicotinamide-adenine dinucleotide

## 4 INTRODUCTION

In this master thesis, we proposed a new method for studying the male reproductive physiological barrier with blood, using an *in-vitro* culture of human epididymis tissue in an organ-on-chip platform. A disruption of the barrier can result in male infertility. Infertility in men has a prevalence between 5 and 10%, globally affecting 30 million men.[1] For half of the cases of infertility the cause is unknown.[2] Studying the barrier of the male reproductive system required the use human tissue since there is a large deviation between anatomy and function between species.[3] This research focused on studying the barrier between the luminal environment of the epididymis and the blood. The epididymis is a long convoluted tubule through which the spermatozoa travel after being differentiated from germ cells in the seminiferous tubules.[3, 4] This platform is an essential tool to obtain information to enhance our understanding on barrier functioning and how dysfunctioning leads to infertility.

Before introducing this organ-on-a-chip platform to study the male reproductive barrier, the anatomy of the male reproductive system is discussed. The consecutive section reviews the pathological conditions of the male reproductive system focus on male infertility. The third section provides some background on organ-on-a-chip technology, focusing on creating barrier models and presenting different approaches for this purpose, and giving a perspective on the field of organ-on-a-chip systems for the male reproductive system. The final section explains the set biological goals and the technological objectives to which our platform was designed.

### 4.1 Anatomy reproductive system

The male reproductive system comprises a convoluted network of tubules through which spermatozoa are consecutively produced, activated and transported. In this report, the first two parts are discussed in more detail, as depicted in Figure 1. The seminiferous tubules are the location where spermatozoa are produced through differentiation from germ stem cells, and the epididymis is responsible for the maturation of sperm cells so that they are able to fertilize an oocyte (egg).[3, 5]

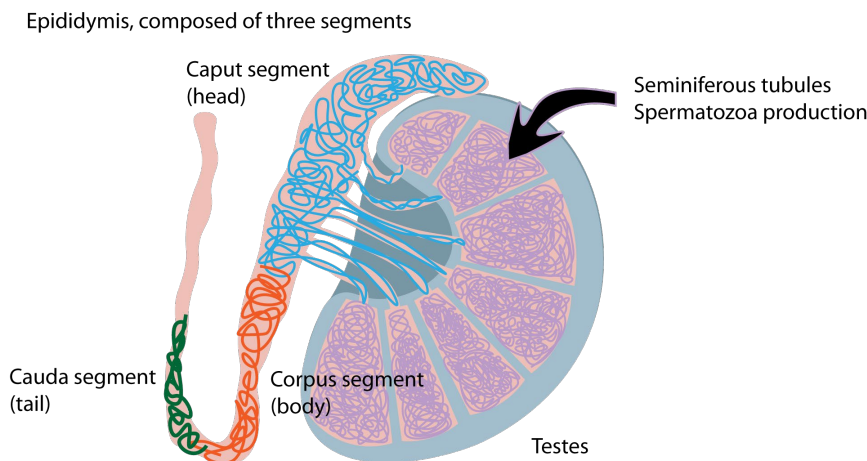


FIGURE 1. ANATOMY OF THE MALE REPRODUCTIVE SYSTEM DISPLAYING A SAGITTAL CROSS-SECTION OF THE TESTES AND THE EPIDIDYMIS. THE MALE REPRODUCTIVE SYSTEM IS COMPRISED OF A LONG CONVOLUTED NETWORK OF TUBULES. THE SEMINIFEROUS TUBULES ARE LOCATED IN THE TESTES AND ARE RESPONSIBLE FOR THE DIFFERENTIATION OF GERM CELLS INTO SPERMATOZOA. CONSECUTIVELY THE SPERMATOZOA ARE TRANSPORTED THROUGH THE EPIDIDYMIS WHILE MATURING BY INTERACTIONS AND MODIFICATIONS BY THE EPIDIDYMIS RESULTING IN A HIGHER CHANCE TO FERTILIZE AN OOCYTE. THE EPIDIDYMIS IS COMPRISED OF THREE DIFFERENT SEGMENTS, THE CAPUT, CORPUS AND CAUDA. THESE DIFFERENTIATIONS IN SECTIONS ARE MADE BECAUSE THEIR CELLULAR COMPOSITION, PROTEIN AND GENE EXPRESSION ALONG WITH THEIR RELATIVE TUBULE DIAMETER IS DIFFERENT. [3, 5]

Both the seminiferous tubules and epididymis comprise of a convoluted network of tubules with a tight barrier to protect spermatozoa from any immune response.[6] As such, a barrier dysfunction can lead to infertility.

#### 4.1.1 **Seminiferous tubules**

The seminiferous tubules are highly convoluted tubules located in the testis and surrounded by interstitial space. The seminiferous tubules comprises of Sertoli somatic cells that maintain the integrity of the tubule. Tight junctions exist between adjacent Sertoli cells, generating an impenetrable immunological barrier, the blood-testis barrier (BTB) to protect the developing spermatozoa and to control their microenvironment. The process of spermatogenesis is illustrated in Figure 2; and it starts with a dividing germ cell (spermatogonium) in the outer layer of the tubule below the basal membrane, through mitosis. One of the dividing cells remains to be a germ cell, and the other passes the blood-testis barrier. [6, 7] After crossing the BTB, the primary spermatocyte continues dividing, first through meiosis I and consecutively through meiosis II to become a spermatozoon.[6, 7] The spermatozoa releases into the lumen and is transported to the next segment of the male reproductive system, the epididymis.

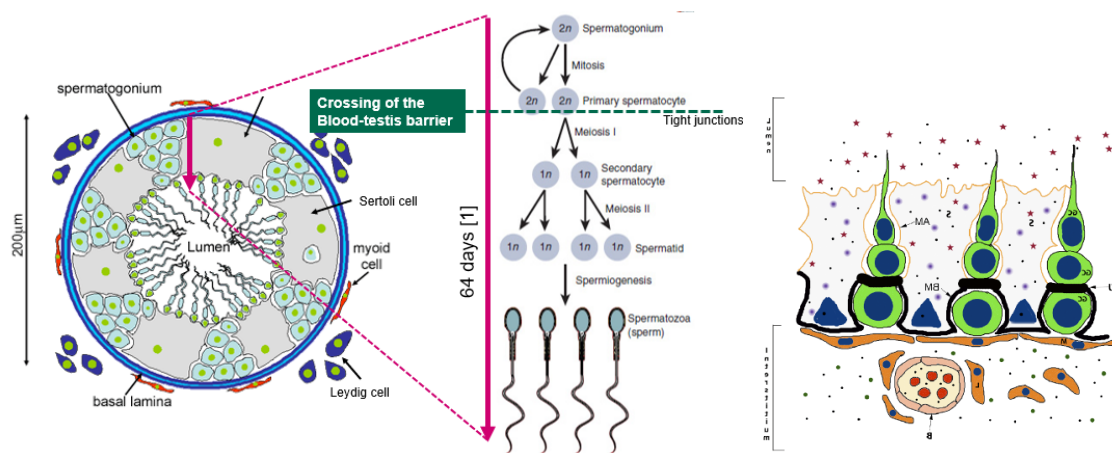


FIGURE 2. SPERMATOGENESIS, THE PROCESS OF MATURATION OF SPERMATOZOA INSIDE THE SEMINIFEROUS TUBULES IN THE TESTIS. ADAPTED AND COMBINED FROM [3, 8, 9]

#### 4.1.2 **Epididymis**

In this research, we focus on the epididymis and hence discuss it in more detail in this section. The first section explains the primary function of the epididymis, followed by a general anatomical and physiological composition of the epididymis. Thirdly, the role of the different cell types within the epididymal barrier wall that comprise the barrier are addressed. Within the epididymis the composition changes between segments which is discussed in the fourth section. The last section explains the differences between species in epididymal composition.

##### **Main function**

The four primary roles of the epididymis are transportation, protection, storage and, the most essential one, maturation of spermatozoa. The spermatozoa that reach the epididymis are not fully mature yet and have a low chance of fertilizing an oocyte. [10, 11] Similar to the seminiferous tubules, the epididymis has its own immunological impenetrable barrier, the blood-epididymis barrier (BEB), which also prevents immune responses towards spermatozoa and it allows controlling their microenvironment. [10]

##### **General anatomical & physiological composition**

Anatomically the epididymis is composed of a long single tubule of about 3-5 meters in adult men. When describing the epididymis, it consists of three different segments, the caput, corpus and cauda. Transportation through the epididymis takes between 2-6 days, and water is resorbed throughout the epididymis leading to an increase in sperm concentration upon transit. [12] These three segments have different intraluminal diameters and cellular barrier thickness, as depicted in Figure 3.[12] It has recently been argued that the epididymis could also be viewed as a series of small organs. [13] This hypothesis is made based on the fact that gene expression, cellular composition and luminal size changes not only between segments but also within segments. [14-16]

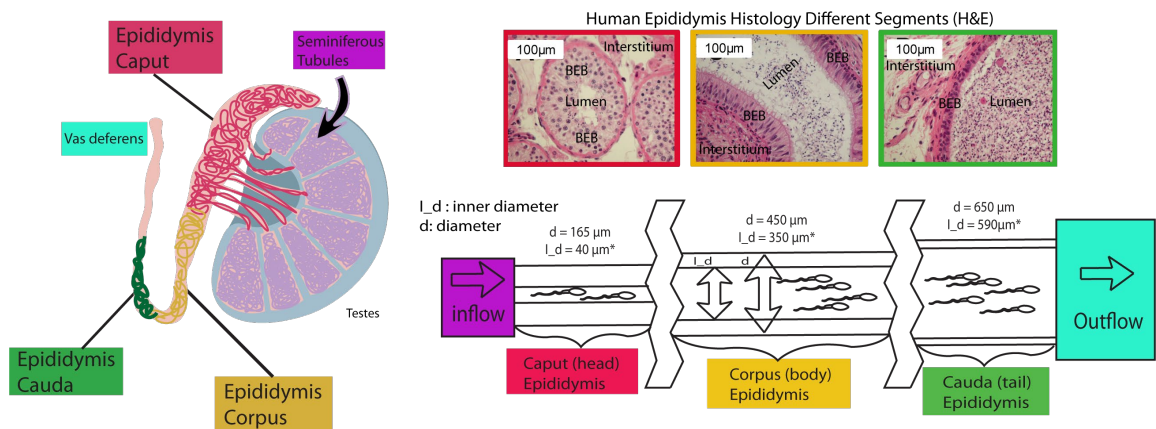


FIGURE 3. SCHEMATIC REPRESENTATION OF THE DIFFERENCES IN DIAMETER FROM THE DIFFERENT LUMINAL PARTS OF THE EPIDIDYMIS. THE THREE IMAGES OF THE EPIDIDYMIS HISTOLOGY WERE HEMATOXYLIN AND EOSIN (HE-STAINING) STAINED. FIGURE ADAPTED FROM [3, 17]

### Cellular composition of the epididymal tubules

The epididymal tubules comprise of principal cells, basal cells, clear cells, halo cells and dendritic cells. [12] The principal, basal and clear cells form the basis of the human blood-epididymis barrier, and in rodents there is an additional cell type (narrow cells) present in the initial segment.[6] The halo cells and dendritic cells found in the epididymal tubules are immune cells.[18] Figure 4 schematically displays the general composition of the epididymis.

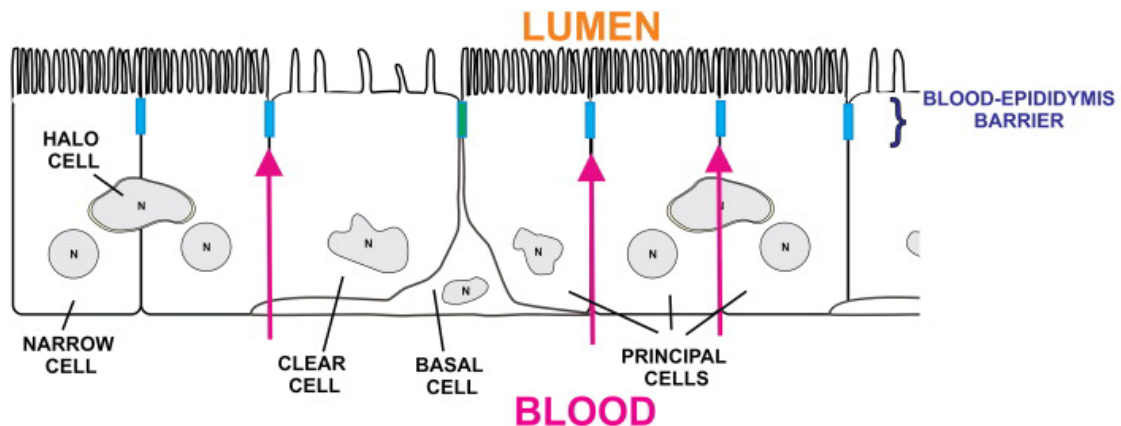


FIGURE 4. THE EPIDIDYMIS IS COMPRISED MAINLY OF PRINCIPAL CELLS (65%), BASAL CELLS (18%) AND CLEAR CELLS (10%). THE GREEN BAR INDICATES THE LOCATION OF THE BLOOD-EPIDIDYMIS BARRIER WHICH IS MAINLY COMPRISED OF TIGHT JUNCTIONS. BASAL CELLS CAN CROSS THE BEB TO SENSE THE LUMINAL MICROENVIRONMENT AND CLEAR AND PRINCIPAL CELLS CONTROL THE INTRALUMINAL PH AND ENSURE PROTEIN RELEASE INTO THE LUMEN THAT CHANGES THE PASSING SPERMATOZOA. THE NARROW CELLS IS A CELL TYPE THAT IS NOT PRESENT IN THE HUMAN EPIDIDYMIS, ALREADY INDICATING ANATOMICALLY SPECIES VARIABILITY BETWEEN SPECIES. FIGURE FROM [10]

The principal cell is the main cell type (65%) in the epididymal epithelium and is responsible for secretion and absorption of fluids, thereby maintaining the composition of the intraluminal environment. The secretion and absorption can be categorized into transport through transporters, mesocrine secretion and apocrine secretion. Transporters secrete and reabsorb ions, water and organic compounds. The mesocrine secretions include the secretion of glycoproteins and resorption of proteins, which is dynamic along the epididymal tubes to create specific microenvironments throughout the epididymis. The apocrine secretion is the process where principal cells release small vesicles originating from the apical membrane called epididymosomes. These vesicles are thought to transfer proteins to the surface of sperm cells to help recognition of the oocyte for fertilization and to contain noncoding RNA that can influence gene expression along the epididymis. [19, 20]

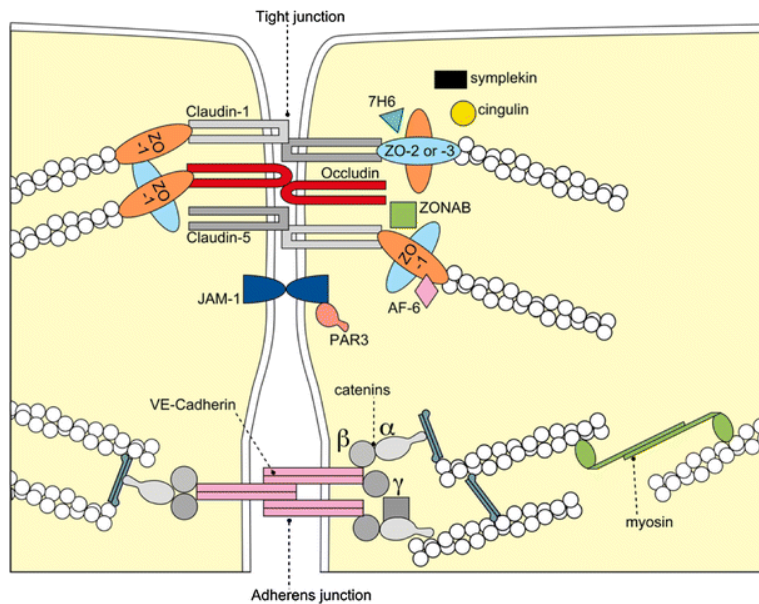


FIGURE 5. DIFFERENT TIGHT JUNCTIONS AND PROTEINS ARE DISPLAYED THAT FORM AN IMPORTANT BASIS OF THE TIGHT IMMUNOLOGICAL IMPENETRABLE BARRIER, THE BLOOD-EPIDIDYMIS BARRIER. THE FIGURE DISPLAYS THE TIGHT JUNCTION PROTEINS (CLAUDIN-1, OCCLUDIN, CLAUDIN-5, ZO-1), ADHERENS JUNCTION (ADHERENS) AND FOR INSTANCE CELLULAR SKELETAL PROTEINS LIKE MYOSIN. FIGURE FROM [21]

Neighbouring principal cells form strong connections through a variety of cadherins, desmosomes (cell-cell adhesion) and tight junctions proteins (occludins: close intracellular gaps). The communication between neighbouring cells is facilitated through gap junctions. These different junction types are schematically depicted in Figure 5. The epididymis has a large variety and number of these different cell-cell interactions (desmosomes, tight junctions), which are also one of the elements that are expected to make this blood-epididymal barrier so strong.[6, 20, 22] The strength of the BEB also correlates with the functioning of cadherins. Dubé *et al.* proved in their research that the strength of the barrier is significantly lower if the cells are not expressing specific cell-cell interaction genes (cadherins: CLDN1, CLDN3, CLDN4 or CLDN7). These cadherins are present between neighbouring cells to promote tightness and make the BEB immune-impenetrable. Understanding their specific role and might lead to an explanation for some cases of male infertility, leading to the development of new therapeutic infertility solutions. [22, 23]

Basal cells are located on the outer perimeter of the epididymal tubes and extend into the lumen. Recently it was found that these cells are sensing the luminal hormonal levels. Furthermore, they have tight junctions with neighbouring cells (mostly principal cell), and their sensing extensions can cross the tight junctions. Moreover, they also have gap junctions, communicating with the principal and clear cells. The crossing of tight junctions is a dynamic process that happens more in the distal corpus and proximal cauda. The function of the basal cells is unclear, but it is hypothesized that it is involved in protecting the intraluminal environment from reactive oxygen species.[11] Another hypothesis about the basal cell function is that they regenerate the epididymal epididymis since it has been found that they present features that are similar to that of adult stem cells.[12]

Research by Jones *et al.* concluded that the intraluminal pH was 6.3 in comparison to a pH of 7.3 outside of the tubes.[24] Clear cells are responsible for the maintenance of this acidic intraluminal environment of the epididymal. The V-ATPase vacuolar proton pump in these cells pump H<sup>+</sup> ions from the interstitium towards the lumen. The acidic environment is thought to keep the spermatozoa in a quiescent state.[4, 12]

On the outside of the intraluminal environment, behind the tight junctions, the epididymis contains mononuclear phagocytes (dendritic cells and macrophages) that are part of the immune system and have a key role in presenting antigens to halo cells (which are intraepithelial lymphocytes) and thereby trigger an immune response.[18, 25] The role of macrophages are not confirmed but four

hypothesis are made. (i) The macrophages present antigens from the lumen, originating from sperm cells to halo cells, initiating an auto-immune response, (iii) they clear debris from the epididymal barrier to maintain the barrier integrity, they undergo interactions with vasculature and (iv) macrophages undergo interactions with nerve cells to regulate the peristaltic movement of the smooth muscle cells in the epididymis, which is hypothesized since recently it was shown that macrophages in the intestine interact with nerve cells to regulate peristaltic movement.[18]

As mentioned earlier the strength of the barrier prevents sperm antigens from escaping the barrier preventing the antigen presenting cells to trigger an autoimmune response, and it also prevents immune cells and immunoglobulins from entering the lumen.[6, 26]

### ***Species-specific variation in anatomy***

The male reproductive system is highly species-specific. Rodents, for instance, have an extra segment before the caput, the initial segment. This segment is not present in humans and large animals.[4, 27] On a histological level, this segment has another type of cells called small cells, which are more cubical than the clear cells while having a similar function.[4] Another notable difference is the segmentation. For rodents, dogs and some primates the epididymis can be clearly divided into different sub-segments when looking at a cross-section. Here a bundle of tubules can be grouped together since they are surrounded with a clear layer of connective tissue. For the human epididymis the same sub-segmentation of the epididymis is not possible since this connective tissue that segments the epididymis is not present.[12, 28] The variation between species also highlights the importance of having a platform and model to study and experiment on human tissue.

## **4.2 Reproductive medicine: pathology**

The male reproductive system is delineated by a barrier, the BTB and BEB in the seminiferous tubules and the epididymis, respectively. If the integrity of this barrier is compromised, by for example a gene mutation or an infection, this could lead to reduced fertility or even to infertility. 15-30% of male infertility cases are attributed to immunological, which affect the barrier strength and thereby trigger the auto-immune response towards the spermatozoa. [29]

Gene mutations that can cause infertility include the mutation of cystic fibrosis transmembrane conductance regulator (CFTR), adhesion G-protein-coupled receptor G2 (ADGRG2). CFTR mutations are often present in patients with cystic fibrosis and can cause infertility suggested to be caused by the congenital absence of the vas deferens (CATVD) leading to epididymal malformation.[27, 29] Most gene mutation related infertilities affect the process of spermatogenesis. [30, 31]

The definition of infertility by the World Health Organization is stated as “the inability of a sexually active, non-contracepting couple to achieve pregnancy in one year”. 15% of the couples (48.5 million couples) do not achieve pregnancy within one year, 7.5% do not within 2 years and about 1% still not after three years. In 50% of the cases, the man is the cause of infertility. Strikingly enough, only half of the cases in a study on 7057 infertile men could be explained. This would mean that 12.5 million cases of male infertility could not be explained overall couples.[1]

Factors that explained infertility included idiopathic abnormal semen (OAT syndrome, 76.4%), urogenital infections (6.6%), increased scrotal temperature (12.3%), immunological factors (3.1%), urogenital congenital genetic disease(2.1%), and endocrine disturbance (0.6%). The OAT syndrome is diagnosed based on sperm analysis and is concluded if the sample has one or several of the following results: (1) a decreased number of sperm cells (Oligozoospermia), (2) a decreased motility (Asthenozoospermia) or (3) a morphological abnormality (Teratozoospermia). For the OAT syndrome, in 30-45 per cent of the cases, the reason for the abnormal semen parameters is not clear.[2, 32] In the case of obstructive azoospermia (OA), which is a condition where there is no spermatozoa or spermatogenic cells in the semen, the largest reason is an obstruction of the epididymis, which can be visualized usually through ultrasound. The main contributor of OA is the obstruction of the epididymis, which is caused in 30-67% of the cases by infection of the urinal tract or by the chlamydial virus, or in 82% of the cases by genetic factors, such as a mutation of the cystic fibrosis gene. [2, 32] In a systematic literature study, Agarwal *et al.* estimated that, when

taking the global factor into account a total of 30 million men are affected by infertility. Here they corrected for the fact that most data originates from western continents.[1] If the cause of infertility is male infertility is equally distributed per global continent this would mean that 15 million cases of infertility have no explanation.

Research on the male reproductive organ is also highly crucial for improving current assisted reproductive technologies (ART). Currently, with ART, the fertilization of spermatozoa is not performed by a natural selection process, which increases the chance of genetic defects in the offspring. Having a system that could mature spermatozoa *in vitro* would allow to improve the current ART techniques. This would increase the chances of a successfully fertilizing an oocyte. Additionally by implementing the natural selection process in ART the offspring from this technique are less prone to have genetic mutations or defects. [27]

#### **4.3 Current methods of studying the epididymis**

In biology, a lot of discoveries in the last century on cellular mechanisms and cellular interaction have been made through *in vitro* cell cultures in Petri dishes. Immortalized and primary cell lines are used for these cultures to study their protein expression or gene expression and how those are altered when exposed to certain chemicals. Immortalized cell lines have been altered to proliferate indefinitely due to a genetic mutation. In contrast primary cells are directly extracted from tissue and do not proliferate indefinitely. For the human epididymis and the human male reproductive system, the information we know is mainly extracted from such static *in-vitro* Petri-dish experiments. These static tests do not provide results that are translatable to *in vivo* situations, where the cells would be subjected to parameters like flow and the interaction with other cell types that are essential for barrier function and maintenance.[33-35]

In the last decade, most studies on the human epididymis used immortalized cell lines or primary cells obtained through vasectomy. These studies have included three analysis methods: *in vitro* culturing of immortalized cells, followed by immunofluorescence staining, electron microscopy or confocal microscopy to visualize the present tight junctions or other markers and to analyze cellular mechanisms; the study of protein expression by mass spectroscopy; and analysis of gene expression through polymer chain reaction (PCR) or reverse transcriptase PCR (RT-PCR).[22, 36]

There is a large variability between species, making the results from animal studies not per se translatable to the human. The current available data on human epididymis function are based on static experiments using primary and immortalized cell lines, which consist of an over-simplified model since only a single cell type is cultured in a not-physiological static environment, resulting in a poor model for studying the human BEB. Here we propose a new model to study human epididymis in a physiologically relevant environment, by culturing all the different cell types of the epididymis at once, to capture the complete physiological interplay between cells and how they form and maintain the blood-epididymis barrier. This new model is created by using organ-on-a-chip technology, which is explained in the next paragraph.[37, 38]

#### 4.4 An introduction to organ-on-a-chip technology

As discussed *in vitro* Petri-Dish experiments do not represent physiological conditions and studying the BEB in animal models is not an option due to species variability of the reproductive system anatomy and function. Organ-on-a-chip technology offers an optimal solution, where tissues are cultivated in a dynamic and physiological condition, using microfluidic technology and tissue with human origin can be used. Microscale structures, chambers and channels, can mimic the organ structure, simulate and mimic blood flow, deliver nutrients and remove waste produced by the tissue.[39] Using this approach, human tissue explants, primary cells, immortalized cells or spheroids (cell clumps) can be used.[36, 40]

Basically, every blood-organ barrier can be recreated in a dedicated organ-on-a-chip platform. Numerous organ-on-a-chip devices have been realized so far including but not limited to the oviduct, gut, heart, brain, lung, liver, kidney and skin on a chip, of which a few examples are presented in Figure 6.[41]

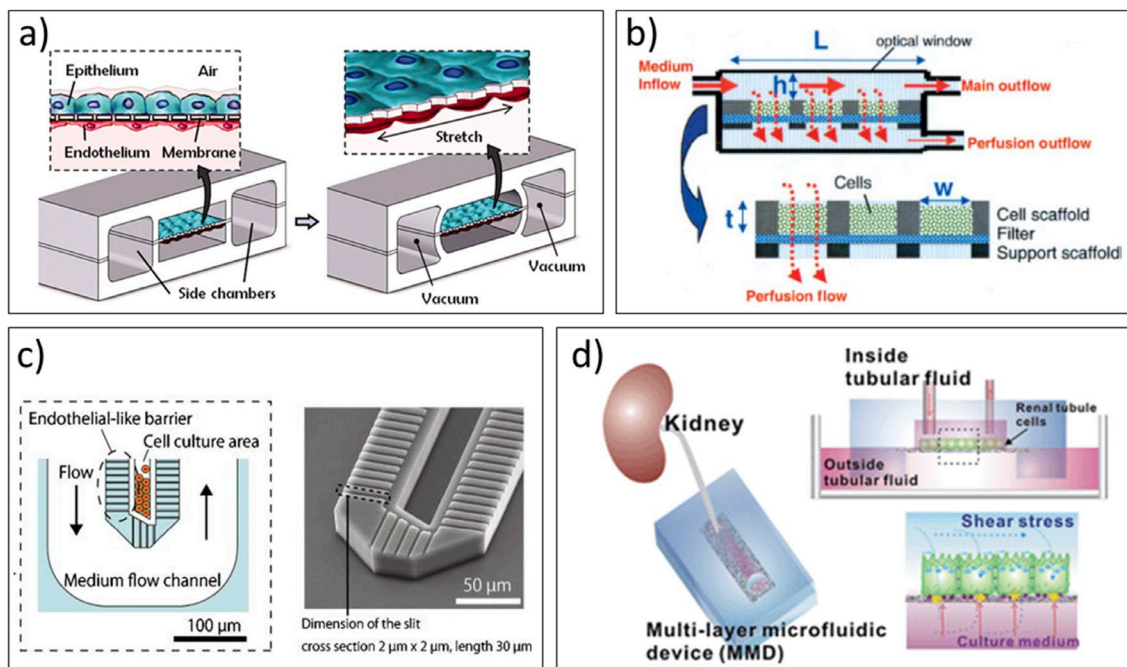


FIGURE 6. ALL BLOOD-ORGAN BARRIERS CAN BE STUDIED EFFECTIVELY INTO AN ORGAN-ON-A-CHIP DEVICE. FOR THE LUNG (A), LIVER (B&C) AND KIDNEY (D) EXAMPLES ARE DISPLAYED. THE LUNG-ON-A-CHIP DEVICE GROWS ALVEOLAR CELLS ON A SURFACE AND THE OUTER CHANNELS CAN BE PRESSURIZED SUCH THAT THE SURFACE ON WHICH LUNG CELLS GROW IS STRETCHED THEREBY SIMULATING THE PHYSIOLOGICAL MECHANICAL STRESS THAT OCCURS WHEN BREATHING. FOR THE LIVER-ON-A-CHIP (B) A 3D PIECE OF LIVER TISSUE IS CULTURED. FOR THE LIVER-ON-A-CHIP (C) A STRUCTURE OF HEPATIC CORD IS PUT ON A CHIP. THE KIDNEY-ON-A-CHIP IS A TWO-LAYER PDMS CHIP, WITH A POROUS BARRIER SEPARATING THE TWO LAYERS AND KIDNEY CELLS GROWN ON THE POROUS MEMBRANE. DIFFERENT EXISTING ORGAN-ON-A-CHIP PLATFORMS. FIGURE COMBINED FROM REVIEW [42]

Most organ-on-a-chip devices comprise of two layers of of a flexible, gas-permeable and transparent elastomer (PDMS or polydimethylsiloxane) with micrometer-sized channels. Due to these properties, inlets for flow of nutrient diffusion can be easily created using biopsy punches, real-time imaging and monitoring is possible and it allows for on-chip analysis and oxygen supply. In this research we focus on barrier models and a typical approach in organ-on-a-chip platforms is to recreate these barriers by co-culturing different cell types usually separated by a membrane. This approach is referred to as the bottom-up approach (creating a barrier from single cells). The second approach is referred to as top-down, where tissue explants or spheroids are cultured in a microfluidic bioreactor.[43]

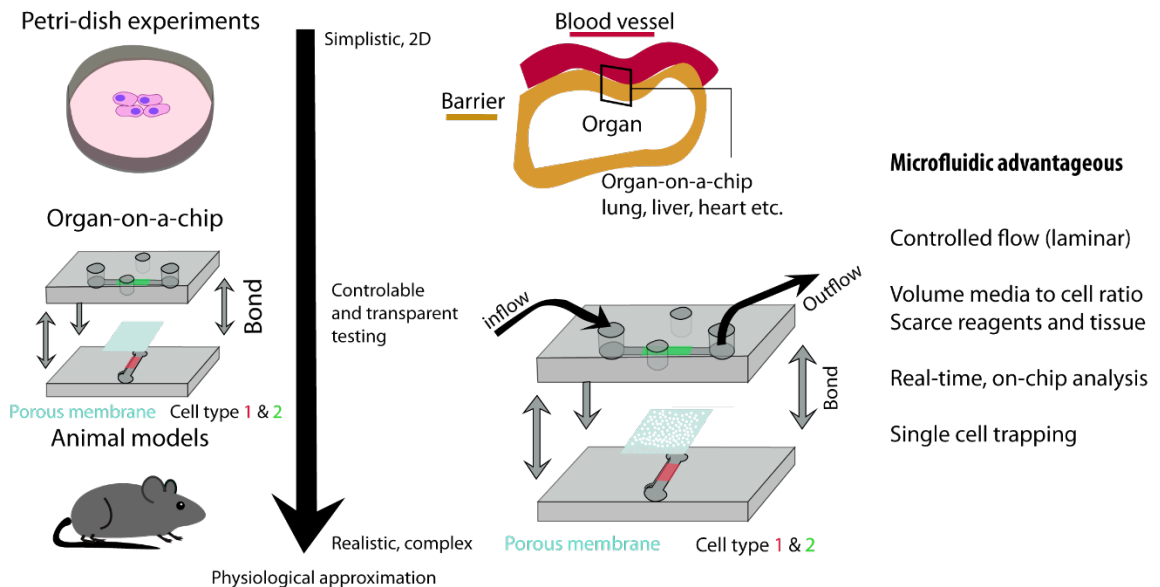


FIGURE 7. HERE THE TREND FROM SIMPLISTIC TO COMPLEX MODELS IS DEPICTED GOING FROM PETRI-DISH (IN VITRO) EXPERIMENTS TO ORGAN-ON-A-CHIP SYSTEMS AND ANIMAL MODELS BEING THE MOST COMPLEX. ORGAN-ON-A-CHIP DEVICES ARE ENGINEERED DEVICES WITH MICROMETER DIMENSIONS AND USING MICROLITERS OF FLUID TO FILL AND CAN BE MANIPULATED TO CREATE DYNAMIC ENVIRONMENTS TO MIMIC PHYSIOLOGICAL CONDITIONS. THESE DEVICES ARE TYPICALLY MADE TO STUDY AND MIMIC BLOOD-ORGAN BARRIERS. THE LOW VOLUMES ARE ALSO ADVANTAGEOUS TO REDUCE COST WHEN USING SCARCE AND EXPENSIVE METABOLITES AND SAMPLES.

Summarizing the benefits of the organ-on-a-chip approach is the fact. The usage of small volumes reduces the amount of expensive metabolites and the amount of scarce sample required. The micrometer sized dimensions of the microfluidic channels lead to a high flow resistance, resulting in laminar flow conditions, which are easy to predict and control. Moreover, extra information can be obtained in real-time through the implementation of electrodes and different type of sensors allowing for electrical, mechanical or optical measurements. [44, 45] Microfluidic platforms can have micrometer-sized objects when created in the cleanroom and about features as small as 25-100µm when using 3D-printing. These fabrication techniques allow to engineer constructs that are able to trap single cells or cell constructs.[37, 38, 46]

For the epididymis, no OoC model has been proposed/reported yet, but Komeya *et al.* describe a testis-on-a-chip [47] platform, in which they culture seminiferous tubules from a neonatal mouse in its entirety under perfusion. These mice were Acr-GFP transgenic, so that they express a fluorescent signal in spermatogenic cells. The height of the dimensions of the seminiferous tubules culture chamber platform was chosen to ensure tissue survival. In their research they proved that if the culture chamber is higher than 300-400 µmm, the cells would not get enough nutrients at a deeper level in the culture chamber and hence would die. They were able to keep the tissue viable for 180 days, but it was more challenging to maintain its function of spermatogenesis.[47]

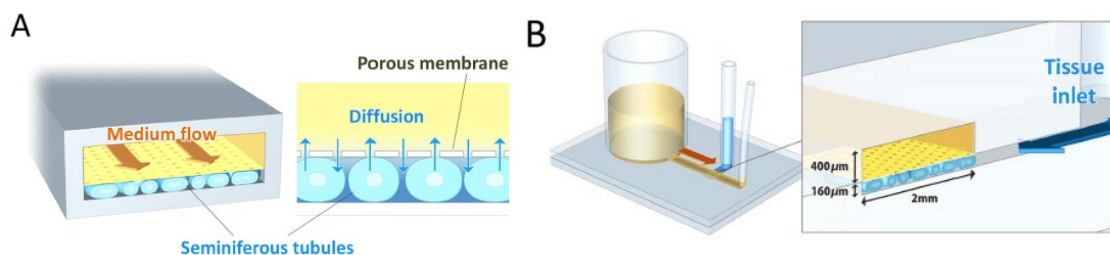


FIGURE 8. THIS FIGURE DEPICTS THE DESIGN BY KOMEYA *ET AL.* FOR CULTURING TESTIS TISSUE. A) THEY SEMINIFEROUS TUBULES INTO A CULTURE AREA WITH A WIDTH OF 2MM AND 160µM HIGH. THE TOP OF THE CULTURE CHAMBER IS COMPRISED OF A POROUS FLOW, AND ON TOP OF THAT, THERE IS A MICROFLUIDIC CHANNEL THAT ALLOWS PERFUSION. B) THE TISSUE IS INSERTED FROM THE SIDE IN THE BOTTOM CHANNEL, AND A LARGE RESERVOIR OF MEDIA ALLOWS FLOW OVER THE CULTURED TESTICULAR TISSUE. THE FIGURE WAS TAKEN FROM [48]

#### **4.5 Epididymis-on-a-chip**

In this collaborative project with the center of reproductive medicine in Münster, *ex vivo* human tissue, collected after sex-change surgery on gender dysphoria patients, are cultured in an organ-on-a-chip platform. The human blood-testis barrier would be difficult to recreate using the bottom-up approach, because its structure is not fully understood, and using animal models or animal derived cells does not lead to physiological relevant research for human BEB function due to variability in BEB function between species.

Interesting biological questions and experiments that can be done using this platform include the studying of barrier regeneration, the interactions between spermatozoa and the epididymis, the effect of endocrine disruptors on barrier integrity, screening of metabolites on their toxicity towards the BEB by barrier disruption and exploring the role of the immune system and in particular of macrophages on barrier functioning. By answering these essential biological questions on BEB functioning, more insight can be gained on how barrier dysfunction can lead to infertility and to design therapeutic treatments against infertility. This would also mean that a portion of the current 50% of unexplained cases of male infertility could then be explained and cured if treatments are created. The next chapter will introduce the different techniques to fabricate the epididymis-on-a-chip platform and will elaborate on the experimental set-ups.

## 5 MATERIAL AND METHODS

The first section describes the different fabrication techniques used for creating the epididymis-on-a-chip platform. The second section explains the handling and staining of the epididymal tissue. Lastly the set-ups for creating and executing the experiments are described.

### 5.1 Fabrication techniques

For this project a set of fabrication techniques have been employed including 3D-printing, soft lithography and glass pulling, to create the epididymis-on-a-chip platform. Therefore, the theory behind these techniques and the setup themselves will be described here.

#### 5.1.1 3D printing theory

For the designing of the platform, 3D printing has been used extensively. There are several different techniques to 3D-print objects, but here we specifically used vat photopolymerization, which is depicted in Figure 9. This technique is a layer-by-layer printing technique, where each layer is illuminated by a digital light projector (DLP). The light source projects light on a vast array of small micrometer-sized mirrors, generating a light projection on the resin. Upon illumination, the resin in the 3D printer cross-links, through activation of a photo-initiator. The micrometer-sized mirrors can be controlled into an on- and an off-state corresponding, allowing to create patterns of light exposure and selectively cross-linking the resin at those locations. When the first layer is cured the building platform (stage) is moved up and the next layer is exposed to (patterned) light, to get cross-linked and attached to the previous layer. This process is repeated to create three-dimensional objects.[49, 50]

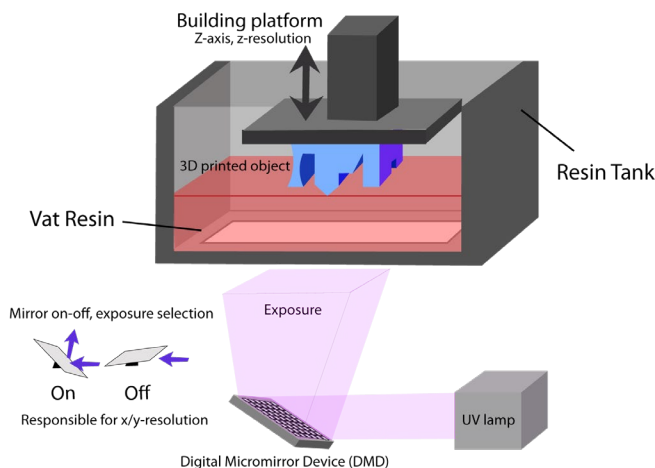


FIGURE 9. AN ADDITIVE VAT POLYMERIZATION METHOD, LAYER-BY-LAYER PRINTING. UV LIGHT IS PROJECTED ON AN ARRAY OF SMALL MIRRORS (DMD) THAT CAN BE INDIVIDUALLY FLIPPED INTO AN ON AND OFF STATE, THEREBY DETERMINING WHERE LIGHT IS PROJECTED ON THE BUILDING PLATFORM AND WHERE A RESIN IS CURED, FORMING A 3D PRINTED OBJECT IN A LAYER-BY-LAYER FASHION.

#### 5.1.2 3D printing: setup

A FlashForge Hunter 3D-printer was used together with a Fun-To-Do Deep Black resin and a Clear transparent resin by Formlabs. The resolution of this 3D printer is 62.5  $\mu\text{m}$  in x and y directions (horizontal plane) and 25  $\mu\text{m}$  in the z-direction.

Designs were drawn in Solidworks, converted to STL files and loaded into the dedicated program from Flashforge, FlashDLPrint. Appendix A summarizes the main settings for printing the used resins (Fun-To-Do Deep Black and Formlabs clear resin) throughout this study. After printing the devices were cleaned/rinsed/washed with isopropanol, acetone or ethanol. Cleaning the parts for too long results in cracks in the final design.

The resin used for 3D printing comprises a mixture of ingredients that usually cross-link through photo-initiators. After printing, some of these components are expected to still be present, and able to diffuse into the cell culture media. It was hypothesized that post-treatment of the 3D printed parts would enhance the biocompatibility

Two main post-treatment steps were executed with different time durations. The first step was an exposure to 405 nm light ( $14 \text{ mW/cm}^2$ ) and the second step heating of the 3D printed parts. For the parts printed with Formlabs clear resin a post-treatment of 1-h exposure to 405 nm and 30 min of hot-plate bake at  $120 \text{ }^\circ\text{C}$  was used. For the parts printed with the Fun-To-Do Deep black resin, the post-treatment was set at 1-h exposure to 405 nm light and 24 h baking on the hotplate.

### 5.1.3 **Soft lithography**

Soft lithography is a highly popular technique for producing microfluidic chips since it is a rapid prototyping technique. Conventionally soft lithography is used in combination with cleanroom fabricated wafers. A wafer contains the inverse design of all the channels and walls. Afterwards it is covered with a polydimethylsiloxane (PDMS) mixture, prepared by mixing the two pre-polymer base and curing agent components in a 10:1 weight ratio (Sylgard® 184 Silicone Elastomer kit (Dow Corning, Midland, MI, USA)). PDMS is then degassed in a vacuum chamber for several minutes and consecutively cross-linked and cured at  $70 \text{ }^\circ\text{C}$  for at least 4 hours. After cross-linking the PDMS structure can be removed from the mold and the mold can be reused to make a new chip. Here, we use 3D printed molds for this step of soft-lithography. The whole process is also depicted in Figure 10

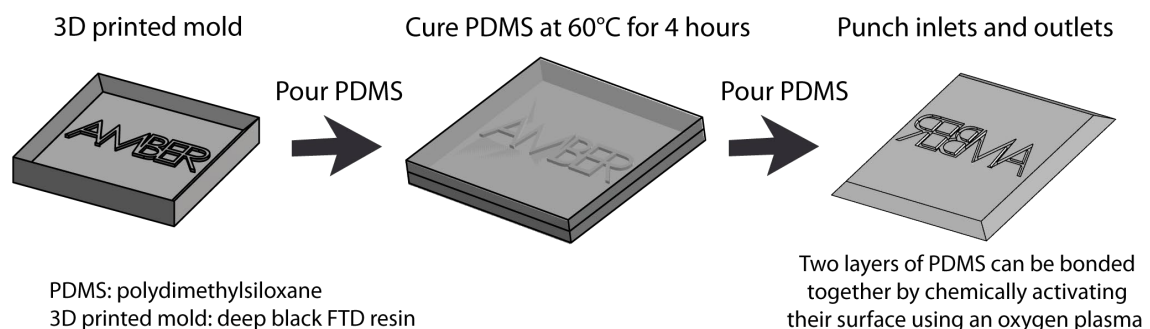


FIGURE 10. SOFT LITHOGRAPHY PROCESS FROM 3D PRINTED MOLDS (PDMS PRODUCTION)

The resulting PDMS chips, containing the desired microfluidic channels, are next bonded to a glass slide, an adhesive tape or another piece of PDMS. For this, the PDMS -with its side of attachment up- is activated in a plasma oven (Cute, Femto Science, 50 W, 40 s, at 50 kHz and 0.09 torr), which allows a chemical bonding that can be further strengthened by an overnight step in the oven at  $70 \text{ }^\circ\text{C}$ . [39]

Another option is to seal the PDMS device with PCR tape, which relies on pressure sensitive adhesion. Serra *et. al* proved that using this commercially PCR tape can be used for biological experiments to seal a PDMS chip that has been activated by an oxygen plasma. This is a low-cost and easy fabrication method and as an additional benefit the tissue can be easily removed from the chip afterwards for further analysis. [51]

### 5.1.4 **Glass pulling theory**

When glass is heated, it becomes fluid. A glass capillary can be pulled into a glass needle by holding it a flame and simultaneously pulling it in opposite directions with tweezers. However, this method is challenging to control to create needles with well-defined and reproducible dimensions. Therefore, we decided to use a dedicated glass puller. These devices can pull glass capillaries with tip sizes with inner diameters as small as  $0.1 \mu\text{m}$ .

In Figure 11 the working principle of the glass puller is displayed. Glass pulling uses glass capillaries to create glass microneedles from  $0.1 \mu\text{m}$  diameter and larger. Glass capillaries are

brought into a flowing state by applying heat to reach the glass transition temperature. Next, the glass is pulled into a needle by velocity sensing or by applying a fixed force. With dedicated glass pullers, needles can be designed with dedicated diameter, length and bevel. Typical applications for glass microneedles include patch-clamping and microinjections.[52-54]

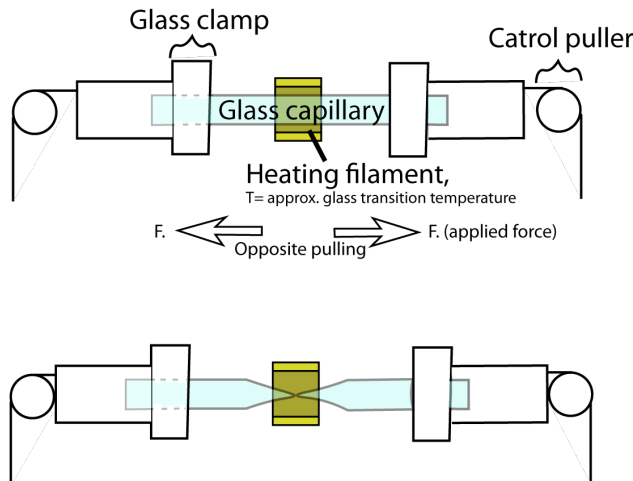


FIGURE 11. IMAGE SHOWING THE USED GLASS PULLER + PRINCIPAL GLASS PULLER [55] GLASS TUBE IS HEATED AT TEMPERATURE  $T$  BY A HEATING COIL. WHEN THE TEMPERATURE IS CHOSEN TO BE SET JUST ABOVE THE GLASS TRANSITION POINT, AT WHICH GLASS BECOMES SOFT. BY APPLYING AN OPPOSING FORCE THE GLASS IS PULLED INTO A NEEDLE. THE FORCE, AMOUNT OF HEATING AND COOLING CAN BE ADJUSTED TO CHANGE TO FINAL APPEARANCE OF THE GLASS NEEDLE.

### 5.1.5 Glass pulling setup

Glass needles were pulled using the Model P-87 Flaming/Brown micropipette puller by Sutter Instruments CO and the P-1000 Sutter Instrument glass puller. The first experiments were performed with the P-87 glass-puller, which was a predecessor (90's) of the newer P-1000 model.

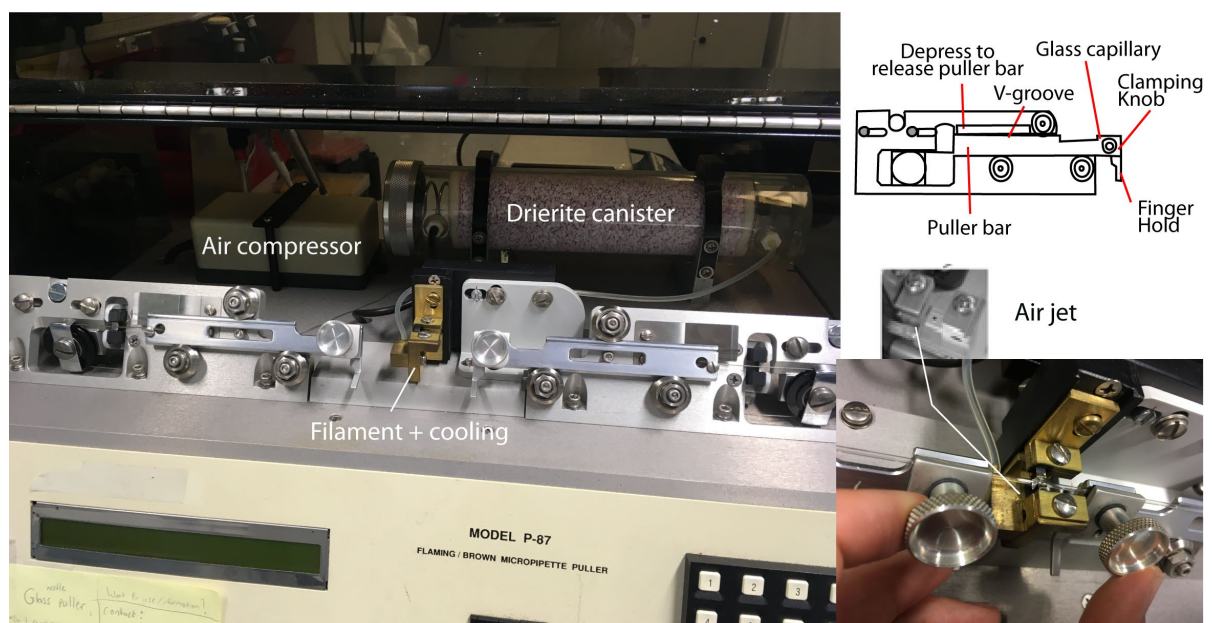


FIGURE 12. P-87 MICROPIPETTE PULLER, SHOWING ALL THE DIFFERENT IMPORTANT ELEMENTS TO UNDERSTAND HOW TO PULL A MICROPIPETTE. FIGURE ADAPTED FROM [56]

### Setting up a glass pulling program:

After inserting a glass capillary (GC150F-15, Clark electromedical instruments), a ramp test is run to determine the heat value for which the inserted glass capillary reaches the glass transition temperature. Based on this value, one can start programming a cycle. A cycle is referred to as a consecutive chosen number of steps each with their own heat, pull, velocity and pull values. Table

1 shows the effect of changing these parameters and the specific special conditions that can be programmed. For a detailed description on how to operate the glass puller Appendix B can be reviewed.

A good starting point for the heat value is the ramp test value or about 5 units above it (which increases the current through the filament with 250 mA). As the tip is heated, less heat is required to put the glass into a flexible state. Thereby heat can be decreased by small steps of 5 throughout the loop, or it can be kept on the same heat throughout as a starting point.

Below the filament there is an air jet that cools the filament and glass pipette. The setting time and delay both control the air cooling. The time indicates how much milliseconds cooling air is applied and the delay setting is a special time setting where the amount of cooling (cooling time) is kept constant, but the value determines at how many milliseconds during the cooling phase a hard pull is done. Higher delay values increase cooling and generate a shorter/steeper tapering. The delay setting is only present for the P-1000 Sutter instruments glass puller. Like the time parameter, it controls the air-cooling control. The time mode indicates the duration of cooling. The delay mode gives a fixed amount and duration of cooling and the given value indicates when the hard pull (when a force is applied actively) will occur during the cooling stage. This mode gives more control over the viscosity of the glass.

By tuning the heat, pull, velocity, time and delay values, tips with different shapes can be created. Here we aimed to create a small, medium and larger sized tip (diameter of 5-10, 20-30, 75-100 µm). Besides the diameter the length of the glass needle will also change between programs, but for now, only the diameter size will be optimized.

TABLE 1. TUNABLE PARAMETERS. L=LENGTH OF THE NEEDLE TIP, D\_TIP=DIAMETER OF THE NEEDLE, R=ELECTRICAL RESISTANCE OF THE TIP. THE PRESSURE CAN BE ADJUSTED, AND 500 IS THE RECOMMENDED VALUE. \*DELAY SETTING CAN REPLACE THE TIME SETTING ON THE P-1000 SUTTER INSTRUMENTS GLASS PULLER WHICH CHANGES THE COOLING TO A FIXED AMOUNT OF TIME AND THE SET NUMBER WILL INDICATE THE TIME WHEN THE HARD PULL WILL OCCUR DURING THE COOLING PHASE.

Cycle Parameters	Value range & advised noticeable step size	1 unit	Effect of increase	Special conditions or tips
Heat	0-999 5	50mA of current through the filament	L=↑, D=↓, R=↑	Start with a value that is similar to the ramp test result or a maximum of 5% more.
Pull	0-255 10	4 mA of current through pull solenoid	L=↑, D=↓, R=↑	If >125, D below 0.1 µm If 0, D becomes at least 1-10 µm If >8 & increasing airflow, will increase D
Velocity	0-255 10-100	1 mV of transducer output	L=↓, D= ↑, R= ↓	>100 for micropipettes
Time / Delay*	0-255 100-200	1 ms if time is larger than 0 otherwise 10 ms	L=↑, D=↑ (if pull>8), R=↓	time=0 vel= nonzero, no cooling. L= ↑ (microinjection pipettes)  time&vel=nonzero, time indicates duration air pulse

## 5.2 Tissue handling and staining

Detailed information on the use of intact epididymal tubules from humans was not extensively described. Setups had to be created to improve tissue dissection. The variability between samples was assessed and protocols for staining important proteins for BEB function and to assess the viability of the tissue had to be explored.

### 5.2.1 Human epididymis sample retrieval

Testicular tissue was obtained from gender dysphoria patients on the day of sex reassignment surgery (SRS).[57] Consecutively seminiferous tubules and the epididymal tubules were

separated. The epididymis was transported in a Styrofoam box filled with ice and stored before experimentation in this box inside of a fridge (4 °C).

Our collaborators from Münster Germany obtain testicular tissue from three different clinics. These three clinics have different treatment plans for time and length during which the patients are treated with anti-androgens and estrogens before surgery. It was shown that patients that stopped the treatment 2 or 6 weeks before the surgery showed blood levels that were back to male physiology and patients that did not stop hormonal therapy had feminized blood levels after surgery.[58]

Matoso *et al.* concluded that in their research out of the 99 patients, 21% had epithelial hyperplasia which means that the macroscopic length of the epididymis (from the top of the caput to the bottom of the cauda) has a length of 2.5 cm or less and the average size was 3.87 cm (3-5.5 cm). 24% expressed fibrosis around the epididymal ducts, and 4% had both conditions. This indicates that about 60% of the received samples are expected to be in normal conditions after androgenic treatment. [59]

### 5.2.2 Tissue preparation

Tissue was dissected on ice using forceps and small scissors. Figure 13 shows the stepwise manner in which the dissection was performed. A small portable USB microscope was used to monitor where to cut and where the connective tissue was located to facilitate the process of extracting 5-10 mm epididymal tubules.

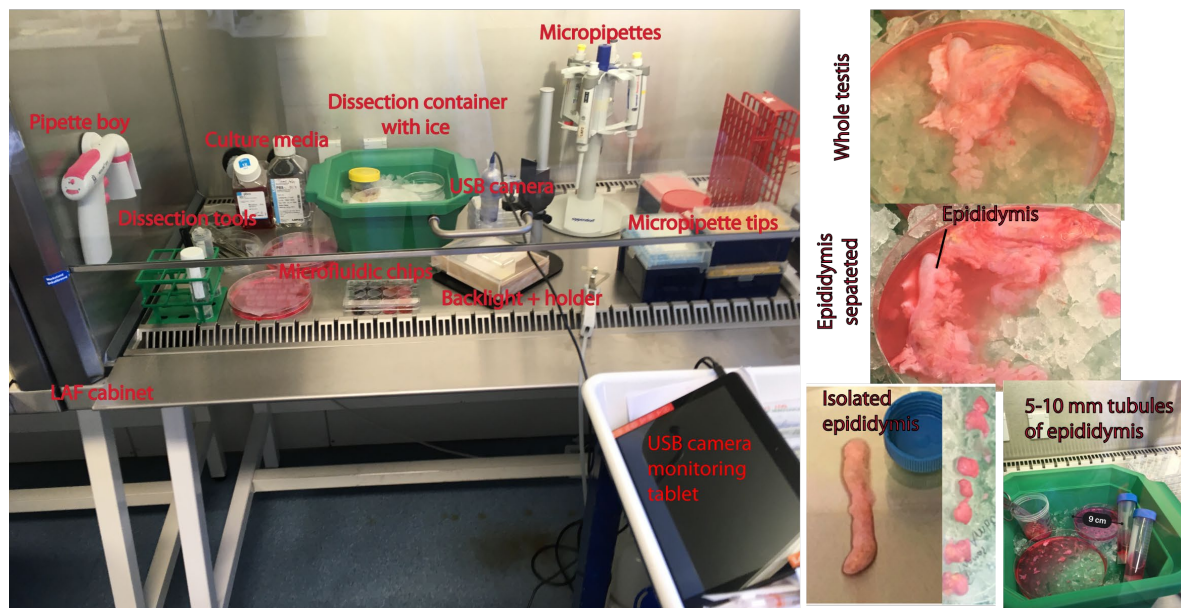


FIGURE 13. DISSECTING SETUP IS SHOWN, AND ZOOMED-IN STEPS FROM THE WHOLE TESTIS TO 5-10 MM EPIDIDYMAL TUBULES ARE SHOWN. THE TISSUE IS DISSECTED ON ICE, AND THE DISSECTION TOOLS CONSIST OF TWEEZERS AND SMALL SCISSORS AND THE USB CAMERA WITH A TABLET ALLOWS TO MONITOR WHERE TO CUT TO OBTAIN 5-10 MM TUBULES.

### 5.2.3 Enhanced survival of epididymis on chip

It was hypothesized that epididymal tubules would be more viable while cultured on chip in a chamber of about 14  $\mu$ L volume, versus in a large volume in a well-plate of 1.5 mL. By reducing the tissue to volume ratio from (1:1500 to 1:14), the surrounding concentration of secreted products would be more physiologically relevant since the tissue would be confined in a tightly packed and small volume *in vivo*. Secreted products are still able in the on-chip condition to diffuse into 1.5 mL of culture medium through a microchannel barrier and nutrients from this bulk medium are provided through this structure as well. Figure 14 demonstrates how the tissue culture on-chip and in a well-plate looks in practice. Appendix C describes the protocol for loading the tissue onto the chip in more detail.

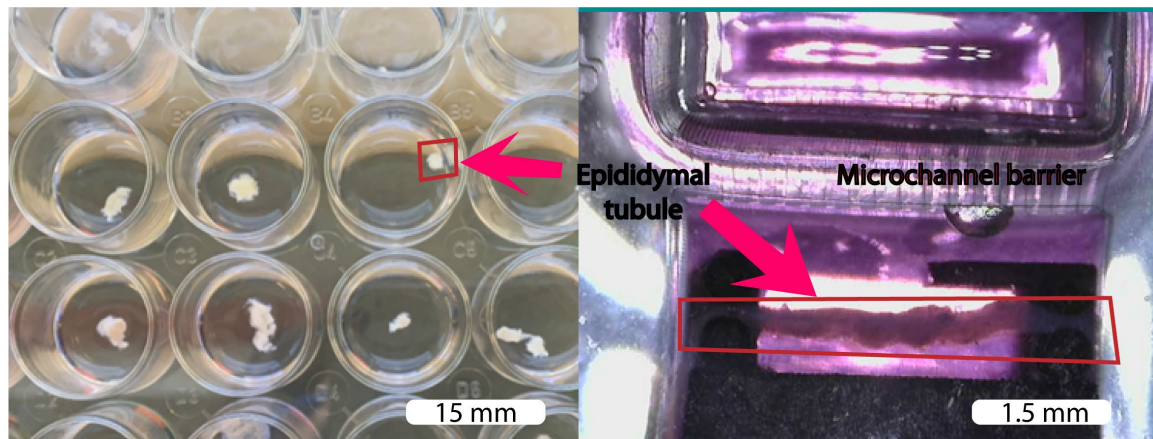


FIGURE 14. THE LEFT IMAGE SHOWS FREE-FLOATING EPIDIDYMAL TUBULES INSIDE OF A 24WELL PLATE, AND THE RIGHT IMAGE SHOWS AN EPIDIDYMAL TUBULE INSIDE A CHIP.

#### 5.2.4 Tissue fixation protocol

Epididymal tissue was fixed using a histopathology fixative, Bouin's solution which is a mixture of picric acid, acetic acid and formaldehyde. Depending on the size of the tubular fragments, the time of fixation varies. For small tubular fragments incubating for 3 hours is sufficient, while for larger tissues like the breast, colon or spleen should be fixed for 10-12 hours. Staining for longer than 24 hours can have an adverse effect. Since we cut the epididymal tubes into smaller pieces here, it was decided to treat for about 5.5 hours. Afterwards, the Bouin's solution was removed and replaced with 70% ethanol.[60]

#### ZO-1 immunohistology of the epididymis

A protocol was developed and optimized for immunological staining of ZO-1 in this tissue. ZO-1 is a tight junction marker, which provides information on the strength of the blood epididymis barrier. The time and concentration values of the primary and secondary antibody were based upon multiple studies on staining optimization of spheroids, *ex vivo* imaging of excised tissues and the iDISCO viskoll tissue protocol.[61-63].

Primary antibody ZO-1 (Life technologies, LOT: QD215339, 250µg/mL) was chosen to be tested in 0.5-2.5 µg/mL range and the stock solution was 250 µg/mL Secondary antibody goat anti-rabbit IgG (Alexa Fluor 568, Life technologies, LOT: 1811756, 2mg/mL) had a stock concentration of 2mg/mL A total of nine different protocols for ZO-1 staining were tested in terms of primary and secondary antibody concentration (Table 2)

TABLE 2. CONDITIONS

Primary antibody → Secondary antibody ↓	1:500, 0.5µg/mL	1:250, 1µg/mL	1:100, 2.5µg/mL
1:500, 5µg/mL	Condition 1	Condition 2	Condition 3
1:250, 10µg/mL	Condition 4	Condition 5	Condition 6
1:100, 20µg/mL	Condition 7	Condition 8	Condition 9

#### Immunostaining protocol

1. 3X wash with PBS for 25 minutes, at 250 rpm on a rocking plate (On 24 well plate)
2. Triton x-100, 1% weight in PBS at RT for 15min at 250 rpm on a rocking plate (From here onwards: in Eppendorf tube 1.5mL)
3. Wash with PBS, 0.2% Tween20 for 30 minutes at 250 rpm on a rocking plate
4. Penetration continue penetration buffer (iDisko) for 60 minutes at 250 rpm on a rocking plate
  - a. Penetration buffer (PBS / 0.2% Triton X-100 / 0.3 M glycine / 20% DMSO)
5. Blocking solution (iDisko) at RT, 3 hours at 250 rpm on a rocking plate
  - a. Blocking solution (PBS / 0.2% Triton X-100 / 6% donkey serum / 10% DMSO)
6. 1<sup>st</sup> antibody 37 °C, 20 hours
7. Wash 2x PBS for 25 min at 250 rpm on a rocking plate

8. 2<sup>nd</sup> antibody 37 °C 25 hours
9. Wash 1x PBS for 25 min at 250 rpm on a rocking plate
10. Transfer the samples into a well plate with fresh PBS and analyse under the microscope.

#### ***Live/dead assay protocol***

1. Prepare live/dead staining in correct concentrations (live/dead viability/cytotoxicity)
2. 2.5µL/mL (5.0 mM) Ethidium ( in PBS)
3. 1µL/mL (2.5 mM) Calcein-AM in PBS
4. 24 well plate, 80-200µL staining solution per well
5. 45min of staining while moving at 100 oscillations/minute ON TOP OF THE SHAKING 37 °C bath.
  - a. Put an empty pipette tip holder (blue/yellow or red part) in the incubator and put the wells plate wrapped in aluminium foil on top.
6. 15 min of rinsing in PSB while shaking as in the previous step

The protocol was optimized throughout the experiments. The results will indicate the specific changes to the described protocol.

#### **5.2.5 *Experiment tissue variability assessment***

The goal of this experiment was to determine the distribution of epididymal tube diameter between the different segments and to check whether there was a variation between samples both for the epididymis and the seminiferous tubules. For transportation and storage, the tissue was kept on ice in a Styrofoam box and stored in a fridge at 4 °C afterwards. To test the viability of the tissue after storage of several days up to three weeks, live dead staining was performed. Staining at day 0 in accordance with the protocol described before was done as a positive control. As a negative control tissue was put either inside Bouin's solution or 70% ethanol for 45 min, which ensures the death of the tissue.

#### **5.3 *Barrier penetration and permeability setup***

To get an idea of the barrier strength of the epididymis on-chip, luminal access was obtained through a glass pulled needle with a tip diameter of about 30 µm to allow capillary filling before entering the lumen. The glass microneedle was pre-loaded with a 10mg/mL FITC-Dextran 40k (fluorescein isothiocyanate-dextran (FITC), FD40S-100MG, MW08261, 19996TH) in PBS solution utilizing a 28 gauge, 97 mm long micro filling needle (World precision instruments, Inc., MF28G-5, 10K) and capillary filling of the glass needle. Upon insertion a time lapse recording (see appendix D to see the protocol how to do so) was initiated to monitor the diffusion of the fluorescent dye out of the epididymal tubule as a measure of barrier integrity. Appendix E shows an extended setup of barrier penetration for testing the effect of differently sized FITC particles and the permeability in combination with an inflammatory inducer TNF-alpha.

## 6 RESULTS: MATERIALS & METHODS

This section discusses the variability between the different human tissue samples, their survival and viability after storage on ice for prolonged periods of time, control live/dead staining and the optimization of the ZO-1 staining protocol.

### 6.1 Setup adaptations and analysis

For the dissection of the tissue it was difficult to determine whether a piece of tubule or a strand of interstitial/connective tissue was dissected. To give more guidance during dissection a dedicated set-up was built consisting of a USB camera with a long working distance connected to a tablet. (see appendix F) Additionally a backlight was fabricated for a better illumination during dissection and a holder to prevent the epididymis chip from moving during insertion of the cartridge and needle insertion. (see appendix F)

Since 3D printed resins are often not reported as biocompatible, the effect of post-treatment protocols was investigated. It was hypothesized that after printing, the parts still contained biologically toxic components for the cells, like polymer chains that are not cross-linked and photo-initiator. By heating the chips afterwards, it was predicted that the weight of the 3D-printed part would decrease, indicating the evaporation of toxic components. Appendix G summarizes the result of weight loss decrease after heating for hours and days. No significant difference was observed when comparing one sided versus two-sided 405 nm treatment for 15 min. In terms of heat, keeping the cartridges at room temperature resulted in a weight loss of 0.3% (+- 0.2% STD, n=6) and 60 °C 0.55% (+- 0.2% STD, n=6) and at 120 °C 4.8% (+- 0.2% STD, n=6). Appendix G also presents data of heating an object of about 2 grams (7 black cartridges on a frame) for up to 31 days at 120 °C. The trend line shows a linear decrease of the weight over time with a confidence value of 0.89. This could indicate that the heat slowly degrades the cross-linked resin on the surface and thereby steadily decreases the weight. For the clear resin the heat treatment of 120 °C the weight loss per day decreases over time. This could

Glass-pulled needles had to be created with a diameter between 5-100 µm for accessing the luminal environment of the epididymal tubules. Recipes with the P-87 and P-1000 Sutter Instruments glass pullers were optimized and tested. (See appendix H & J) Figure 15 depicts the resulting pulled pipettes using the P-1000 glass pulling recipes summarized in appendix I.

Glass needles with a diameter around 30 µm seem to be the easiest to fill with fluid through capillary filling and filling with a flexible microneedle that can be attached to a syringe. Diameters around 5-15 µm were often too fragile, breaking quickly upon insertion in the glass needle insert. Glass needles around 30 µm were used to access the lumen of an epididymal tubule.

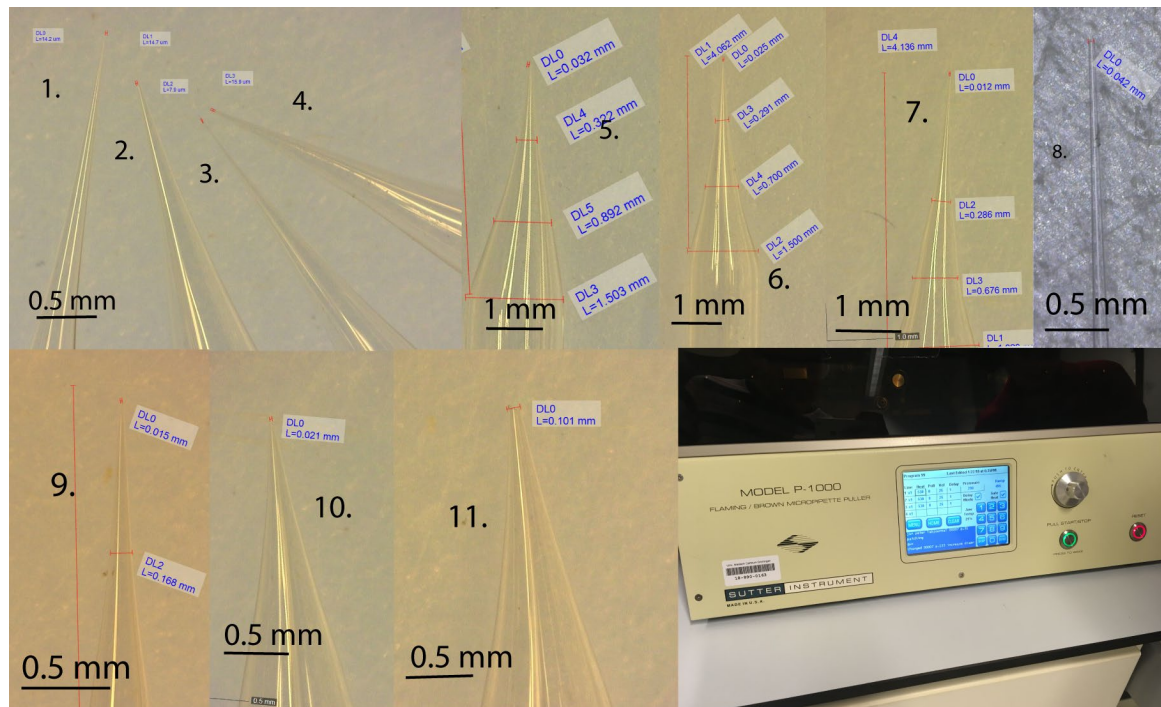


FIGURE 15. HERE THE ELEVEN GLASS PULLING RECIPES RESULT FROM THE SUTTER INSTRUMENT P-1000 GLASS PULLER THAT WERE TESTED ARE SHOWN. FROM ONE TILL ELEVEN IN ORDER THE DIAMETER OF THE TIP IS 14, 15, 8, 16, 32, 25, 12, 42, 15, 21, 100  $\mu\text{m}$ . THE P-1000 PIPETTE PULLER IS SHOWN IN THE IMAGE AT THE BOTTOM RIGHT. THE DETAILED ELEVEN PROGRAMS ARE DESCRIBED IN APPENDIX I.

## 6.2 Tissue variability

Since the obtained epididymal tissue originates from patients undergoing sex reassignment surgery that had hormonal treatment before surgery it is important to screen whether there is a large variability between the samples and whether this can be explained by the hormonal treatment or other factors such as the age of the patient. If the tissue varies too much, then the variability between experimental results may be high if different tissues are used. The goal was to check whether the diameter of the different segments and macroscopic size of the epididymis varied between samples. This was also important to check to see the range of diameters to make sure to design clamping structures with an appropriate spacing or that perhaps different trapping structures should be designed.

Figure 16 displays the variability in diameter between sample A and F till J in the different epididymal segments. In terms of tissue variability, there was no observable correlation between epididymal tissue height and the diameter of the tubules. However, a possible trend could be that the epididymal tubule diameter was larger for smaller epididymis. It is known that androgenic treatment can result in enlarged epididymal tissue, which could explain this trend. In appendix J the additional weight, age and hormonal data of the patients A, F, G, H, I and J is included. However, more patient data is needed from similar age categories and/or hormonal data to see trends.

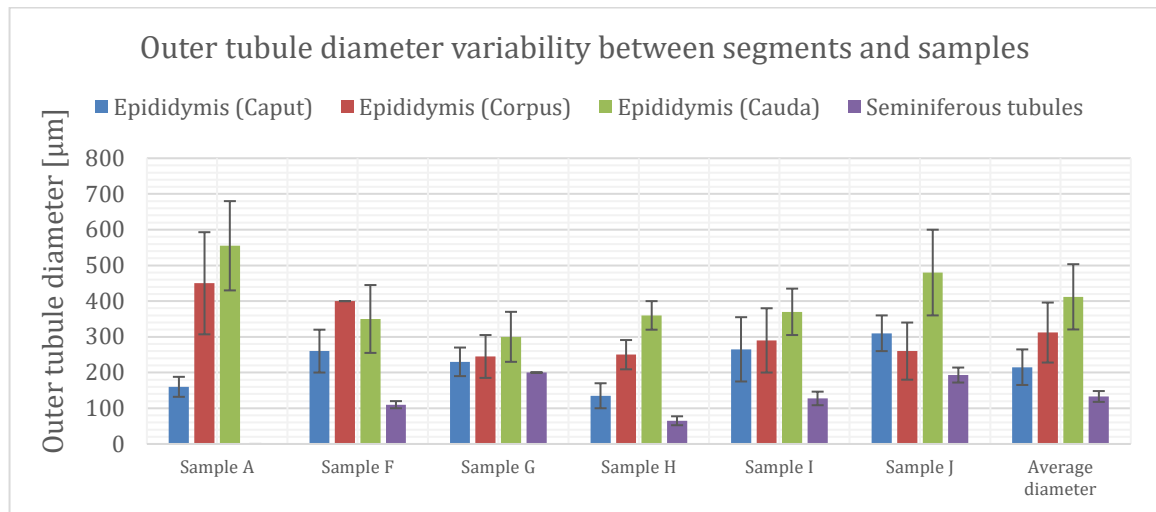


FIGURE 16. MEASUREMENT OF HUMAN EPIDIDYMAL TUBULE (SAMPLE A AND F TILL J, SEE APPENDIX J) DIAMETERS IN DIFFERENT SEGMENTS (CAPUT, CORPUS, CAUDA). ALSO INCLUDED ARE THE MEASUREMENTS OF THE SEMINIFEROUS TUBULES FOR COMPARISON. ALL DIMENSIONS ARE IN  $\mu\text{m}$ . ERROR BARS INDICATE  $\pm 1$  STANDARD DEVIATION

Especially in the caput region, where the tubule diameter is smallest, being around 200-250 $\mu\text{m}$ , it can sometimes be difficult to distinguish blood vessels from epididymal tissue. One way to keep them apart would be to check whether the tubule branches. If it does, then it is a blood vessel. Other methods would include epididymal specific staining or blood vessel specific staining.

### 6.3 Tissue survival when stored for prolonged time on ice

For some experiments only small amounts of epididymal tissue are required. The number of samples that could be obtained through our collaborators in Münster varied between one per week to one per one and a half month. To use as much of the tissue as possible and to be able to do experiments in periods when less sample is available a test was performed to check the viability of the tissue after storing it for several days up to three whole weeks. Live/dead staining was done on tissues after storing them 1, 8, 16 and 21 days respectively.

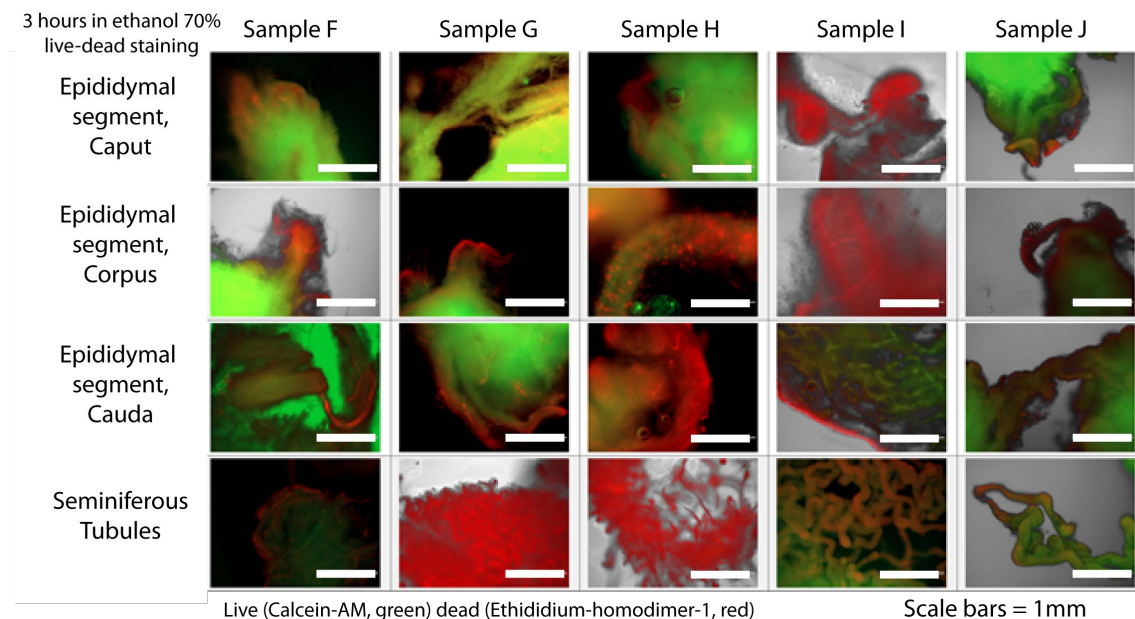


FIGURE 17. SEMINIFEROUS TUBULES AND EPIDIDYMAL TUBULES WERE PUT IN 70% ETHANOL FOR 3 HOURS AS A NEGATIVE CONTROL. THE COLUMNS INDICATE THE DIFFERENT SAMPLES. THE DIFFERENT SAMPLES WERE HELD FOR DIFFERENT AMOUNT OF TIME ON ICE IN A STYROFOAM BOX IN THE FRIDGE AT 4 °C. SAMPLE F AND G WERE 21 DAYS OLD, H 16 DAYS, I 8 DAYS, J 1 DAY. THE WHITE SCALE BARS INDICATE 1000 $\mu\text{m}$

500µL of calcein (live, 1µL/mL) and ethidium (dead, 2µL/mL) staining in PBS were incubated with the tissue in a 24 well-plate for 1 hour. A negative control was performed, where the different epididymal tubules were put in 70% ethanol for 3 hours to ensure cell dead, removing the sample variability and giving a comparison of how a dead tissue would be stained with the same live/dead protocol. Figure 18 depicts live/dead staining after storage of the sample after 1, 8, 16 and 21 days. One thing that can be noticed is that the samples G, H and I look alive (green) in particular. Samples F and J are in a worse state although the seminiferous tubules of sample F look alive.

Comparing the age, weight, and hormonal levels that are denoted in appendix J a few things stand out. Sample H has an FSH that is twice as high as the upper normal range which could be an explanation for the state of the seminiferous tubules. However, the epididymal tubules seem to be in a living state, especially the corpus segment, which could indicate that the epididymis is not sensitive to very high FSH levels. Sample I had an epididymis weight of 15 grams, which is twice or almost three times as high as the other samples. Additionally, this patient had testosterone levels that were closer to normal levels. This could mean that a large epididymis with the prescribed medication does not result in tremendous reduced genetically male hormonal levels. Sample G and J were almost similar in terms of hormonal data although sample J had less testosterone. It could be that the epididymis is in a worse state if the epididymis is very light. Sample J is 5 grams whereas sample G is 6 grams and the other samples all testis that are heavier. Another noticeable thing is that samples G, H and I are from patients between 37 and 41 years old whereas samples J and F are both 26 years old. There are too many parameters and too little samples analyzed to see a trends between tissue viability, sample weight, patient age, length, weight and hormonal data.

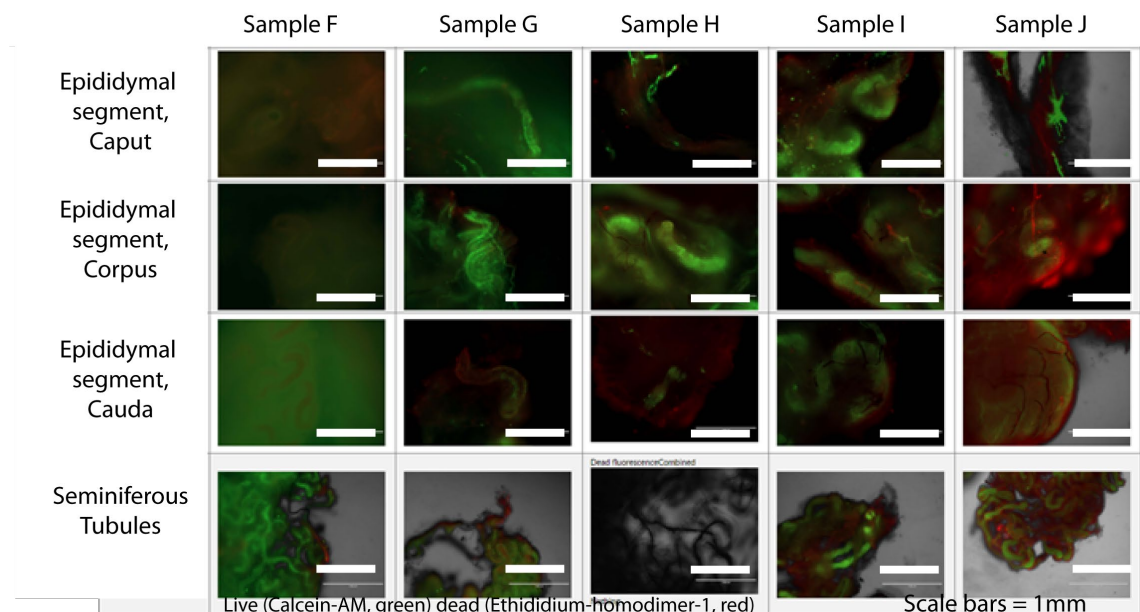


FIGURE 18. SEMINIFEROUS TUBULES AND EPIDIDYMAL TUBULES WITH DIFFERENT TIMES STORED IN A STYROFOAM BOX IN THE FRIDGE AT 4 °C WERE COMPARED. SAMPLE F AND G WERE 21 DAYS OLD, H 16 DAYS, I 8 DAYS, J 1 DAY. THE WHITE SCALE BARS INDICATE 1000µM EXCEPT FOR TISSUE G AND ROW A WHICH HAS A SCALE BAR OF 400µM

#### 6.4 Live dead staining control experiments

As a positive control for the samples when culturing on-chip, live dead staining are performed at day 0 of the culturing to create a baseline of tissue viability before culturing. The previous section also proved that the time after surgery does not translate directly to a highly viable tissue (Tissue I, 1 day post-surgery), but that it is sample dependent. Figure 19 displays the results from the positive and negative live/dead staining. For the positive control (meaning live/dead staining at day 0) an additional confocal image is made. Important to note here is that especially on the confocal image there is an apparent trend that a certain cell type does not survive in the tissue. This could be attributed to random cell death, barrier defects or a selective cell type survives less. An

hypothesis for selective cell survival is that the cell culture media that is currently used does not provide all the required metabolites for the survival of this specific cell type. Based on the number and distribution of the cell death and assuming that all these cells would die, these could be immune cells (macrophages, dendritic cells or t-cells), since they are also present outside the epididymal tubules. When zooming in closer to the epididymal tubules (objective of 20x or higher), movements of tissue can also be observed, probably caused by the peristaltic movement of smooth muscle cells. Another clear observation that can be made in the confocal image is the presence of small blood-vessels on the surface of the epididymal tubule.

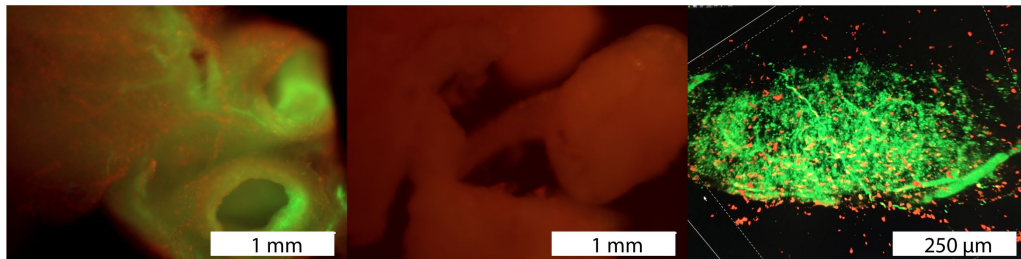


FIGURE 19. THE LEFT IMAGE IS A POSITIVE CONTROL OF FRESH 1 DAY POST SURGERY TISSUE FROM A 22 YEAR OLD PATIENT AND ON THE MIDDLE A NEGATIVE CONTROL WHERE THE TISSUE IS KILLED BY PUTTING THE TISSUE IN BOUIN'S SOLUTION FOR 45 MINUTES. THE IMAGE ON THE RIGHT IS A CONFOCAL IMAGE OF EPIDIDYMAL TISSUE WITH LIVE/DEAD STAINING. THE LARGER GREEN STRUCTURES RESEMBLE VASCULATURE THAT IS WRAPPED AROUND THE EPIDIDYMAL TUBULES. LIVE (GREEN: CALCEIN-AM) DEAD (RED: ETHIDIUM HOMODIMER-1)

### 6.5 ZO-1 immunostaining of the epididymis

Cell-cell interactions form the basis of tight barriers throughout the human body. One of the proteins responsible for maintaining the tightness in a barrier is ZO-1, which is a tight junction protein. By immunostaining this protein an indication of barrier strength can be obtained. Staining of ZO-1 in whole epididymal tubules is not reported in literature. A protocol was designed for staining the ZO-1 protein and nine different combinations of primary and secondary antibody were tested. The results depicted in Figure 20 clearly indicate that a concentration of 2.5  $\mu\text{g/mL}$  of primary antibody has the best results. However, the lowest primary antibody concentration together with the middle secondary antibody concentration also leads to a good result. A possibility could be that the amount of tissue in the Eppendorf tube was less during staining was less. The epididymal tissue also contains biomolecules that emit fluorescent light as described later in this MSc thesis. The intensity of the ZO-1 in this experiment was similar to the auto fluorescence intensity of the cells. Therefore, for future experiments it is suggested to either analyse the ZO-1 staining by confocal microscopy or use a different secondary antibody, that emits a different wavelength or lastly the incubation time with the primary and especially the second antibody should be increased.

	Secondary antibody 1:500 (4 $\mu\text{g/mL}$ )	Secondary antibody 1:250 (10 $\mu\text{g/mL}$ )	Secondary antibody 1:100 (20 $\mu\text{g/mL}$ )
Primary antibody 1:500 (0.5 $\mu\text{g/mL}$ )			
Primary antibody 1:250 (1 $\mu\text{g/mL}$ )			
Primary antibody 1:100 (2.5 $\mu\text{g/mL}$ )			

FIGURE 20. NINE DIFFERENT COMBINATIONS OF PRIMARY AND SECONDARY ANTIBODY CONCENTRATION. SCALEBARS INDICATE 200  $\mu\text{m}$

## 7 DESIGNING THE EPIDIDYMIS-ON-A-CHIP

The aim for designing the epididymis-on-a-chip platform was to access the luminal environment of the epididymal tubules to study the BEB. Obtaining more information on barrier function is important since it can lead to understanding the cause of infertility that are currently unexplained (12-15 million). To be able to design a biological relevant model it was important to first set several biological and technological requirements that had to be met.

The first biological objective was to be able to maintain the tissue alive for at least 7 days, by succeeding to do so, it is possible to study the barrier function over time as a result of microenvironmental changes.

The second biological objective was to obtain access to the luminal environment, which has never been reported *in vitro* in human derived tissue before. From a technological perspective the length of epididymal tissue to be put in a microfluidic device had to be defined, in a confined microfluidic culture chamber was set to have a length between 5 and 10 millimeters. Since the total length of the epididymis ranges between 3 and 6 meters, a large amount of experiments can be performed from one sample, removing variability parameters between samples. The epididymis comprises of three segments, and here the corpus segment (body) was chosen to be used, since the diameter of the segment are about 350µm, which is 100µm bigger than the caput segment. A larger lumen would allow easier access of the barrier. The cauda segment is even larger with a diameter of about 500-550µm, but function of the cauda segment is thought to mainly function as a storage of spermatozoa before ejaculation. The corpus segment of the epididymis and the exact processes occurring in there are less studied, making it more interesting to study.

The technological decision was made to attempt luminal access by puncturing it with a needle. Glass-pulled needles were chosen since they allow to create tip diameters that are below the size of the epididymal tubule lumen. To make sure that the luminal environment does not interact with the surrounding media, disturbing the measurement of the barrier function, the endings of the 5-10 millimeter tubules were required to be sealed. This can technologically be achieved by creating structures that trap/clamp the tubule and thereby separating the luminal microenvironment from the fluid outside of the BEB. Hence, the only method for fluid exchange between the two would be through the BEB. Figure 21 schematically depicts and summarizes the approach taken, to fulfill the main biological goals of tissue survival for at least 7 days and luminal fluid access.

In the Chapters 8 till 11 the three designs created for the epididymis-on-a-chip are described. Each of the designs will discuss its results and why it was required to design a new design for the platform.

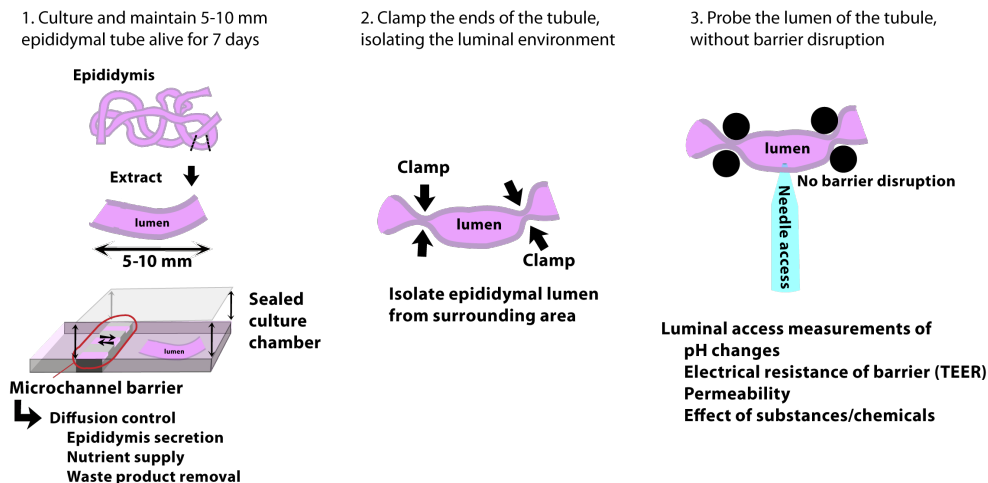


FIGURE 21. THE THREE OBJECTIVES THAT THE EPIDIDYMIS-ON-A-CHIP SHOULD BE ABLE TO FULFILL.

## 8 DESIGN ITERATION 1: CULTURING THE EPIDIDYMIS ON A MICROFLUIDIC CHIP

The first design was aimed to mainly culture the epididymal tissue and to check whether tissue viability is enhanced or better preserved when cultured in a confined area (microfluidic culture chamber). It was hypothesized that due to the increased concentration of secreted products in the microenvironment (more physiological) as opposed to culturing in a 1-1.5mL well the viability would increase.

### 8.1 Introduction

The first design is depicted in Figure 22 which comprises of a culture chamber, a nutrient supply channel and a microchannel barrier. The dimensions of the microchannel barrier were chosen based on research done during the beginning of the project together with our collaborator where the effect of flow on cultured seminiferous tubules on a chip were modeled by COMSOL Multiphysics (See appendix K). This design managed to maintain seminiferous tubules viable up to at least eleven days and shear stresses simulated were not damaging. This indicated that these dimensions were large enough for tissue survival by nutrient supply with an applied of 100 $\mu$ L/hour. A detailed overview of the simulation data with the according assumptions can be found in Appendix L. In the presented design in this section the supply of nutrients is caused by diffusion and not by flow (as was simulated). If a diffusion mediated nutrient supply in this design results in cell dead, it gives an indication that a flow is required. If this would be the case, the design can be easily adjusted to provide a flow as modelled, knowing it is not damaging to the tissue. Molds for fabricating the PDMS chip design were created by 3D printing as described in the material and methods section and PDMS chips were sealed with PCR tape.[51]

As a control to check whether the PCR tape is biocompatible with the use of epididymal tissue, the same design and experiments were done with a PDMS-PDMS sealed chips. The PDMS chips and PDMS thin slabs (for PDMS-PDMS chip) were both plasma treated before tissue placement and it was aimed to insert and close the tubule within 15 min after plasma treatment to enhance bonding strength. The whole chip was placed in a 12 well plate filled with about 1.5 mL of culture medium (Dulbecco's modified eagle medium (DMEM), 1% penicillin/streptomycin (pen/strep)).

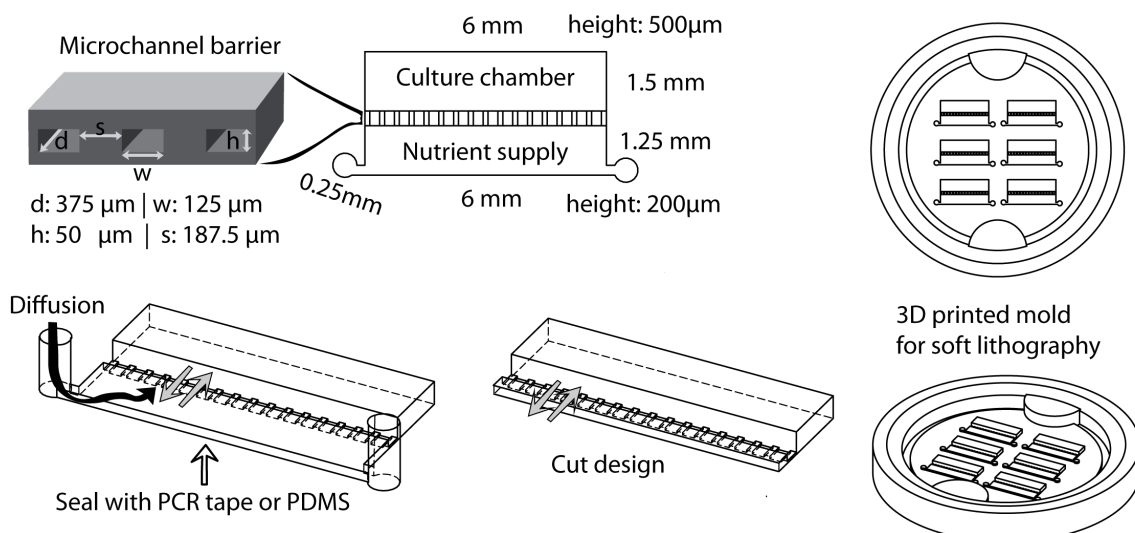


FIGURE 22. IN THE TOP LEFT A SOLIDWORKS IMAGE OF THE 3D PRINTED MOLD IS MADE. NEXT TO THE IMAGE THE DIMENSIONS OF THE DIFFERENT COMPONENTS ARE NOTED. THE ROUND SHAPES NEAR THE ENDS OF THE SUPPLY NUTRIENTS SECTION GETS PUNCHED WITH A 1 MILLIMETER DIAMETER BIOPSY PUNCHER. ON THE BOTTOM LEFT A SCHEMATIC REPRESENTATION OF THE MICROCHANNEL BARRIER IS SHOWN WITH DIMENSIONS AND ON THE RIGHT THE RESULTING 3D PRINTED MOLD. PCR: POLY CHAIN REACTION ADHESIVE TAPE (PRESSURE SENSITIVE ADHESIVE TAPE), PDMS (POLYDIMETHYLSILOXANE)

Besides the comparison of tissue viability between culturing epididymal tubules in PDMS-PCR and PDMS-PDMS chips it was also tested whether the distance from the microchannel barrier to the bulk medium would influence the viability. Two conditions were created, the cut design and the hole design that are also displayed in Figure 22. Here the nutrient supply chamber for the PDMS-PCR and PDMS-PDMS chips were either removed or holes were punched in the nutrient supply chamber. This leads to a longer diffusion pathway for the holes design from the microchannel barrier to the bulk of the media.

## 8.2 Results & discussion

An experimental image of the tubules loaded on the chips in the microfluidic culture chambers and the consecutive chip sealed with the PCR tape are depicted in Figure 23. Closing the chip with PCR tape was preferred since fabrication was easier and cheaper, and the tissue could easily be extracted for off-chip analysis.[51]



FIGURE 23. CHIPS ARE APPROXIMATELY 12MM BY 6MM. THE PDMS CHIPS ARE LOADED WITH EPIDIDYMAL TUBULES ORIGINATING FROM THE CORPUS SEGMENT AND ARE CLOSED WITH PCR TAPE. THE RIGHT IMAGE SHOWS A PIECE OF EPIDIDYMAL TUBULE INSIDE A CHIP AND CONFINED IN THE CULTURE CHAMBER WITH THE MICROCHANNEL BARRIER ON THE RIGHT.

The viability results of the tissue after 11 days by live dead staining with Calcein-AM and Ethidium-homodimer-1 respectively are depicted in Figure 24. All on-chip culturing of epididymal tubules lead to viable tissue. From the experiments it can be concluded that there is no difference in toxicity between PCR and PDMS bonded chips and that the diffusion path length towards the bulk media is not too long for the hole design (Figure 22). The free-floating epididymal tubule, which was an off-chip control of a tubule floating in 1.5 mL (1:1500 tissue:volume ratio instead of 1:14) of medium was less viable than the on-chip tissue. This confirmed the hypothesis that confining the tissue in a micron-sized dimensional chamber, with a relatively low tissue volume to culture chamber volume ratio (1:5 or lower), improves tissue viability.

One of the tested chips during the experiment did not have properly developed microchannels, which heavily reduced the possibility of nutrients exchange (Figure 24). between the bulk media and the microfluidic culture chamber. This epididymal tissue was not viable, which acts as a control that nutrient supply through the microchannel barrier is essential.

Another advantage of the on-chip culturing of epididymal tubules found during culturing is that it prevented the tubules from being aspirated while refreshing media. The microchannel barrier reduces the inflow and outflow of liquids due to the increased resistance (also modeled in appendix G). The free-floating tissue does experience direct shear stress when refreshing media which could be damaging to the tissue.

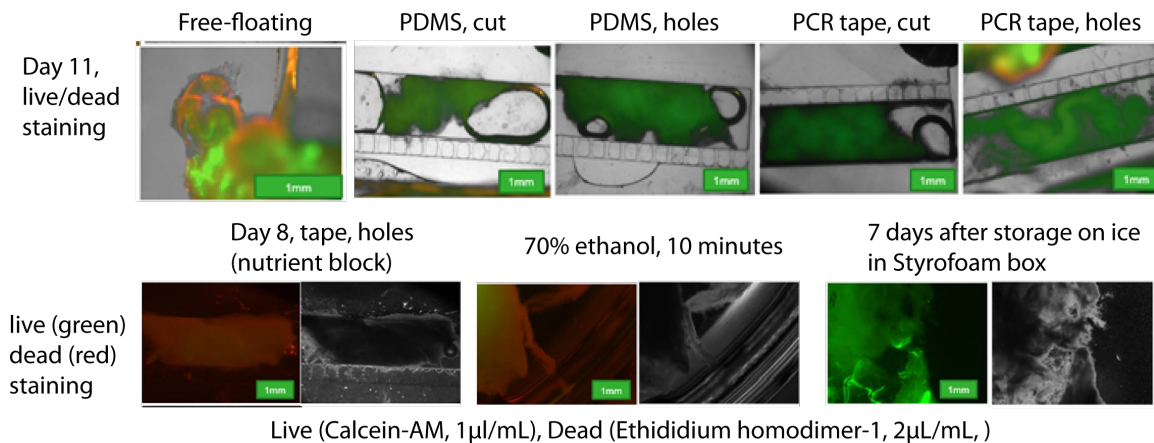


FIGURE 24. COMPARING THE VIABILITY OF EPIDIDYMAL TISSUE WITH THE DIFFERENT CONDITIONS OF CHIP FABRICATION. CUT INDICATES CONDITIONS WHERE THE CHIP IS CUT IMMEDIATELY AFTER THE MICROCHANNEL BARRIER TO ENSURE THE SHORTEST DISTANCE BETWEEN BULK MEDIA AND THE CULTURE CHAMBER, WHEREAS HOLES MEANS THAT HOLES ARE PUNCHED IN THE CHIP WHICH HAS A LONGER DIFFUSION LENGTH FROM THE BULK MEDIA TOWARDS THE MICROCHANNEL BARRIER. TAPE INDICATES THAT THE PDMS CHIP IS SEALED WITH PCR TAPE AND PDMS INDICATES THAT THE PDMS CHIP IS SEALED WITH A PDMS SLAB. FREE MEANS THE CONDITION WHERE EPIDIDYMAL TISSUE IS CULTURED SEPARATELY IN 1 ML OF MEDIUM IN A 24 WELL PLATE. LIVE (GREEN: CALCEIN-AM) DEAD (RED: ETHIDIUM HOMODIMER-1)

An unforeseen problem of the PDMS-PCR tape chip designs was that during the culture, the tape could sometimes delaminate and was poorly attached for all (shaking the well plate already could lead to delamination). For all the designs and different time points three chips were prepared (triplicate experiments). However, for the different time points only 1 or 2 out of the 3 chips for each condition at each time point remained attached (PDMS-PDMS and PDMS-PCR). It is unclear whether the poor attachment lead to the supply of extra nutrients, although the chip with tissue where the microchannel barrier was blocked suggest that it still not sufficient to maintain cells alive and suggest that this is most likely not true.

It was hypothesized that the poor bonding between PDMS and PCR tape could be appointed to the culture media it was floating in and that the adsorption of for instance the proteins interfered with the bonding strength. A microfluidic chip was designed to test this hypothesis. (experiment and design described also in appendix L). PDMS-PCR bonding strength in air, deionized water (DI water), phosphate buffered saline (PBS), culture media (DMEM and 1% pen/strep) and culture media supplemented with 10% Fetal Bovine Serum (FBS) was compared. After 69 hours of incubation at 37 °C and 5% CO<sub>2</sub> after bonding, all of the PCR tape was delaminated in the case of culture media with FBS, while for DI water, PBS and DMEM culture media only 1 out of 4 chips delaminated. Bonding in air did not cause delamination at all. FBS contains a high amount of proteins which can indicate that the hypothesis is true that the proteins interfere with PDMS-PCR bonding. Optionally it could be tested whether it would work better if tissue would be loaded and bonded in air before submerging the chip in media. Although it should be kept into consideration that this method would also increase the chance of incorporating large air pockets/bubbles in the culturing area.

Tissue was viable for 11 days inside a confined area delineated with a microchannel wall and expressed more cell death for the off-chip tissue (free-floating). However, the final goal of the project was to design a device that enables access of the luminal environment to measure barrier function. Therefore, a new platform had to be designed that could also fulfill these goals.

## 9 DESIGN ITERATION 2: EPIDIDYMIS-ON-A-CHIP USING PDMS-PCR TAPE CHIP AND 3D PRINTED CLAMPING STRUCTURE

This second design was aimed to fulfill all the set goals of the epididymis-on-a-chip system to culture and maintain tissue integrity for at least 7 days, clamp the tissue and provide luminal access. This chapter will discuss the design approach, idea and validation, followed by the results and the discussion on these results.

### 9.1 Introduction

The results from the previous design did not indicate difference in tissue viability between PDMS-PDMS bonded chips and PDMS-PCR tape bonded chips. Since the PCR tape provides a very convenient and easy fabrication method and it showed no toxic effects on the epididymal tissue in the previous design, it was decided to use this for sealing the PDMS chip for this design. Figure 26 displays the principle of this design. Like the first design a culture chamber was created that confined the tissue and allowed nutrient replenishment, waste removal and as hypothesized a physiological matching secretion concentration, enhancing viability.

The additional goal of this design in comparison with the previous one is to obtain luminal access and closing the endings of the epididymal tubule to ensure that the luminal environment has no direct fluid contact with the surrounding media. To close the endings of the epididymal tubules it was envisioned to use a 3D-printed stick. This approach was inspired by Venzac *et al.* where they used sliding walls to pattern for instance agarose.[64] They placed walls before inserting uncured agarose, after cross-linking the agarose the sliding walls are removed, resulting in patterned agarose.

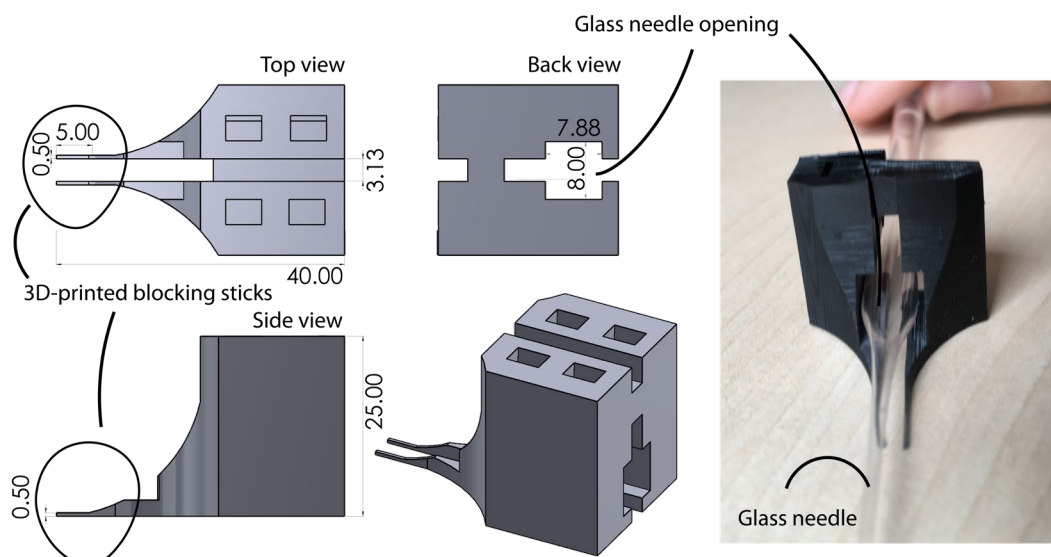


FIGURE 25. HERE THE 3D-PRINTED OBJECT WITH DEEP BLACK FTD RESIN USING THE FLASHFORGE HUNTER PRINTER IS SHOWN. ALL DIMENSIONS INDICATED ARE IN MILLIMETER. THE 3D-PRINTED BLOCKING STICKS ARE CIRCLED AND WILL CLOSE THE LUMEN OF THE EPIDIDYMIS. THE LARGE OPENING IN THE STRUCTURE IS MEANT FOR THE INSERTION OF A GLASS NEEDLE THAT CAN BE CONSECUTIVELY INJECTED INTO THE EPIDIDYMAL TUBULE.

The first step for accessing the lumen barrier was plasma treatment of the PDMS chip, putting the tissue inside the culture chamber and sealing the PDMS chip with a PCR tape. Next, a 3D printed

block is inserted from the side of the chip through designed channel with matching dimensions (see Figure 25). The 3D printed block then pushes against the tubule and compresses the epididymal tubule against the wall and hence seals the lumen. The procedure of luminal sealing is displayed in Figure 26. The 3D-printed blocking stick from Figure 25 included a opening between the blocking sticks for insertion of a glass needle. To ensure ease of handling and positioning of the glass needle and the blocking sticks, indentations were created that allow to pick up the whole object by tweezers.

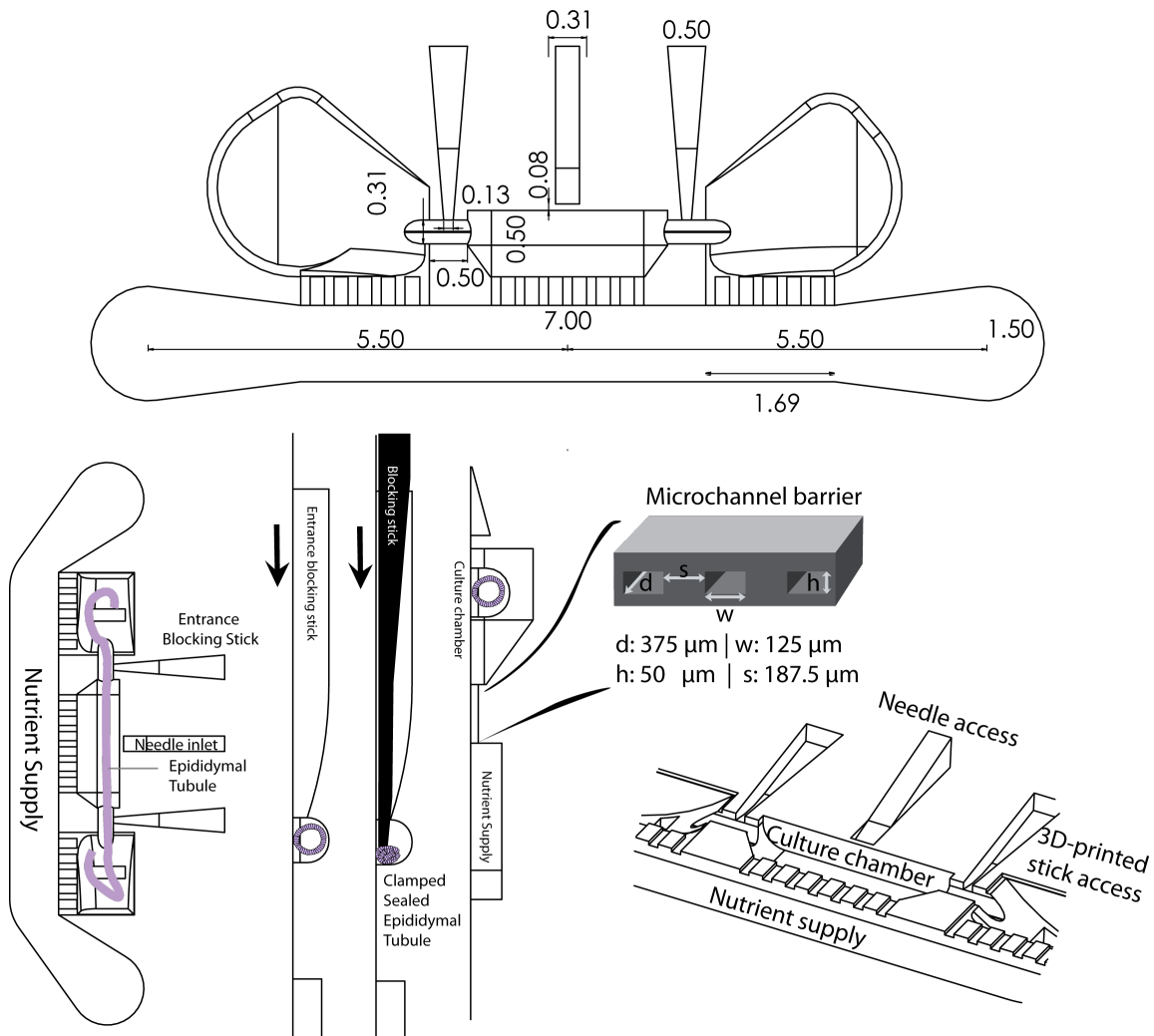


FIGURE 26. HERE THE SECOND EPIDIDYMIS-ON-A-CHIP DESIGN IS SHOWN. THE TISSUE IS LOADED IN A CULTURE CHAMBER AND THE CHIP IS SEALED WITH A PCR TAPE. THE CULTURE CHAMBER IS CONNECTED TO A NUTRIENT SUPPLY CHANNEL THROUGH A MICROCHANNEL BARRIER OF WHICH DIMENSIONS ARE INDICATED IN THE FIGURE. THE 3D-PRINTED OBJECT FROM FIGURE 25 CONTAINS TWO 3D-PRINTED STICKS THAT CAN BE INSERTED THROUGH THE INDICATED MICROFLUIDIC CHANNELS. A CARTOON IMPRESSION OF HOW THE INSERTION OF THESE BLOCKING STICKS LEADS TO CLAMPING OF THE EPIDIDYMAL TUBULE IS DEPICTED.

## 9.2 Results & discussion

Epididymal tubules were put on the chip and live/dead staining was done on-chip as schematically depicted in Figure 27. Although this staining was done only after one day, the dimensions are similar to the previous design with the PDMS-PCR tape and tissue survival was assumed similar as such. However, the two remaining goals of closing the endings of the epididymal tubules and the needle access proved to pose more problems here. The positioning and insertion of the blocking sticks was straight forward and easy but lead to delamination of the PCR tape. In Figure 27 images of the PCR tape delamination after 3D-printed stick insertion is shown. The bonding

strength between PDMS and PCR tape was found to be too poor for the application. The delamination of the PCR tape caused the microfluidic culture chamber to not be a confined chamber anymore. This would therefore decrease viability as was proven by the free-floating epididymal tubule culture with the previous design as a control. Other methods were tried for sealing the tubules such as clamping by using thin thread filaments, but that turned out to be hard to position and manipulate.

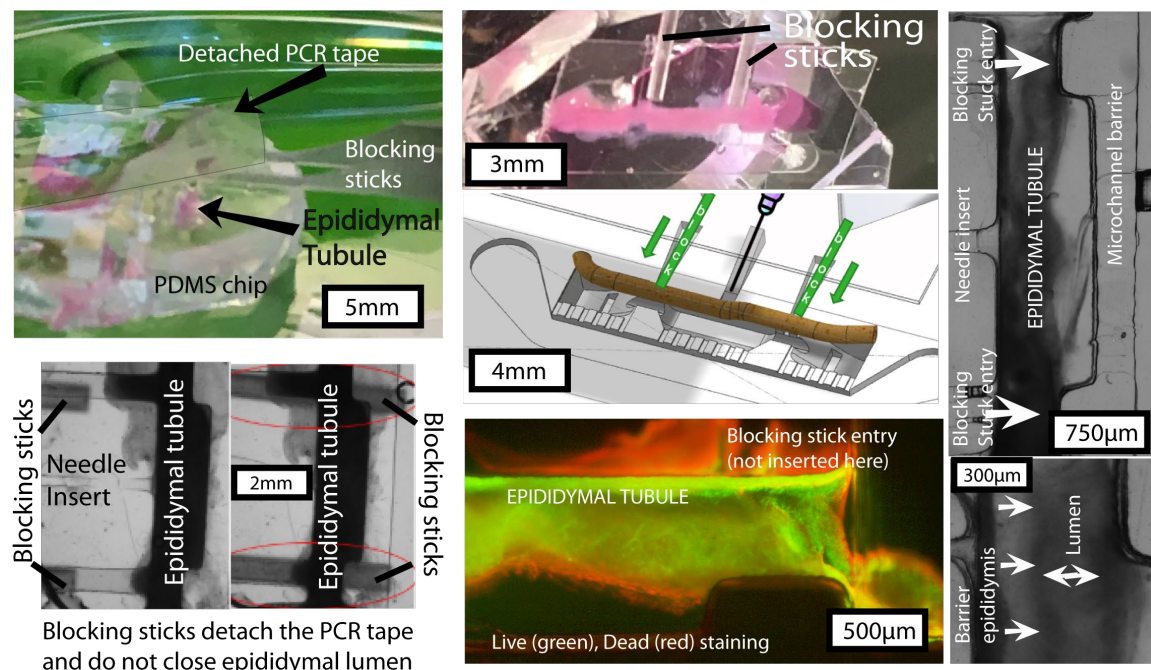


FIGURE 27. TAPE DETACHMENT AFTER INSERTING 3D PRINTED BLOCKING PILLARS. TUBULE FROM THE CORPUS SEGMENT AND A PICTURE OF A PDMS-PCR TAPE CHIP LOADED WITH EPIDIDYMAL TISSUE. SCALE: THE WHOLE TISSUE CHAMBER HAS A LENGTH (TOP TO BOTTOM) OF 5.5 MILLIMETER. LIVE (GREEN: CALCEIN-AM) DEAD (RED: ETHIDIUM HOMODIMER-1)

This chip design was promising at first by fulfilling the goals of capturing, clamping and obtaining luminal access of the epididymis. The proposed design allowed the loading of epididymal tissue into the microfluidic culture chamber. The microchannel barrier, responsible for providing nutrients to the epididymal tubule had the same dimensions as in the previous design. Long-term viability assays were not performed since the design was also a PDMS-PCR tape bonded device with similar dimensions and which was able to maintain tissue viable for up to eleven days.

As discussed in previous section, the attachment of PCR tape to the PDMS is not very strong mainly because temperatures above at least 50-60 °C are required for tighter bonding, but that would not be compatible with tissue culturing since tissue is most viable at 37 °C for humans and above that it becomes apoptotic and starts to die. Therefore a different method was designed for placing the epididymal tubule in a microenvironment with the ability to access the luminal barrier.

## 10 DESIGN ITERATION 3: EPIDIDYMIS-ON-A-CHIP, A PDMS-PDMS BONDED CHIP, WITH SIDE CONNECT TO INSERT TISSUE LOADED 3D-PRINTED CARTRIDGE

This final design should fulfill the three main goals of the epididymis-on-a-chip system to culture and maintain integrity tissue for at least 7 days, clamp the tissue and provide luminal access. This chapter will discuss the design approach, idea and validation, followed by the results and the discussion on these results.

### 10.1 Introduction

Solutions were explored to solve the poor bonding of the PCR tape to PDMS in the previous design. An option that would not require the bonding of chips after tissue loading would be to create a PDMS-PDMS bonded chip (PDMS housing) with an opening on the side. This opening could be utilized as an entry point for epididymal tissue and after loading the tissue into the culture chamber the chips could be sealed. Like the previous design the culture chamber would be replenished with nutrients through a microchannel barrier. The closing of the culture chamber after tissue insertion was first thought to be done by using a PDMS fabricated lid. Although this is possible, it does allow for barrier access by a needle and the tissue is not kept in place to do so. To enable needle access to the lumen a 3D-printed structure was designed that could be used to capture the epididymal tissue in place, closing the endings of the tubule and allowing for needle access. This part is referred to as the cartridge and this part also seals of the culture chamber in its entirety.

Figure 28 presents the concept of this design. The use of this design requires to first dissect the epididymal tissue in a piece of about 5-10 millimeter and load it onto the cartridge afterwards, where the lumen is closed by the compression between the cartridge pillars with a spacing of  $250\mu\text{m}$ . The PDMS housing is composed of two layers of PDMS. In the next paragraphs the design and fabrication of the PDMS housing, 3D-printed cartridge and glass-pulled needles are discussed separately in more detail.

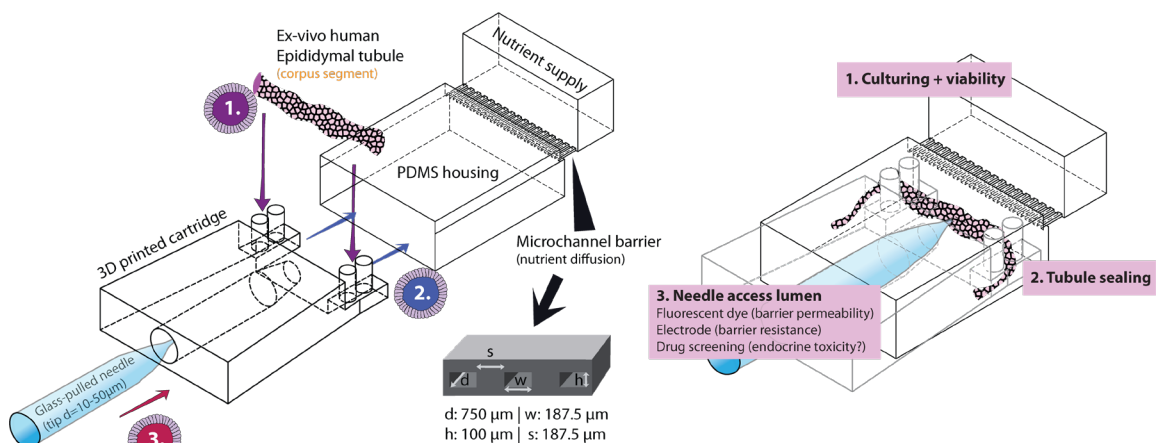


FIGURE 28. DESIGN 3, PRINCIPLE OF THIS DESIGN. A PDMS-PDMS BONDED CHIP IS CREATED AND A 3D PRINTED CARTRIDGE, LOADED WITH AN EPIDIDYMAL TUBE IS INSERTED. EPIDIDYMAL TISSUE CLAMPED BETWEEN 3D PILLARS IN A CUSTOM-DESIGNED 3D PRINTED CARTRIDGE, WHICH IS NEXT INSERTED IN A PDMS HOUSING CHIP. THE MICROCHANNELS ENSURE THAT THE TISSUE IS ABLE TO CREATE ITS OWN MICRO-ENVIRONMENT. LASTLY THE BARRIER CAN BE PROBES USING A GLASS-PULLED NEEDLE.

The PDMS housing part of the design allows to have a side-entry for the tissue into the culture chamber and has appropriate dimensions to allow the 3D-printed cartridge to seal the culture

chamber. Dimensions of the design are indicated in Figure 29. The microchannels allow for nutrient diffusion and luminal environment control like in the last two designs since it proved to result in viable tissue up to 11 days after culturing.

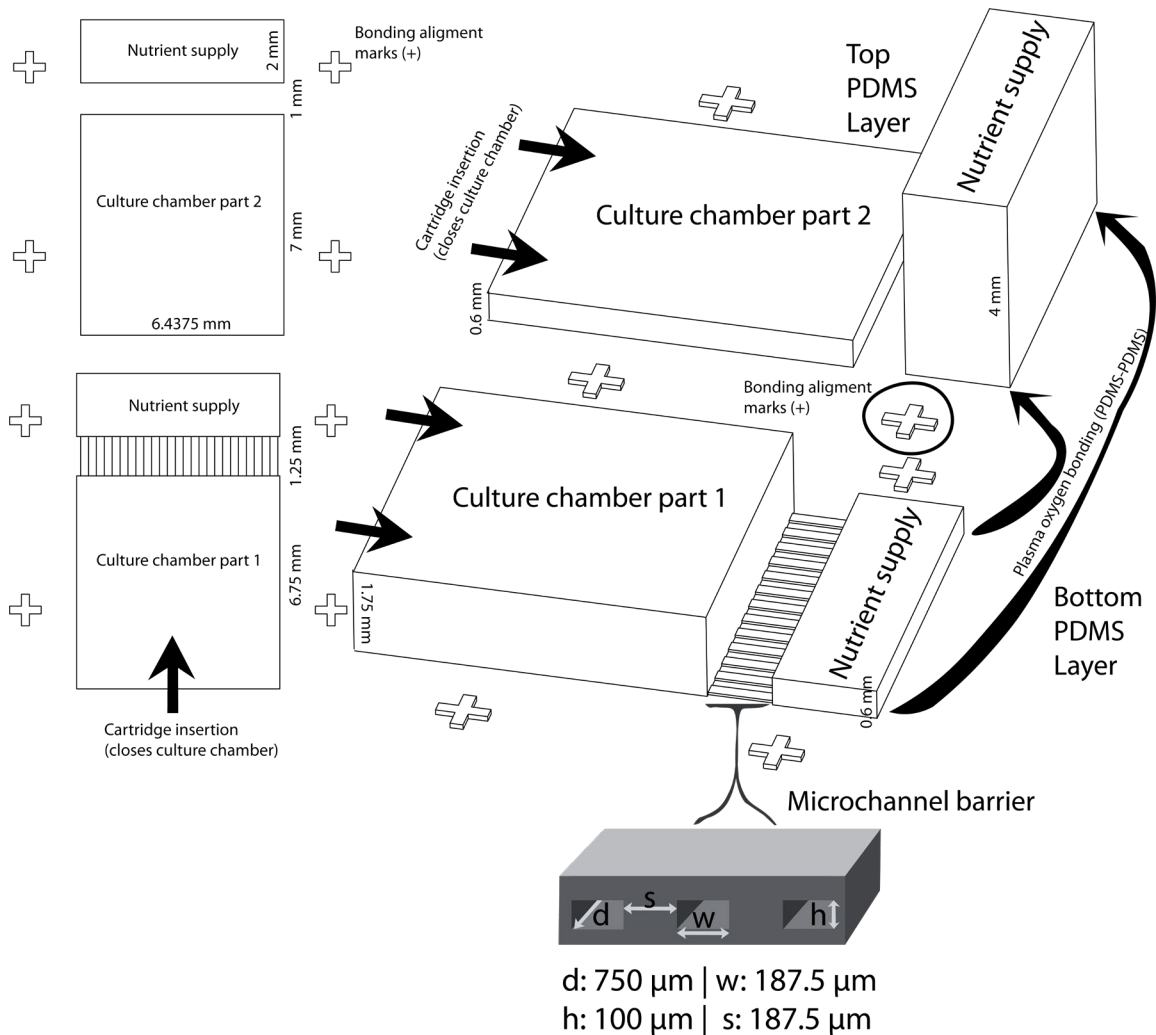


FIGURE 29. THE PDMS HOUSING IS COMPRISED OF TWO OXYGEN PLASMA BONDED PDMS LAYERS. TOGETHER THESE FORM THE CULTURE CHAMBER IN WHICH LATER THE 3D PRINTED CARTRIDGE LOADED WITH THE EPIDIDYMAL TUBULE CAN BE INSERTED THROUGH. THE CARTRIDGE EFFECTIVELY SEALS THE CULTURE CHAMBER AND ENSURES THAT NUTRIENTS ARRIVE THROUGH THE MICROCHANNEL BARRIERS WHICH ARE CONNECTED TO THE NUTRIENT SUPPLY THAT IS CONNECTED TO THE CULTURE MEDIUM IN THE WELL PLATE IN WHICH THE WHOLE CHIP DESIGN IS INSERTED.

The 3D printed cartridge design from Figure 30 comprises of two pillars on the front of the design that create a trapping structure for the epididymis. This structure ensures that the luminal environment of the tubule and the surrounding volume cannot directly interact, but only through the blood-epididymis barrier. Upon insertion of the epididymal tubule between the trapping pillars the cartridge can be inserted as depicted in Figure 28 and Figure 30. The next step is to access the barrier by inserting a glass pulled needle through the needle insert which is designed in the cartridge. By monitoring through the microscope, it can be observed when the needle punctures the epididymis.

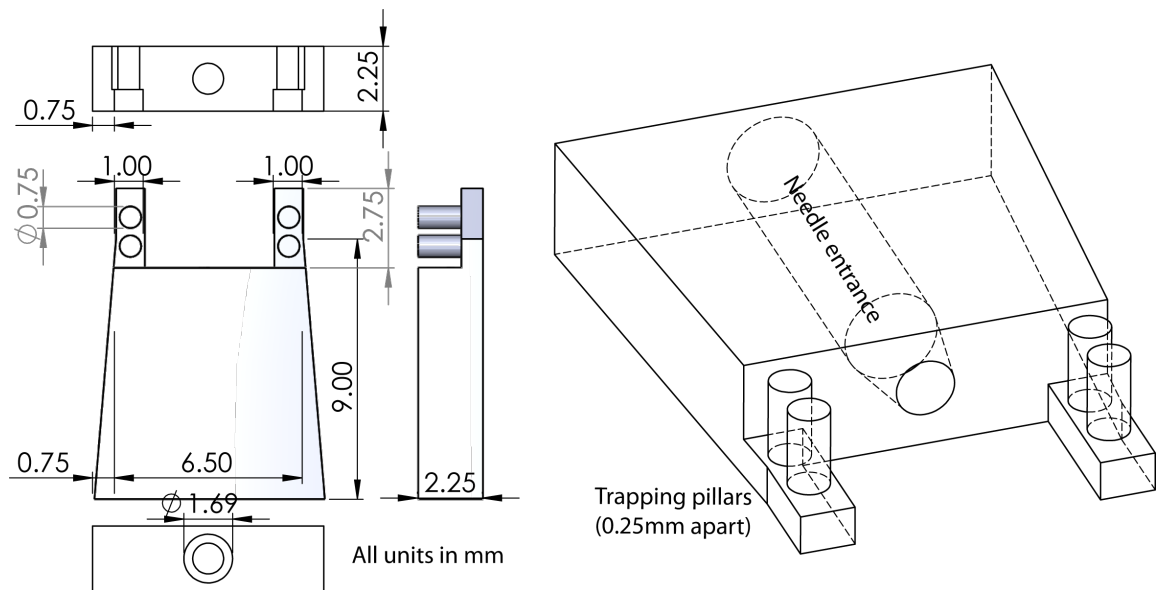


FIGURE 30. CARTRIDGE SOLIDWORKS DESIGN. THIS DESIGN IS PRINTED WITH THE FLASHFORGE HUNTER 3D PRINTER WITH FUN TO DO DEEP BLACK RESIN. ALL VALUES IN THE DRAWING ARE IN MILLIMETER.

## 10.2 Results & discussion

The first result of the final epididymis-on-a-chip device of the ability to access the lumen of the epididymal tubule is visible in Figure 31. However, here the tissue was not submerged in media, but it was hanging in air. Positioning of the needle was not difficult for this experiment, but other later experiments revealed that it is more complicated to access the luminal barrier. The complicated parts include the insertion of the glass needle by hand, since its fragile tip can easily break, enlarging the tip diameter. When the glass-pulled needle breaks during insertion in the cartridge, it is not possible to re-insert a different needle due to debris of the glass remaining in the needle entry. When a glass-needle breaks into a large amount of small glass fragments it can damage the epididymal tubule barrier, which would also result in an inconclusive experiment about barrier strength.

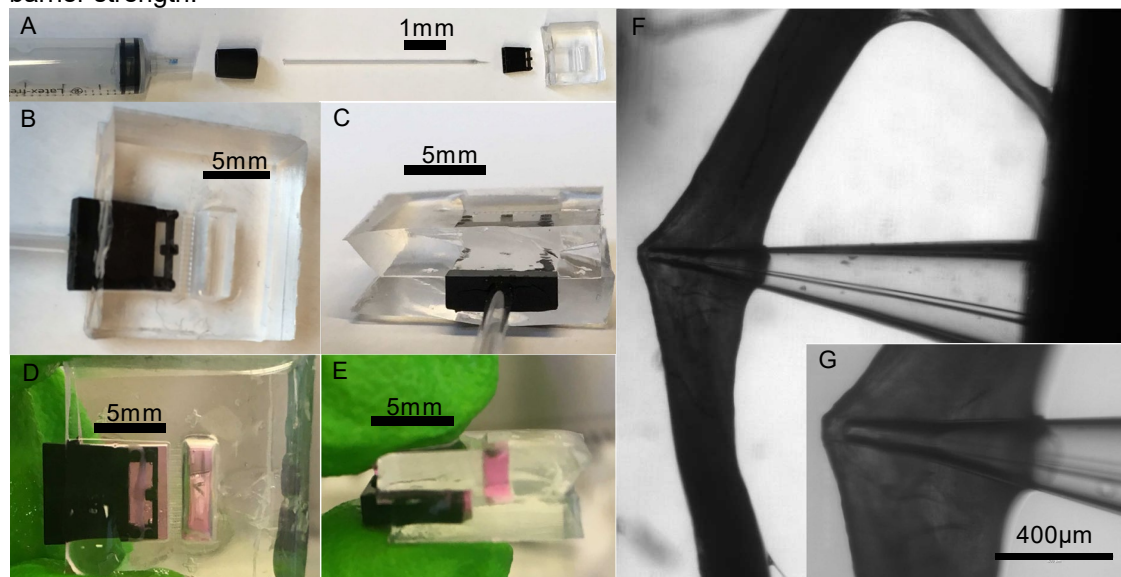


FIGURE 31. PICTURES DEPICTING THE ENTIRE DEVICE. INDIVIDUAL COMPONENTS FOR INJECTING EXOGENOUS SUBSTANCES (A) ALONG WITH DIFFERENT ORIENTATIONS OF THE PDMS HOUSING AFTER INSERTION OF THE 3D-PRINTED CARTRIDGE AND GLASS MICROPIPETTE (B-C), AND LOADING OF EPIDIDYMAL TISSUE (D-E). MICROSCOPIC IMAGE OF A GLASS MICROPIPETTE PROBING THE LUMINAL REGION OF A HUMAN EPIDIDYMAL TUBE (F-G).

Figure 32 depicts the live/dead staining results where the viability of the tissue was tested when cultured on a 3D-printed cartridge versus a PDMS cartridge. Additionally, the culture conditions

were varied, where tissues were cultured with DMEM and 1% pen/strep versus culturing with DMEM, 10% FBS and 1% pen/strep. As a control the tissue was stained also at day 0 and stained at day 0 after killing it by putting it in Bouin's solution for 30 minutes.

An observation of live/dead staining on-chip revealed that tissue around the clamping pillars appeared to be dead. It is unclear what caused this. Hypothesis included that clamping reduces the accessibility of nutrients, contact with 3D printed materials induced apoptosis in the cells, mechanical pressure from the clamping induces apoptosis. On top of that from the barrier penetration experiment it seemed that the spacing between the clamping pillars in the 3D printed cartridge might still be too large. However, there is a deviation between tubule diameters, therefore it could be that different spacing for clamping is required for different epididymal tubules.

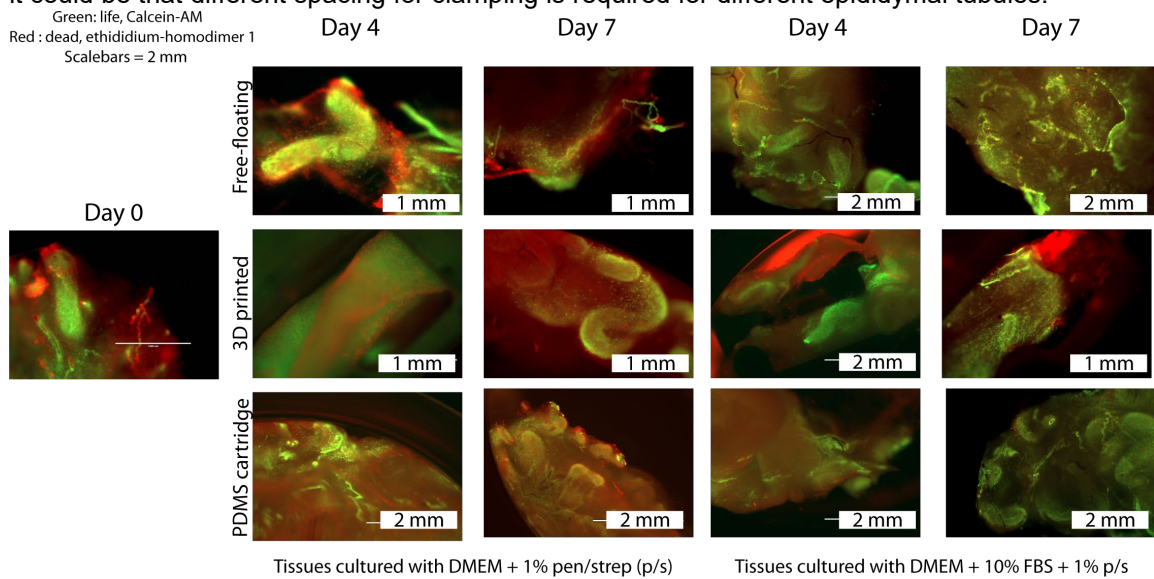


FIGURE 32. LIVE/DEAD STAINING RESULTS COMPARING TWO DIFFERENT CULTURE MEDIA CONDITIONS (WITH AND WITHOUT 10% FBS) AND COMPARING THE VIABILITY DIFFERENCES BETWEEN TISSUE CULTURED IN PRESENCE OF A PDMS CARTRIDGE ON CHIP, 3D-PRINTED CARTRIDGE AND OFF-CHIP IN A WELL PLATE (FREE-FLOATING). AS A NEGATIVE CONTROL TISSUE WAS KILLED IN BOUIN'S SOLUTION FOR 30 MINUTES BEFORE STAINING ON DAY 0. LIVE (GREEN: CALCEIN-AM) DEAD (RED: ETHIDIUM HOMODIMER-1)

The results from Figure 32 also compare the difference in viability between free-floating (epididymal tubule of about 5-10 millimeter floating in 1.5mL medium), on-chip with a 3D printed and an on-chip with a PDMS cartridge (a PDMS block with the size of the 3D printed cartridge to create a similar-sized microchannel culture chamber). The reason for this experiment was to investigate whether the 3D-printed on-chip culturing is inducing toxicity or whether it is the same if it would be cultured by using a PDMS cartridge which is and proven biocompatible. The live/dead staining results were not conclusive. It appeared that the PDMS cartridge condition survival is better for the 3D-printed cartridge condition. The differences could also be a normal deviation in viability between different segments of the patient.

Another trend from this live/dead staining (Figure 32) which is more evident, is the effect of an addition of 10% Fetal bovine serum (FBS) to the culture medium. Fetal bovine serum (FBS) contains proteins that can provide more nutrients to the tissue. It was hypothesized that cell viability might increase due to increased protein content and that these proteins are essential for the viability of certain cell types. From the live dead staining (Figure 32) it can be concluded that tissue seems to be more viable when cultured with 10% FBS, meaning that FBS contains essential proteins for cell survival in the epididymis. This experiment was a first test to optimizing the cell culture conditions, however further extensive tests have to be done to ensure tissue viability. In the recommendation this point is discussed in more detail together with some suggestions on what changes in culture media conditions to test.

Something to consider when evaluating fluorescent data of the epididymal tubules are their auto fluorescent properties. Figure 33 displays images of the auto fluorescent behaviour of a one-day post-surgery epididymis along with the fluorescence filter used, exposure time and light intensity. Auto-fluorescent properties of dead tissue were not explored. The red fluorescent protein (RFP) and green fluorescent protein (GFP) filter were used for the dead and alive staining respectively. The gain and exposure values in the figure of the RFP and the GFP were chosen to be like the values used throughout the live/dead staining in previous experiments.

If auto fluorescence would differ between live and dead tissue it might be a good method to monitor cell viability without immunolabeling the cells. This would be a great real-time assessment tool. If both dead and alive tissue exhibit similar auto fluorescent signal than in previous data, the tissue might be more alive than actually is the case.

When looking back at previous data however, it does seem that the auto fluorescent signal mainly stains areas that are lid up green or red. However, the live/dead staining used stains cell bodies and appear brighter than the auto fluorescent background

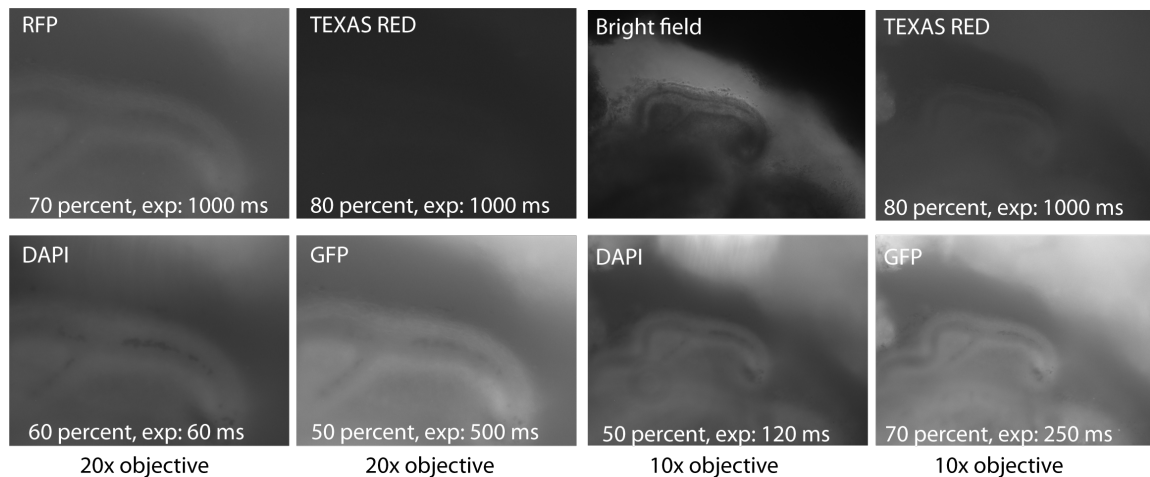


FIGURE 33. AUTOFLUORESCENCE OF EPIDIDYMAL TISSUE WITH DIFFERENT FILTERS. EXPOSURE TIME (EXP) AND LIGHT INTENSITY (PERCENT) IS GIVEN FOR EACH OF THE FILTERS. THE GFP AND RFP FILTERS WERE USED THROUGHOUT THE PROJECT WITH APPROXIMATELY THE SAME EXPOSURE TIME. 10x CORRESPONDS TO THE IMAGES WITH SCALEBARS OF 400µM AND 20x CORRESPONDS TO SCALEBARS OF 200µM

To monitor the strength of the blood epididymis barrier a barrier penetration test was performed where FITC-dextran 40k was injected and diffusion of the tubule was monitored. In Figure 34 the results are depicted from the barrier penetration test where FITC-dextran 40k at a concentration of 10mg/mL was inserted in a glass pulled tip of approximately 25-40 µm. The diffusion of dye was monitored for 25 minutes. Originally the plan was to first insert a cartridge loaded with tubule onto the PDMS but here the tubules were loaded onto the cartridge and the cartridge was submerged in media. A glass needle with a tip diameter of 30µm (program 7 of P-87 glass puller, appendix H) was used.

Friction between the glass entry wall and the needle caused the needle to catch a small part of the epididymal tubule. This resulted in the instantaneous filling of the epididymis, by capillary filling. The fluorescent FITC dye occupied the whole epididymal tubule. However, it was not clear whether the dye was inside of the tubule or also in the lumen. Furthermore, the part of the epididymis that is attached to the glass needle is very thin (+-100µm). It could be that this is an extremely stretched tubule, a piece of interstitial tissue or perhaps a damaged part of a tubule. To make any conclusions medium was put on top of the 3D-printed cartridge with the epididymal tubule that lid up.

Drawing conclusions from the single succeeded time-lapse in Figure 34 is difficult. When critically looking at the pictures it appears that there is a segment in the middle of the tubule where the blood-epididymis-barrier seems to be intact. Over time the intensity next to this border does not seem to increase. From the right side the intensity is growing slowly over time, which after stopping

the experiment, originated from the tip of the glass needle due to diffusion and a minor flow (evaporation of media).

Two other needle injections in the tissue were successful. In Figure 34 these two cases in the two bottom right images are imaged. Luminal access was achieved on-chip but off-chip as shown in the left image(not in PDMS-housing chip), and the needle was freely aimed to puncture the barrier since the needle entry of the 3d-printed cartridge was a few micrometres too small for glass-needle insertion. For the other experiment (right bottom image), it appeared that the tubule did penetrate the barrier and that clamping was achieved, causing the tubule to not light up with fluorescent dye due to capillary forces. Time-lapse imaging was not possible since not enough light could be obtained by the microscope camera, indicating that the camera settings or the camera itself should be changed for this experiment.

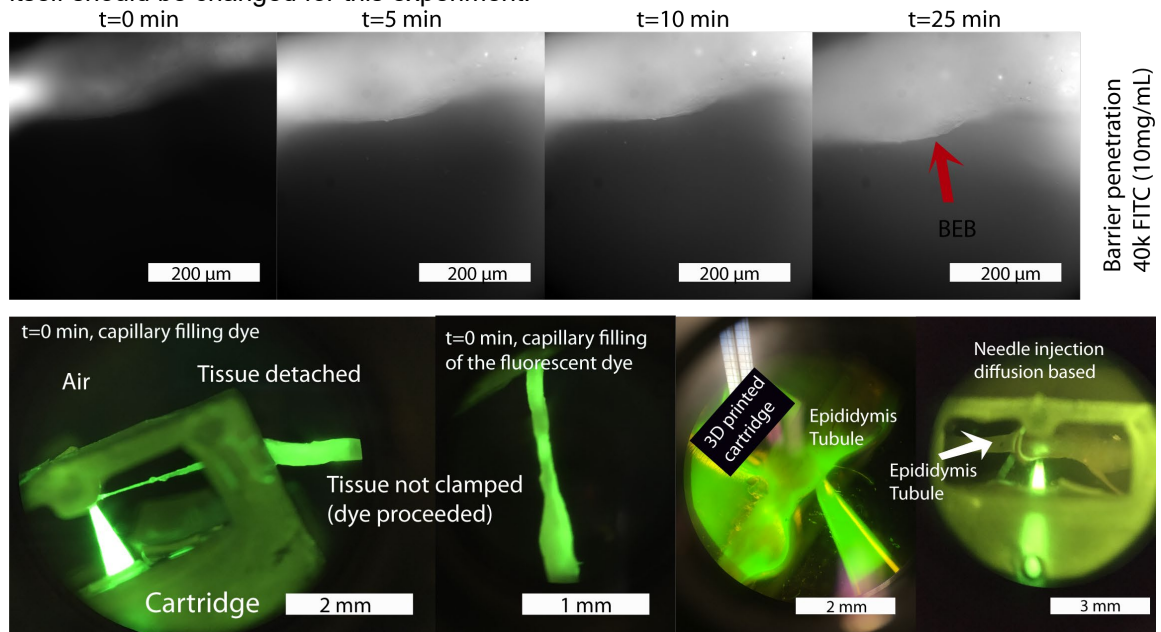


FIGURE 34. THE DIFFUSION OF THE FITC 40k (10MG/ML) IN PBS IS OBSERVED OVER TIME. THE SECOND ROW OF IMAGES DISPLAYS IMAGES OF THE LUMINAL ACCESS SECONDS AFTER INSERTION OF THE GLASS-PULLED NEEDLE. THE TUBULE LID UP THE MOMENT THE NEEDLE WAS INJECTED, WHICH WAS HYPOTHESIZED TO BE DUE TO CAPILLARY FLOW THROUGH THE TUBULE.

# 11 DISCUSSION

Three goals for the design were set to create a platform that can answer the biological questions of how the barrier functions and how does the luminal composition environment change. For the three goals that included culturing of the tubules for 7 days, clamping of the epididymis and luminal access of the epididymis are discussed separately in this chapter.

## 11.1 Objective 1: culturing the epididymis

### 11.1.1 *Tissue quality*

As can also be seen from appendix A, there is a large variance between patient samples in terms of hormonal data and state of the epididymis. Here we did not investigate the impact of the treatment and the different samples on the epididymal barrier. It might appear that the hormonal data can predict the quality of the barrier of the epididymal tubules. Control samples of patients with epididymal tubules that were not affected by hormonal drug treatment might be obtained from patients that undergo vasectomy. Fortunately for this experiment it also seems that the seminiferous tubules are more affected by the pre-surgery medication and for the epididymis it mainly leads to more swollen tubules. [4]

### 11.1.2 *Cell culture media and culturing conditions*

The most basic culture media was used in this research since the tissue is comprised of a mixture of cell types. Different cell types need different nutrients and some metabolites can trigger differentiation of cells or enhance cell division. Here the main goal was to keep the tissue in a viable and physiological state. The most basic cell culture media is DMEM and 1% pen/strep was added to reduce the chance of infection during culturing. Additionally FBS was tested as an extra component to the culture media and cell viability was compared. Addition of 10% FBS to the basic culture media resulted in an enhanced cell viability. In the recommendations suggestions for adapting the cell culturing media are made, which could potentially further enhance tissue viability.

For the culturing of the epididymis throughout the experiments temperatures of 37 °C were used. However, *in vivo* the scrotum temperature is 3 °C lower.[65] In future experiments a separate incubator should be used with a lower set temperature to see whether this has an effect on the epididymal barrier and tissue viability. Another improvement that can be made in terms of physiological conditions is the oxygen percentage in the incubator.

The oxygen percentage in air equals 21% and the culture media thus also becomes 21% in oxygen percentage. Oxygen concentrations of about 1.5% (12-15 mm Hg) were reported for the interstitial tissue in the testicles of rat. [66] Oxygen concentrations in human tissue can be as low as 0.5% up to 12.5% depending on the organ. [67]

### 11.1.3 *Tissue loading, 3D-print toxicity and fungal infections*

The 3D-printed cartridge in the design is not labeled as biocompatible by the supplier and it is not clear whether post-treatment with 405 nm light and heating as described here offers sufficient removal of toxic elements, thereby making the cartridge biocompatible. The attempt to test the toxicity of 3D printed cartridges did not succeed due to a fungal infection.

### 11.1.4 *Autofluorescence and live-dead staining*

Epididymal tissue showed autofluorescence properties. Literature gives suggestions that green (around 470-530nm) might indicate the presence of flavins and blue the presence of nicotinamide-adenine dinucleotide NAD. Flavoproteins and NAD are involved in the protection against reactive oxygen species, which is one of the known functions of the epididymis.[68] Furthermore, cells that are necrotic have a decreased cellular metabolism which in turn increases their autofluorescence

(in particular 488nm). Knowing this might reveal some information about the state of the tissue without doing immunological stainings.[69] Other autofluorescence elements could be red blood cells, collagens and elastins.[70]

### **11.2 Objective 2: Clamping the epididymal lumen**

The luminal environment of the epididymal tubule was required to be sealed from the surrounding medium. This ensures that communication between both microenvironments would occur through the BEB. To achieve this, it was aimed to seal the endings of the epididymal tubule by introducing a structure that could clamp the tubule. Different methods for clamping were tried. (i) The first idea was to seal the endings of the epididymal tubule by wrapping them with a thread. A filament with a diameter of 60 $\mu$ m was used to achieve this but experimentation showed that positioning these threads at the endings of the tubule was difficult. (ii) The second idea included sealing of the lumen by placing the epididymal tubule in a confined chamber and pressing a 3D-printed stick against it, thereby compressing the tubule between the stick and the wall and sealing the lumen. This method of clamping could have worked, however as presented earlier the tissue was placed in a PDMS chip that was closed with a PCR tape. The delamination of this tape caused to redesign the chip. (iii) A third method for clamping was tried that would not require manual positioning of the 3D-printed stick, simplifying the design.

The 3D-printed cartridge that was designed included two sets of two pillars with a spacing of 250 $\mu$ m. Epididymal tubules placed between the pillars, trapped the epididymis and sealed the lumen at the same time. A few of the tissues that were stained with a live/dead assay on chip showed cell death around the clamped area, which could be hypothesized to be caused by the toxicity upon contact with 3D printed material, mechanical stress or lack of nutrients.

The diameter of the epididymal tubule is variable between samples. Epididymal tubules from the corpus region were used for the experiments and when looking back at Figure 16 where the diameter of the tubules are compared, it can be seen that for some samples the tubule diameter is below 300 $\mu$ m. Trapping these tubules between two pillars with a spacing of 250 $\mu$ m will not result in a sealed lumen. Therefore the distance between the pillars should be reduced. The resolution of the 3D printer in the horizontal plane equal 62.5 $\mu$ m, thus a smaller spacing can be achieved although with the current design.

An additional adjustment that could simplify the insertion of the tubule would be to change the two pillars with constant spacing into a variable spacing, starting large (+1mm) at the top and 62.5 $\mu$ m at the bottom (parabola-shaped pillars). This will ensure that tubules with every diameter can be sealed instead of only those with a diameter above 350-400 $\mu$ m.

### **11.3 Objective 3: access the lumen of the epididymal tubules**

The principle of the design is clearly described, but the fabrication and variability upon printing generates some more difficulties. The 3D-printed FTD deep black resin has a recipe that is well defined and printing something multiple times results in the same design almost every time. However, for printing with the clear resin resulted in a large variance in outcome in terms of size and stiffness. This could be due to the printer being out of focus or perhaps the much higher viscosity of the clear resin compared to the FTD deep black plays a role. The glass capillaries were 1.5 millimeter in size with a deviation of about 0.05 millimeter. However, for the black resin the hole was already designed to be 1.6875 millimeter to ensure a good fit of the glass needle.

For the cartridges made out of Formlabs clear resin, a hole size of 1.75 millimeter or even 1.825 millimeter did not always result in the possibility to insert the glass needle. It was thought that the reason for this was the limited ability of cleaning the needle entry. To test this hypothesis a design with openings along the needle guide was created to enhance access of the ethanol for cleaning of the uncured resin. However, this still resulted in cartridges that did not allow the insertion of a glass needle. Therefore a second hypothesis was made that the current 3D-printing settings for

the clear resin lead to overexposure, resulting in the cross-linking of resin that was not patterned to be cross-linked by the design. This could be explained to be caused by scattering of photons. Described more visually this would mean that a line that is 1mm in width would result in a cross-linked structure of 1.2 mm in width.

Accessing the lumen of the epididymal tubule was achieved as well as 25 minute monitoring of the diffusion, which resulted in reduced diffusion of FITC-40k dextran molecules in a specific part of the epididymal tubule wall. Due to a limited amount of time the time-lapse duration was not extended beyond 25 minutes. Originally the sequence of this experiment would be to insert the tubule onto the chip between the trapping pillars, insert the cartridge with tissue in the PDMS housing chip, fill the needle with fluorescent dye, insert the needle in the cartridge and access the lumen. However, here the tissue was first loaded and the needle was partially inserted into the cartridge to have a better control over inserting the needle. At this point the needle that was filled with fluorescent dye caught a piece of the tubule or interstitial fluid and within seconds lid up the whole epididymal tissue. (Figure 34) It was unclear whether capillary forces filled the lumen of the tubule or whether the dye also lid up the outer layer of the epididymal tubule (outside BEB).

In the other permeability experiment shown in Figure 34 (right bottom image) was executed as planned. Injection of the needle did not result in the whole tissue becoming fluorescent, which could indicate that there was no capillary filling, thus the epididymal tubule was sealed by the trapping pillars. However, focusing the camera for capturing the diffusion of the fluorescent dye was difficult and the sensitivity fo the camera to monitor the diffusion was not clear. When trying to improve the focus and slightly moving the chip, the needle broke.

Glass-pulled needles are very fragile, and the tight fit between the glass-pulled needle and the 3D-printed cartridge needle inlet caused high friction and difficulty to insert the needle. However, the difficulty of inserting the needle is different per cartridge which can be explained by the variability in glass diameter (1.44-1.50mm) and the slightly variability in 3D-printed cartridge dimensions estimated at approximately 30 $\mu$ m. Therefore, for future experiments it is recommended to match glass capillary before pulling with a 3D-printed cartridge that allows effortless insertion. This ensures that the glass-pulled needle can easily access the cartridge and reduces the chance of breaking the glass needle during the experiment.

## 12 CONCLUSION

An epididymis-on-a-chip device was designed and fabricated that allowed for culturing of epididymal tubules with maintained cell survival in a microfluidic chip for at least eleven days. Putting the epididymal tubules of 5-10 millimeter in length in a confined microenvironment, where the volume of the tissue chamber was maximally 10 times larger than the tissue volume resulted in an enhanced viability in comparison to the same tubules in a traditional well plate (free-floating condition, 5-10 millimeter tubule floating in 1.5mL medium). Due to the small amount of sample required, a minimum of 100 on-chip experiments can be run from a single epididymis sample up to 600 for a long epididymis.

The best way to create a sealed culture chamber is through having a side entry for the tissue which can be sealed afterwards with a material of choice (preferably biocompatible). Tight sealing of a PDMS culture chamber with another layer of PDMS, involves plasma bonding and heating which is not compatible with living tissue. The same applies for the convenient PDMS-PCR tape bonding, which results in a temporary seal that is easily disrupted/delaminated over time.

Culturing conditions for the whole *ex vivo* human epididymis was not researched in literature. Basic DMEM medium with 1% penicillin/streptomycin still resulted in cell viability after 11 days but the addition of 10% FBS to the media enhanced the viability of the tissue.

3D-printed objects, referred to as cartridges, were designed such that epididymal tubules could be loaded on it and allowed for perpendicular access to the barrier with a needle.

The 3D-printed objects used in cell culture were not officially labeled as biocompatible, leading to a series of experimentation with post-treatment to make them biocompatible. Even after 14 days of heating of the cartridges weight was still lost. However, the major decrease of about 4% in weight occurred over the first 4 days. After that the next 10 days only decreased it by an extra 2%.

Samples were retrieved at irregular time intervals ranging from two samples in one week up to one sample in 6 weeks. Tissue survival after prolonged storage on ice in the fridge at 4 °C in a Styrofoam box was tested by live-dead staining. Epididymal tubules that were stored 21 days in the fridge had similar viability as the samples that were stored for 1 day on ice.

Tissue was found to be variable in terms of epididymal tubule diameter and viability. More samples should be analyzed to predict which values are important for epididymal viability.

Epididymal tissue exhibits autofluorescence properties which is predicted to be caused by collagens. The presence of autofluorescence should be considered when doing immunological imaging.

## 13 RECOMMENDATION

The recommendations can be divided into four different categories. Recommendations for handling of the tissue, for imaging suggestions, design adaptations and future perspective of the device.

### 13.1 Tissue treatment and handling

Epididymal tissue was cultured using basic cell culturing media, however in literature there are multiple more complex media types for culturing primary or immortalized cell lines for the epididymis. It might be a good recommendation to check whether these media types would result in a better viability or regeneration of the tissue barrier on chip. For dissecting the tissue it is recommended to check whether it is easier if the tissue is first cleared of connective tissue by using collagenase (enzymatic reaction). However, the collagen present in the epididymis might also play a role in the regulation of the barrier.

#### 13.1.1 *Culturing the tissue: media type*

Trying to maintain the tissue alive on a chip was not described previously in literature before. Since the tissue was comprised of a large variety of cells it was decided that using basic medium composition was tried first also since here the goal is not necessarily to have the cells divide faster but mainly to maintain the integrity. In literature there are a few examples of single type cell lines cultures. These studies use more complex culture media. Therefore, it would be a good recommendation to try these different cell culture media and analyze the viability to check whether the integrity is increased.

Literature study	Cell type	Dissection	Medium	Culture conditions
Leir <i>et al.</i> [36]	Human primary epididymal epithelial cells	Collagenase	15% FBS, 2 mmol/L L-glutamine, 1µg/mL hydrocortisone, 0.2 U/mL insulin,	
Dubé <i>et al.</i> [22]			DMEM/HAM F12 media, glutamine 2mM, penicillin/streptomycin 50U/mL,	32 °C , 5% CO <sub>2</sub>
Ruan <i>et al.</i> [71]	Immortalized epididymal cell line principal cells		Iscove's modified Dulbecco's medium, 5alpha-di-hydrotestosterone (DHT, 1nm) and 10% FBS	33 °C , 5% CO <sub>2</sub>
Moore <i>et al.</i> [72]	Principal cells human	Treated with 0.05% collagenase type 7 at 37 Degrees in media for 24 hours	RPMI1640, 10% FBS, 1mM sodium pyruvate, 100 nM insulin, 200mM hydrocortisone, 200 mM testosterone, 1 l'm dihydrotestosterone, 5 l'g transferrin/mL, 1 l'g retinol/mL	n/a

A research by Reyes-moreno *et al.* have shown that conditioned epididymal culture medium that contained pyruvate (main component), inositol, glycerol and lactate and not carnitine had improved motility of bovine spermatozoa. [73] The experiments resulted in fungal infections two times, which indicates that perhaps a higher concentration of penicillin/streptomycin should be used, or different methods of sterilizing chips should be used. Perhaps UV treating the whole chip after conditioning instead of only doing ethanol treatment would work better. Sterilizing the 3D-printed cartridges is hypothesized to be the most important to investigate, since previous experiments with seminiferous tubules from the same patient origin were not prone to getting these fungal infections.

### 13.1.2 *Dissecting the tissue: collagenase*

Tissue autofluorescence was thought to be a contribution by the autofluorescence properties of collagen which is contained in the extracellular matrix. Enzymatic removal of the collagen by using collagenase will result in less fluorescence. However, it should also be kept in mind that it might have a function in barrier strength. Another advantage of enzymatic removal of collagen could be that the extraction of tubules from the epididymis is easier since this convoluted network of tubules are tightly interconnected through collagen.

### 13.2 *Imaging of the epididymis*

Imaging of the epididymis after culturing on chip can also provide information on barrier tightness and integrity. Recommendations for different immunological markers are given. Furthermore, it is suggested to investigate the matter of autofluorescence and what information can be extracted from this. The autofluorescent properties of the tissue make fluorescent imaging more difficult due to a background signal. This background signal can be reduced by imaging with a confocal microscope. Another option is to use clearing protocols (for example the iDisko visikol clearing protocol). These clearing protocols remove the main scattering components of the tissue (for instance fat tissue) but keeps the integrity. This would allow to image the composition of the barrier and the location of the chosen immunolabels.

#### 13.2.1 *Immunolabeling the epididymis*

Literature has shown staining of epididymal principal cells using a variety of antibodies. [36] Table 3 displays a list of possible antibodies that can be used to stain specific cell types. Nuclei can be stained with propidium iodide. Cytokeratin8 can be stained to locate epithelial cells and not vimentin (VIM) for mesenchymal cells.

TABLE 3. CELL TYPES AND CELLULAR COMPONENTS AND WHAT SPECIFIC PROTEINS THEY EXPRESS

Cell types	Immunological marker	Source
Clear cells (10%)	V-ATPase, P2X4, A2B	[10]
Principal cells (65%)	CFTR, Claudin1 (minor staining), A2B,	[3]
Basal Cells (18%)	COX1, Claudin1, A2B	[27, 74]
Tight junctions	ZO-1, Clatherin, A2B, Claudin3 and Claudin4, CLDN1, CLDN2, CLDN3 (not for corpus), CLDN4, CLDN7, CLDN8, TJP1 (caput), Occludin	[29, 74]
Adherins	CDH1, CDH2	[3]
Desmosomes	DSP	[3]

### 13.3 *Adapting the design*

Adapting the design might be a next step to optimize the ease for needle access. Regarding the 3D printed cartridge it is recommended to look further into the toxicity of the cartridges. COMSOL simulations can be performed to enhance and validate nutrient supply and secretion product concentrations. An interesting adaptation to the design would be the implementation of transendothelial resistance measurements (TEER). Furthermore, in physiological conditions the spermatozoa flow through the epididymis and it would be interesting to analyze the effect of flow through the epididymis on the barrier function.

#### 13.3.1 *COMSOL simulations*

Absorption and consumption of for instance glucose can be experimentally determined by using fluorescently labeled glucose. This would allow to more precisely determine the consumption rate and metabolism of a typical 5-10 millimeter epididymal tubule and see whether the consumption rate is linear (constant consumption) or dependent on concentration. This data can then be used to run more accurate and physiological resembling COMSOL simulations. An old report by Setchell and Waites of glucose and oxygen uptake in the epididymis and testis of the ram can be used for modelling.[75]

### 13.3.2 *Permeability and inflammation induction*

Appendix E shows an experimental setup for permeability and inflammation induction by TNF-alpha. These experiments were planned but due to limitation in time, tissue and number of microfluidic chips were not performed. A glass-syringe connector was designed (appendix M) but due to air leakage was not the optimal setup for aspirating fluids. Another option to investigate might be to look at glass capillaries that can be connected to a standard syringe. An option here could be a filling glass needle from Hilgenberg GMBH.

### 13.3.3 *TEER measurements*

The current design can be adapted to allow measurements with TEER. The current setup available in the group is a Millicell ERS-2. This setup is designed for use with well plates. However, it can also be used here by putting one part in the chip culture reservoir and to adapt the glass-syringe connector (appendix M) such to have a side opening with a small reservoir where the other end of the electrode could be inserted into. In Figure 35 an image of the setup that was imagined is displayed, but requires require optimization since the fittings were leaking.



FIGURE 35. TRIAL FOR CREATING TEER MEASUREMENTS.

Another option would be to adapt the measurement electrodes for the TEER. Electrodes can be created and inserted into the pulled glass needles. Silver wire can be used for this, the outer layer can be sanded off with sandpaper. Agarose could be put between glass-syringe connector opening and the bath to allow electron transport but to prevent degradation of the electrodes.

### 13.3.4 *Adapt the design to allow perfuse the epididymis at physiological rates*

Spermatozoa transit time through human epididymis takes 2 to 6 days. Assuming a total length of 3-5 meters, taking 300µm the average diameter of the luminal space across the epididymis leads to a total epididymal volume ( $2.12e-7 - 3.53e-7$  m<sup>3</sup>). The resulting estimation of the flow velocity in the epididymis by the spermatozoa equals 1.47e-9 to 7.36e-9 m<sup>3</sup>/hour, which in more clear units ranges from 1.47 to 7.36 µL per hour. [27]

Here the idea would be to perfuse the epididymis by putting two needles in the tissue and connecting this to a syringe pump to perfuse it at a rate of about 5 µL per hour. This would have shown how the luminal fluid gets changed by the epididymis and substances could be exposed and presented to the epididymis externally and the outflow could be monitored to check whether these have crossed the barrier and in what amounts.

### 13.4 *Effect of administration to microplastics / testosterone / androgens etc.*

While the tissue can be exposed to endocrine disruptors or fluorescent molecules from the inside through injection with a glass needle, it can also be done in a reversed manner. Molecules can be presented to the epididymis from the surrounding area. This would be a manner more like how blood vessels supply the epididymis with nutrients and expose it to potential endocrine disruptors.

The current chip design would allow for these types of measurements, but it is expected to be more difficult to assess whether for instance a fluorescent dye is inside the epididymal lumen or around the epididymal tissue. Therefore, it could be a good idea for these types of experiments to adapt the design.

Figure 36 depicts two example concept drawings that were imagined to be able to do these types of measurements. This chip that can be made of 3D-printed material and closed by sliding a glass slide on top, which would also be an additional benefit for imaging. Multiple epididymal tubules can be loaded in parallel and clamped by triangular clamping structures. Since this method allows to perfuse fluid on two sides, it is possible to generate gradients, and to monitor the effect of different concentrations. However, this method does make accessing of the barrier more difficult. Needle access might be able to implement by making the height of the culture area larger than the perfusion area, thereby generating enough space for creating a needle access perpendicular to the perfusion area. However, this would still only allow barrier access in the outer epididymal tubules. The second design idea is more simplistic and would allow to perfuse media across the epididymis.

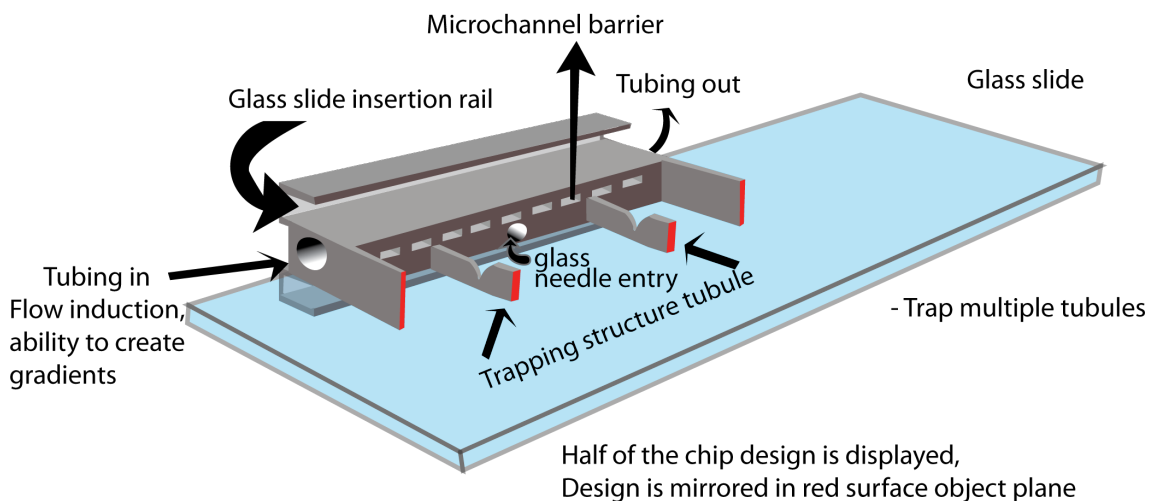


FIGURE 36. CONCEPT DRAWING FOR TRAPPING THE EPIDIDYMIS AND BARRIER ACCESS AND CREATING A GRADIENT OF CHEMICALS.

Since the tissue used in these experiments has been treated with androgenic drugs before surgery it might also be a good idea to assess the platform to simulate the changes that occur upon exposure to these drugs. One could imagine that as a normal situation control epididymal tissue could be obtained from a vasectomy.

### 13.5 Future perspective of the device

The future perspective of the epididymis-on-a-chip can have more impact than just providing more information on how the blood-epididymis-barrier barrier is maintained and how spermatozoa become fertility active after passing the epididymal tube. The first application with impact could be the implementation in the process of drug development.

#### 13.5.1 Drug development in reproductive toxicology

Introducing a new drug to the market, which requires federal drug agency (FDA) approval is very expensive and is getting more expensive every year, mainly due to new regulations. The whole process can take up to 10 years, and the cost increased exponentially costing 179 million dollars in 1970 to 2.5 billion dollars in 2014. because of the entire procedure of clinical tests that need to be done.[76, 77]The first step to bringing a newly discovered drug to the market requires experimental evidence which is usually validated by testing for efficacy on immortalized cancer lines in Petri-dishes. If successful, the drugs can be tested on animals. This step is time-consuming because of the administrative requirements before experiments can start and the duration of the

experiment itself. A drug that has proven to be effective in animals does not guarantee that it will get to the market. In total, studies concluded that the likelihood of getting FDA approved ranges between 12 and 19 per cent.[78-80] Humans and animals are intrinsically different which we described in this thesis during the introduction. This could also lead to high failure rates for drugs on reproductive toxicology. The epididymis-on-a-chip device might help to decrease these failure rates since they utilize human tissue and allow experimentation with a relatively short time for assessment. 0.6% of the male infertility is caused by endocrine disruptors and thus the platform can also be used to screen for new endocrine disruptors or chemicals that are thought to have such an effect.[32]

#### 13.5.2 ***Seminiferous-tubules-on-a-chip***

The seminiferous tubules, in which the spermatozoa develop from germ cells in the process called spermatogenesis is also an interesting organ to study. Just like the epididymis this part of the male reproductive system is comprised of convoluted tubules. Glass needles can be pulled to a size of about 0.5 $\mu\text{m}$ , thus putting these tubules with a diameter of between 100-150 $\mu\text{m}$  should still be possible although the spacing for clamping might need to be adjusted as well as the position where the needle enters the chip.

## 14 ACKNOWLEDGEMENTS

First of all I would like to thank my daily supervisor Bastien Venzac who provided me with guidance in the project both in terms of scientific discussions and learning new skills both practical, in writing and in presenting scientific work. Next, I would like to thank Séverine Le Gac for her detailed look at my data, feedback and scientific discussions. I would also like to thank the staff of the AMBER and DBE group for their fruitful discussions and support.

Our collaborators in Münsters, Stefan Schlatt and Swati Sharma helped to discuss and educate about the biological aspect and provided epididymal tissue throughout the project through their contact with the clinical hospitals.

For the glass pulling I would like to thank the BSS group for lending their P-87 group leader, Armagan Kocer for letting me use their P-1000 pipette and educating me on patch clamping and electrical measurements on single cells. Myrthe Bruning of the physics of fluids group for the fruitful discussions on glass pulling and designing glass pulling programs for the p-87 puller.

Mert Kaya also has been helpful throughout the project for exploring other options for producing the epididymis-on-a-chip, scientific discussions and the use of a laser cutter.

Lastly, I would like to thank Tom Kamperman for helping me out on how to use the glass puller and the basic principles and Michelle Koerselman for providing me with TNF-alpha.

## 15 REFERENCES

1. Agarwal, A., et al., *A unique view on male infertility around the globe*. Reproductive biology and endocrinology, 2015. **13**(1): p. 37.
2. Jungwirth, A., et al., *European Association of Urology guidelines on Male Infertility: the 2012 update*. European urology, 2012. **62**(2): p. 324-332.
3. Robaire, B. and B.T. Hinton, *Knobil and Neill's physiology of reproduction*, ed. T.M. Plant and A.J. Zeleznik. 2015: Academic Press.
4. Sullivan, R., et al., *Revisiting structure/functions of the human epididymis*. Andrology, 2019.
5. Shum, W.W., et al., *Establishment of cell-cell cross talk in the epididymis: control of luminal acidification*. Journal of andrology, 2011. **32**(6): p. 576-586.
6. Mital, P., B.T. Hinton, and J.M. Dufour, *The blood-testis and blood-epididymis barriers are more than just their tight junctions*. Biology of reproduction, 2011. **84**(5): p. 851-858.
7. Stanton, P.G. *Regulation of the blood-testis barrier*. in *Seminars in cell & developmental biology*. 2016. Elsevier.
8. Paxon, S., *Male reproductive system: spermatogenesis*. University of Leeds: Histology Guide Faculty of Biological sciences.
9. J. Gordon Betts, K.A.Y., James A. Wise, Eddie Johnson, Brandon Poe, Dean H. Kruse, Oksana Korol, Jody E. Johnson, Mark Womble, Peter DeSaix, *The*, in *Anatomy and Physiology*. 2013, OpenStax, Houston, Texas.
10. Gregory, M. and D.G. Cyr, *The blood-epididymis barrier and inflammation*. Spermatogenesis, 2014. **4**(2): p. e979619.
11. Bernabò, N., et al., *The maturation of murine spermatozoa membranes within the epididymis, a computational biology perspective*. Systems biology in reproductive medicine, 2016. **62**(5): p. 299-308.
12. Sullivan, R. and C. Belleannée, *Cell biology of the epididymis*. 2018.
13. Domeniconi, R.F., et al., *Is the epididymis a series of organs placed side by side?* Biology of reproduction, 2016. **95**(1): p. 10, 1-8.
14. Syntin, P., et al., *Characterization and identification of proteins secreted in the various regions of the adult boar epididymis*. Biology of reproduction, 1996. **55**(5): p. 956-974.
15. Browne, J.A., et al., *Expression profiles of human epididymis epithelial cells reveal the functional diversity of caput, corpus and cauda regions*. MHR: Basic science of reproductive medicine, 2015. **22**(2): p. 69-82.
16. Da Silva, N., et al., *Proteomic analysis of V-ATPase-rich cells harvested from the kidney and epididymis by fluorescence-activated cell sorting*. American Journal of Physiology-Cell Physiology, 2010. **298**(6): p. C1326-C1342.
17. Turner, T.T., *De Graaf's Thread: The Human Epididymis*. Journal of Andrology, 2008. **29**(3): p. 237-250.
18. Da Silva, N. and C.R. Barton, *Macrophages and dendritic cells in the post-testicular environment*. Cell and tissue research, 2016. **363**(1): p. 97-104.
19. Sullivan, R. and F. Saez, *Epididymosomes, prostasomes, and liposomes: their roles in mammalian male reproductive physiology*. Reproduction, 2013. **146**(1): p. R21-R35.
20. Belleannée, C., V. Thimon, and R. Sullivan, *Region-specific gene expression in the epididymis*. Cell and tissue research, 2012. **349**(3): p. 717-731.
21. Förster, C., *Tight junctions and the modulation of barrier function in disease*. Histochemistry and cell biology, 2008. **130**(1): p. 55-70.
22. Dubé, É., et al., *Assessing the role of claudins in maintaining the integrity of epididymal tight junctions using novel human epididymal cell lines*. Biology of reproduction, 2010. **82**(6): p. 1119-1128.
23. De Grava Kempinas, W. and G.R. Klinefelter, *Interpreting histopathology in the epididymis*. Spermatogenesis, 2014. **4**(2): p. e979114.

24. Jones, R., *To store or mature spermatozoa? The primary role of the epididymis*. International journal of andrology, 1999. **22**(2): p. 57-67.
25. Da Silva, N. and T.B. Smith, *Exploring the role of mononuclear phagocytes in the epididymis*. Asian journal of andrology, 2015. **17**(4): p. 591.
26. Beagley, K., et al., *Immune responses in the epididymis: implications for immunocontraception*. JOURNAL OF REPRODUCTION AND FERTILITY-SUPPLEMENT-, 1998: p. 235-245.
27. Cornwall, G.A., *New insights into epididymal biology and function*. Human Reproduction Update, 2009. **15**(2): p. 213-227.
28. Sullivan, R. and R. Mieuxset, *The human epididymis: its function in sperm maturation*. Human reproduction update, 2016. **22**(5): p. 574-587.
29. Breton, S., A. Nair, and M. Battistone, *Epithelial dynamics in the epididymis: role in the maturation, protection, and storage of spermatozoa*. Andrology, 2019.
30. Massart, A., et al., *Genetic causes of spermatogenic failure*. Asian journal of andrology, 2012. **14**(1): p. 40.
31. Poongothai, J., T. Gopenath, and S. Manonayaki, *Genetics of human male infertility*. Singapore Med J, 2009. **50**(4): p. 336-347.
32. Rowe, P.J., et al., *WHO manual for the standardized investigation and diagnosis of the infertile male*. 2000: Cambridge University Press.
33. Fermi, B., S.T. Coyne, and K.P. Coyne, *Clinical trials in a dish: A perspective on the coming revolution in drug development*. SLAS DISCOVERY: Advancing Life Sciences R&D, 2018. **23**(8): p. 765-776.
34. Huh, D., et al., *Microengineered physiological biomimicry: organs-on-chips*. Lab on a Chip, 2012. **12**(12): p. 2156-2164.
35. Bhatia, S.N. and D.E. Ingber, *Microfluidic organs-on-chips*. Nature biotechnology, 2014. **32**(8): p. 760.
36. Leir, S.-H., et al., *Characterization of primary cultures of adult human epididymis epithelial cells*. Fertility and sterility, 2015. **103**(3): p. 647-654. e1.
37. Mehling, M. and S. Tay, *Microfluidic cell culture*. Current opinion in Biotechnology, 2014. **25**: p. 95-102.
38. Sackmann, E.K., A.L. Fulton, and D.J. Beebe, *The present and future role of microfluidics in biomedical research*. Nature, 2014. **507**(7491): p. 181-189.
39. Nguyen, H.-T., et al., *Low-Cost, Accessible Fabrication Methods for Microfluidics Research in Low-Resource Settings*. Micromachines, 2018. **9**(9): p. 461.
40. Park, S.E., A. Georgescu, and D. Huh, *Organoids-on-a-chip*. Science, 2019. **364**(6444): p. 960-965.
41. Srinivasan, B., et al., *TEER measurement techniques for in vitro barrier model systems*. Journal of laboratory automation, 2015. **20**(2): p. 107-126.
42. Kimura, H., Y. Sakai, and T. Fujii, *Organ/body-on-a-chip based on microfluidic technology for drug discovery*. Drug metabolism and pharmacokinetics, 2018. **33**(1): p. 43-48.
43. Halldorsson, S., et al., *Advantages and challenges of microfluidic cell culture in polydimethylsiloxane devices*. Biosensors and Bioelectronics, 2015. **63**: p. 218-231.
44. Kieninger, J., et al., *Microsensor systems for cell metabolism—from 2D culture to organ-on-chip*. Lab on a Chip, 2018. **18**(9): p. 1274-1291.
45. Du, G., Q. Fang, and J.M. den Toonder, *Microfluidics for cell-based high throughput screening platforms—A review*. Analytica chimica acta, 2016. **903**: p. 36-50.
46. Sosa-Hernández, J.E., et al., *Organs-on-a-chip module: a review from the development and applications perspective*. Micromachines, 2018. **9**(10): p. 536.
47. Komeya, M., et al., *Long-term ex vivo maintenance of testis tissues producing fertile sperm in a microfluidic device*. Scientific reports, 2016. **6**: p. 21472.
48. Komeya, M., T. Sato, and T. Ogawa, *In vitro spermatogenesis: A century-long research journey, still half way around*. Reproductive medicine and biology, 2018. **17**(4): p. 407-420.
49. Cullen, A.T. and A.D. Price, *Fabrication of 3D conjugated polymer structures via vat polymerization additive manufacturing*. Smart Materials and Structures, 2019. **28**(10): p. 104007.

50. Kadry, H., et al., *Digital light processing (DLP) 3D-printing technology and photoreactive polymers in fabrication of modified-release tablets*. European Journal of Pharmaceutical Sciences, 2019. **135**: p. 60-67.
51. Serra, M., et al., *A simple and low-cost chip bonding solution for high pressure, high temperature and biological applications*. Lab on a Chip, 2017. **17**(4): p. 629-634.
52. Wei, C., et al., *Easy-to-operate fabrication of tapered glass capillaries for microdroplet generation*. J. Micromech. Microeng, 2019. **29**(037001): p. 9pp.
53. Purves, R., *The mechanics of pulling a glass micropipette*. Biophysical journal, 1980. **29**(3): p. 523.
54. Stockslager, M.A., et al., *Optical method for automated measurement of glass micropipette tip geometry*. Precision engineering, 2016. **46**: p. 88-95.
55. Tamizhanban, R., K. Sreejith, and G. Jayanth, *An automated pipette puller for fabrication of glass micropipettes*. Review of Scientific Instruments, 2014. **85**(5): p. 055105.
56. Instruments, S., *P-1000 Flaming/Brown tm Micropipette Puller System, operation manual rev. 3.05B (20170927)*.
57. Schneider, F., et al., *Comparison of enzymatic digestion and mechanical dissociation of human testicular tissues*. Fertility and sterility, 2015. **104**(2): p. 302-311. e3.
58. Schneider, F., et al., *Testicular functions and clinical characterization of patients with gender dysphoria (GD) undergoing sex reassignment surgery (SRS)*. The journal of sexual medicine, 2015. **12**(11): p. 2190-2200.
59. Matoso, A., et al., *Spectrum of findings in orchiectomy specimens of persons undergoing gender confirmation surgery*. Human pathology, 2018. **76**: p. 91-99.
60. BioGnost. *Bouin's solution*  
14-10-2019]; Available from: <http://www.novogen.com.tr/wp-content/uploads/2016/09/Bouins-solution-IFU.pdf>.
61. Smyrek, I. and E. Stelzer, *Quantitative three-dimensional evaluation of immunofluorescence staining for large whole mount spheroids with light sheet microscopy*. Biomedical optics express, 2017. **8**(2): p. 484-499.
62. Johnson, S. and P. Rabinovitch, *Ex vivo imaging of excised tissue using vital dyes and confocal microscopy*. Current protocols in cytometry, 2012. **61**(1): p. 9.39. 1-9.39. 18.
63. Matryba, P., L. Kaczmarek, and J. Gołab, *Advances in Ex Situ Tissue Optical Clearing*. Laser & Photonics Reviews, 2019. **13**(8): p. 1800292.
64. Bastien Venzac, Y.L., Ivan Ferrante, Pablo Vargas, Ayako Yamada, Rémi Courson, Marine Verhulsel, Laurent Malaquin, Stephanie Descroix and Jean-Louis Viovy, *Sliding walls: a new paradigm for fluidic actuation and protocols implementation in microfluidics*. Microsystems and Nanoengineering, 2019.
65. Jones, R.E. and K.H. Lopez, *Human reproductive biology*. 2013: Academic Press.
66. Reyes, J.G., et al., *The hypoxic testicle: physiology and pathophysiology*. Oxidative Medicine and Cellular Longevity, 2012. **2012**.
67. Oomen, P.E., M.D. Skolimowski, and E. Verpoorte, *Implementing oxygen control in chip-based cell and tissue culture systems*. Lab on a chip, 2016. **16**(18): p. 3394-3414.
68. Surre, J., et al., *Strong increase in the autofluorescence of cells signals struggle for survival*. Scientific reports, 2018. **8**(1): p. 12088.
69. Hennings, L., et al., *Dead or alive? Autofluorescence distinguishes heat-fixed from viable cells*. International Journal of Hyperthermia, 2009. **25**(5): p. 355-363.
70. Monici, M., *Cell and tissue autofluorescence research and diagnostic applications*. Biotechnology annual review, 2005. **11**: p. 227-256.
71. Ruan, Y.C., et al., *ATP secretion in the male reproductive tract: essential role of CFTR*. The Journal of physiology, 2012. **590**(17): p. 4209-4222.
72. Moore, H.D., et al., *The culture of human epididymal epithelium and in vitro maturation of epididymal spermatozoa*. Fertility and sterility, 1992. **58**(4): p. 776-783.
73. REYES-MORENO, C., et al., *Addition of specific metabolites to bovine epididymal cell culture medium enhances survival and motility of cryopreserved sperm*. Journal of andrology, 2000. **21**(6): p. 876-886.

74. Shum, W.W.C., et al., *Transepithelial projections from basal cells are luminal sensors in pseudostratified epithelia*. Cell, 2008. **135**(6): p. 1108-1117.
75. Setchell, B. and G. Waites, *Blood flow and the uptake of glucose and oxygen in the testis and epididymis of the ram*. The Journal of physiology, 1964. **171**(3): p. 411.
76. Hay, M., et al., *Clinical development success rates for investigational drugs*. Nature biotechnology, 2014. **32**(1): p. 40.
77. DiMasi, J.A., H.G. Grabowski, and R.W. Hansen, *Innovation in the pharmaceutical industry: new estimates of R&D costs*. Journal of health economics, 2016. **47**: p. 20-33.
78. Mohs, R.C. and N.H. Greig, *Drug discovery and development: Role of basic biological research*. Alzheimer's & Dementia: Translational Research & Clinical Interventions, 2017. **3**(4): p. 651-657.
79. Dowden, H. and J. Munro, *Trends in clinical success rates and therapeutic focus*. Nat. Rev. Drug Discov, 2019. **18**: p. 495-496.
80. Takebe, T., R. Imai, and S. Ono, *The Current Status of Drug Discovery and Development as Originated in United States Academia: The Influence of Industrial and Academic Collaboration on Drug Discovery and Development*. Clinical and translational science, 2018. **11**(6): p. 597-606.
81. Griep, L., et al., *BBB on chip: microfluidic platform to mechanically and biochemically modulate blood-brain barrier function*. Biomedical microdevices, 2013. **15**(1): p. 145-150.
82. Förster, C., et al., *Differential effects of hydrocortisone and TNF $\alpha$  on tight junction proteins in an in vitro model of the human blood-brain barrier*. The Journal of physiology, 2008. **586**(7): p. 1937-1949.
83. McLean, I.C., et al., *Powering ex vivo tissue models in microfluidic systems*. Lab on a Chip, 2018. **18**(10): p. 1399-1410.

## 16 APPENDIX

### Appendix A. Recipe for Flashforge Hunter printer using the DLPrint software

Resin	Base time (s)	Attach time (s)	Gradual time layers	Light intensity	Layer height ( $\mu\text{m}$ )	Post-treatment
FunToDo deep black resin	2	20	8	85	25	1 hour 405 nm 24 hours 120 °C
Formlabs Clear resin	6.5	25	8	110	25	1 hour 405 nm 24 hours 120 °C

### Appendix B. Operating the glass puller

1. Make sure the power is on and open the hood of the glass puller
2. Look at Figure 12 for locating the different parts
3. Depress the spring stop near the pulley of the puller cable to release the puller bar on both sides
4. Loosen glass clamping knobs
5. For the P-1000 model
  - a. Insert glass capillary onto a v-groove on one of the puller bars and tighten the clamping knob (not too tight to prevent breaking of the glass)
  - b. Pull the puller bar towards the middle and guide the glass capillary through the box filament
  - c. Press both puller bars as close as possible towards each other (leaning against the filament box) and tighten the other clamping knob as well
6. For P-87 model
  - a. Insert glass capillary in the v-groove in the puller on either of the puller bars
  - b. Tighten the clamping knob (not too tight to prevent breaking of the glass)
  - c. Guide the glass capillary in the v-groove of the other puller bar
7. Select the correct program on the glass puller
8. Close the lid and press pull or start
9. For a more detailed description also on how to program one can visit the extensive manual: [sutter.com/manuals/P-1000\\_OpMan.pdf](http://sutter.com/manuals/P-1000_OpMan.pdf)

### Appendix C. Loading epididymal tubules onto a chip and precondition of the chip

1. Prepare the culture media, containing DMEM, 1% penicillin/streptomycin and 10% FBS
2. Rinse the chip twice with ethanol and twice with PBS
3. Put the PDMS chips in culture media at least 24 hours in the incubator at 37°C, 5% CO<sub>2</sub>, before culturing to ensure higher viability. Possible explanations for this phenomenon might be that the oxygen concentration in the media is higher, the PDMS absorbs culture media molecules, or lastly, the conditioning could remove final oligomers in the PDMS that have not been cured that are toxic.
4. Put the tissue on the cartridge using tweezers and guide it into the PDMS chip.

### Appendix D. Time-lapse setup and fluorescence microscopy setup

Setting up the time lapse for the fluorescence microscopy (Olympus IX51, top-lamp) setup involves three steps, initialize Putty which is the program that can turn the fluorescence lamp on and off by keyboard commands. To automate the time-lapse setup, an automatic and programmable keyboard presser was installed and a script was generated. The time-lapse itself is run through the hokawa imaging software (version 2.1) that controls the microscope camera (C11440-424, S/N: 000025, orca flash 4).

1. Initialize Putty

- a. Session, toggle serial, speed 9600
- b. Type in COM3 (device manager, ports, check which port belongs to the serial bus of the fluorescent lamp)
- c. Go to the terminal, put both settings to force on
- d. Go to serial, set flow control to none
- e. Open Putty

EXTRA INFO: inserting the command 'mm r' in putty opens the lamp and 'zz r' shuts it down

2. Program autosofted keyboard presser v1.9
  - a. Click on edit script
  - b. Load the following lines
    - i. Press {SPACE} for 0 seconds Pause 100 Milliseconds
    - ii. Press m for 0 seconds Pause 100 Milliseconds
    - iii. Press m for 0 seconds Pause 100 Milliseconds
    - iv. Press {SPACE} for 0 seconds Pause 100 Milliseconds
    - v. Press r for 0 seconds Pause 100 Milliseconds
    - vi. Press {ENTER} for 0 seconds Pause 3000 Milliseconds
    - vii. Press z for 0 seconds Pause 100 Milliseconds
    - viii. Press z for 0 seconds Pause 100 Milliseconds
    - ix. Press {SPACE} for 0 seconds Pause 100 Milliseconds
    - x. Press r for 0 seconds Pause 100 Milliseconds
    - xi. Press {ENTER} for 0 seconds Pause 116350 Milliseconds
  - c. Set start/stop hotkey to a hotkey (eg. F1)
  - d. Set play hotkey to a hotkey (eg. F2)
  - e. Troubleshooting
    - i. If you want to change the timing at which a picture is made, make sure to match the total pause time in the script with the time in the hokawa time lapse setup settings
3. Running the time lapse
  - a. Start hokawa imaging software and make sure that the camera is on
  - b. Start the script (press F2), wait for approximately 1.5-2 seconds and then start the time lapse in Hokawa imaging
  - c. Click back to the Putty input screen as fast as possible to make sure that the next line of text ('zz r') is inserted in time.
  - d. Troubleshooting
    - i. If you find that the lamp does not turn off after making the picture, make sure that you really clicked back to the putty input screen. If you cannot match the speed at which to do this, one can increase the time the lamp is open.
    - ii. Make sure to restart and reload the script every time before running the time lapse. When stopping the autosofted keyboard presser during an action it will continue again where it left off. It will crash when you try to stop it during a long wait step, in that case force quit the program.

### Appendix E. Extended permeability experiment

The aim of this experiment is to see the monitor the barrier integrity. TNF-alpha (Recombinant TNF-alpha, 200 µg/mL, Biolegend 570102, 21-03-2018. 2µg/mL) is used in combination with a fluorescein isothiocyanate-dextran (FITC), FD40S-100MG, MW08261, 19996TH) to monitor the diffusion through the barrier. As a control FITC without TNF-alpha is used. For this experiment, we choose to use TNF-alpha together with FITC-40k, since their molecular weights and therefore diffusion coefficients are similar. TNF-alpha is a bit lighter, indicating that it will reach the barrier earlier. The mixtures of FITC and FITC with TNF-alpha will be inserted in the barrier by using a glass needle.

Different diameters are tested for the glass needle (10,20,75µm) to see which one does not rupture the barrier and delivers enough of the mixture to the barrier.

Literature was studied to estimate physiological levels of TNF-alpha, which showed that for exposing tissue to TNF-alpha under flow conditions can be done by using 1µL/min, 1ng/mL TNF-alpha.[81] For static conditions, as is the case in our experiments TNF-alpha can be used at a concentration of 17.4 ng/mL [82] These studies also showed that TNF-alpha after mechanical stimulation decreased TEER by 10 fold inflow conditions and 2 fold in static conditions. [81, 82]

A syringe was connected to a glass needle to aspirate the different test conditions from Table 4. Afterwards, the needle was injected, and time-lapse recordings were made using autosofted keyboard presser to turn light on and of every 10 minutes, monitoring diffusion and prevent bleaching of fluorophores

TABLE 4. TESTED CONDITIONS FOR BARRIER PENETRATION EXPERIMENT FD4-100MG, FLUORESCEIN ISOTHIOCYANATE-DEXTRAN 098K1230 // FD40S-100MG, FLUORESCEIN ISOTHIOCYANATE-DEXTRAN SIGMA ALDRICH MW08261, 19996TH // FD250S-100MG, FLUORESCEIN ISOTHIOCYANATE-DEXTRAN SIGMA ALDRICH MW08121, 04809KH // 10 MG/ML FITC // 20 NG/ML & 200NG/ML TNF ALPHA

400k FITC-dextran + TNF-alpha	
40k FITC + TNF-alpha	10 mg/mL   20 ng/mL or 200 ng/mL
4k FITC + TNF-alpha	
400k FITC-dextran	
40k FITC-dextran	
4k FITC-dextran	
Control: 400k FITC-dextran (no tissue)	
Control: 40k FITC-dextran (no tissue)	
Control: 4k FITC-dextran (no tissue)	

**Appendix F. USB camera, backlight and chip holder**

Dissecting the tissue in the laminar flow hood proved to be difficult, since it was hard to distinguish when an epididymal tubule was extracted or when it was just interstitial tissue. To offer a solution for this problem and to enhance the positioning of tissue in a microfluidic chip a portable USB microscope (Dino-Lite ProX AM4013MTL long working distance) was purchased together with a dedicated holder (MS35B) for the USB microscope (see Figure 37). The USB camera could be steered through DinoLite imaging software both on PC and tablet. Inside the lab the USB camera was connected to the tablet by using an on the go connector (USB OTG hub). Software was used to take images and videos.

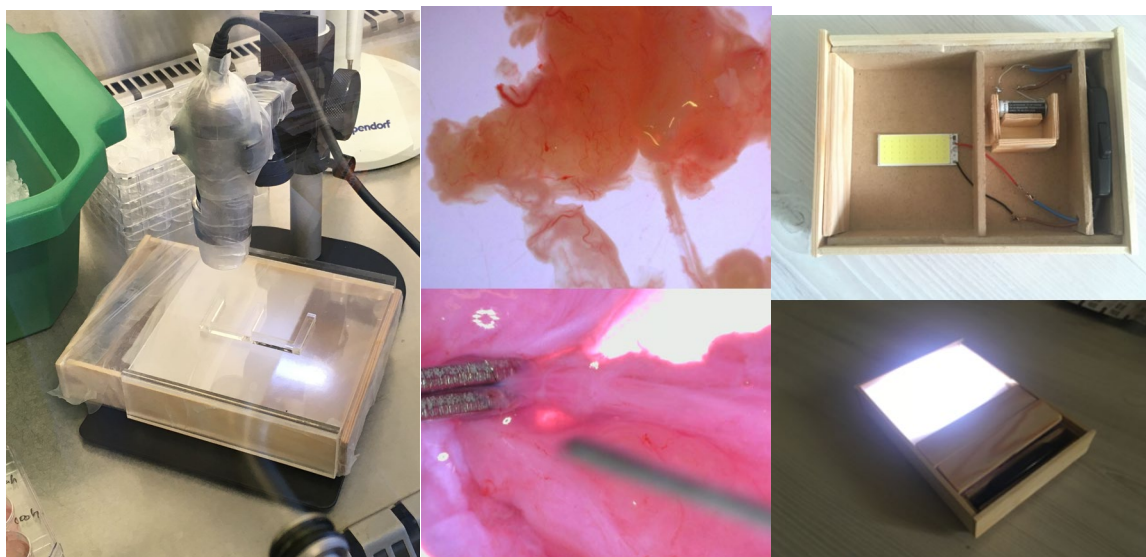


FIGURE 37. USB CAMERA SETUP AND IN THE TWO RIGHT IMAGES DISSECTION IS SHOWN. IN THE BOTTOM RIGHT IMAGE THE TWEEZERS HAVE A WIDTH OF 2MM FOR REFERENCE OF SCALE AND THE TOP RIGHT IMAGE THE SIZE FROM LEFT TO RIGHT IS ABOUT 20 MILLIMETER. THIS BACKLIGHT WAS MADE FROM A 12V POWERED COB LED, 12 VOLT BATTERY, A POWER SWITCH AND SOLDERED ELECTRICAL CONNECTIONS. A DIFFUSER PLATE EXTRACTED FROM A FLAT SCREEN PROVIDED AN EQUALLY DISTRIBUTED LIGHT AND THE HOUSING WAS MADE OF WOOD. FOR USAGE DURING CELL CULTURING AND DISSECTING IN THE LAF CABINET THE BACKLIGHT WAS WRAPPED IN PARAFILM

The internal light of the USB microscope, caused high reflections, reducing the visibility of the chip. Therefore, an inhouse backlight was created, using a 12V battery, 12V powered COB LED, power switch and electrical wires which were soldered to create a functional backlight. The housing was made of wooden panels and an LCD panel that was cut to size. The final resulting device is shown in Figure 37

From early experiments it was found that inserting the needle while imaging under the microscope induces a challenge. Monitoring the insertion of the needle through the microscope was impossible. The gentle force required to insert the needle causes movement of the chip out of the monitoring area. To resolve this issue a sample stage was built from Plexiglass. This object was designed in Solidworks, saved as a dxf file and laser cut. Also a chip holder was created for the microscope, both resulting holders are displayed in Figure 37.

**Appendix G. 3D printing, post-treatment and biocompatibility**

Since these resins are not officially biocompatible the effect of post-treatment protocols was investigated. It was hypothesized that after printing, the parts still contained biologically toxic components for the cells, like polymer chains that are not cross linked and photo-initiator. By heating the chips afterwards, it was predicted that the weight of the 3D-printed part would decrease, indicating the evaporation of toxic components.

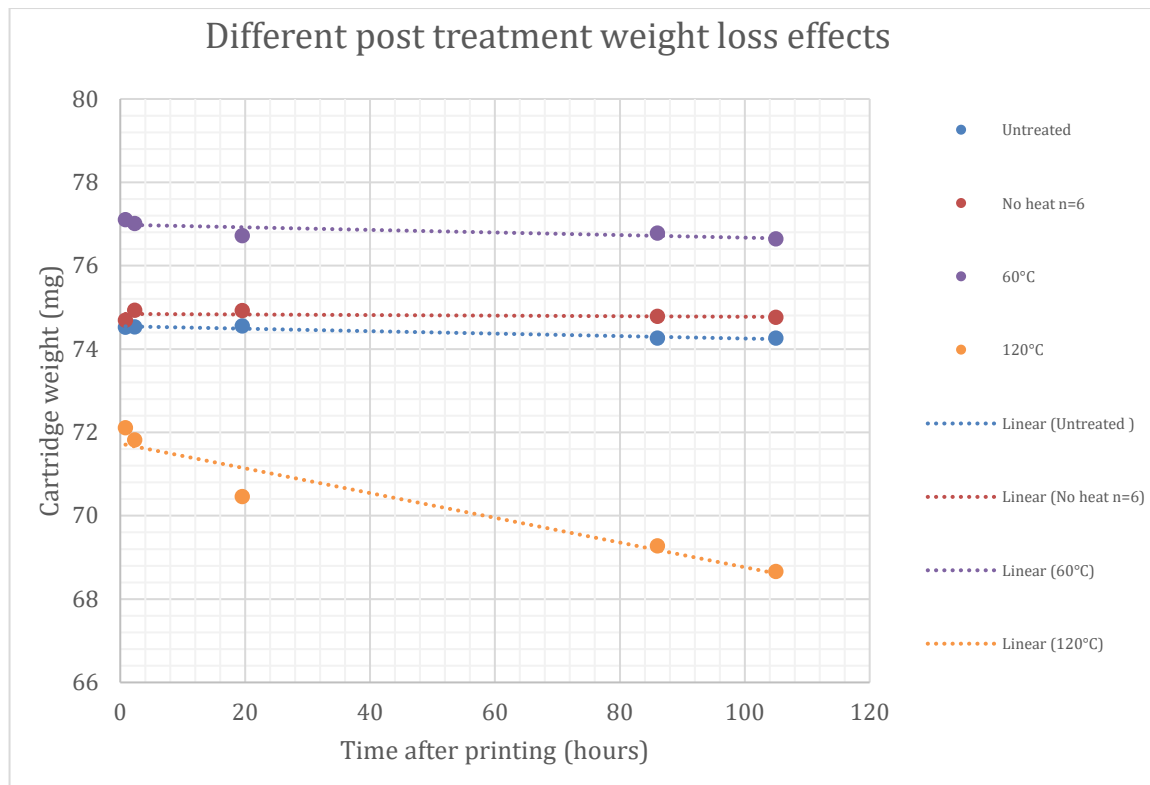


FIGURE 38. DIFFERENT CONDITIONS OF POST TREATMENT WERE TESTED AND COMBINATIONS OF THE FOLLOWING TWO CONDITIONS WERE TESTED I) ONE SIDED VS. TWO SIDED UV POST-TREATMENT II) ROOM TEMPERATURE VS. 60 °C VS. 120 °C.

Post-treatment steps included 405nm wavelength light treatment where one side or two sides of the printed objects can be treated during 15 minutes per side. The second post-treatment step includes heat treatment, comparing room temperature, 60 degrees Celsius and 120 degrees Celsius. Figure 38 depicts the results where these conditions of post treatment are tested against each other. Statistical significance differences did not occur based on heat treatment after one versus two-sided UV treatment. Post-treatment of room temperature showed a decrease in 0.3%

(+/- 0.2% STD) and 60 Degrees Celsius 0.55% (+/- 0.2% STD) and at 120 Degrees Celsius 4.8% (+/- 0.2% STD).

Figure 39 displays an extended experiment of post-treatment with heat at 120 °C, where the weight loss after up to 22 days are described. Seven cartridges with clear resin were measured at once and eleven black cartridges were measured at once.

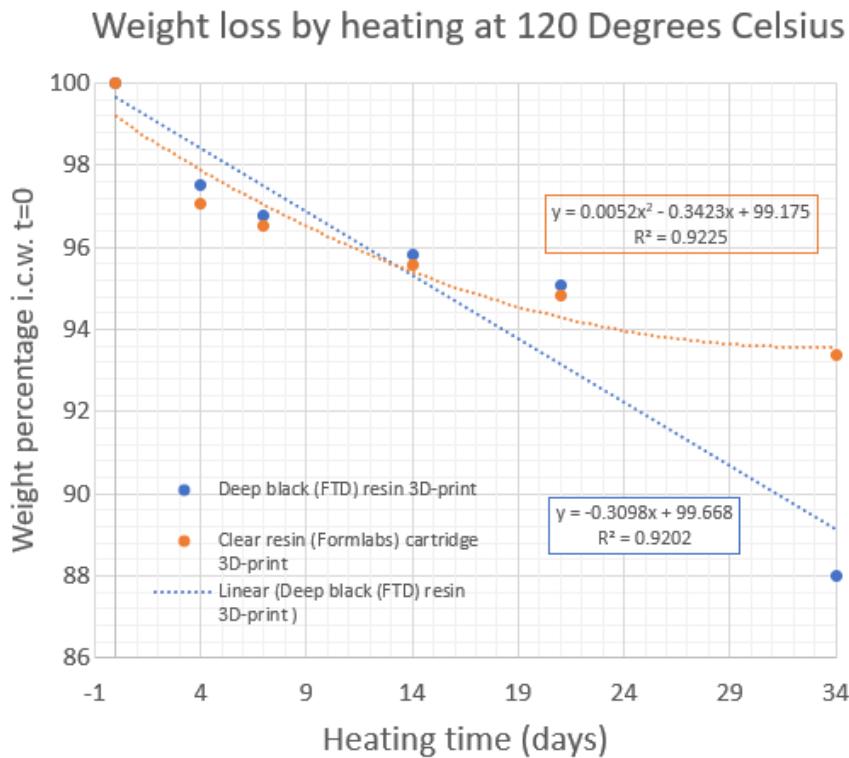


FIGURE 39. WEIGHT LOSS OF TWO TYPES OF 3D PRINTED MATERIAL (CLEAR FORMLABS & DEEP BLACK FTD) BY POST-TREATMENT ON A HOT-PLATE AT A TEMPERATURE OF 120 °C.

**Appendix H. P-87 Sutter Instruments glass puller recipes**

TABLE 5. RAMP TEST ON THE P-87 PIPETTE RESULTED IN A VALUE OF 358. THE FIRST SIX STEPS WERE EQUAL FOR ALL PROGRAMS AND THE LAST STEP IN THE CYCLE WAS ADAPTED. FIRST SIX STEPS: [HEAT: 360/350/335/325/325/300, PULL: 0/0/0/0/0/0, VELOCITY: 50/40/30/30/20/20, TIME: 200/200/200/200/200/200] RAMP TEST: 353+2 (N=3). PRESSURE IS SET TO 601 FOR ALL PROGRAMS. D IS THE DIAMETER OF THE GLASS CAPILLARY AFTER PULLING AND D\_LEFT AND D\_RIGHT REFER TO THE GLASS NEEDLE OBTAINED FROM THE LEFT PULLER BAR AND THE RIGHT PULLER BAR RESPECTIVELY.

Program	Heat	Pull	Vel	Time	D left ± 1STD (n=3)	D right ± 1STD (n=3)	D ± 1STD (n=6)	Shape
1	300	0	35	0	4.0±0.2 (n=2)	3.7±0.3	3.8±0.3 (n=5)	
2	310	0	35	0	4.5±0.5	6.3±0.9	5.4±1.1	
3	310	20	35	200	18.7±7.5	22.9±7.6 (n=2)	20.4±7.8 (n=5)	
4	320	0	35	0	3.7±0.5	3.3±0.7	3.5±0.6	Very pointy and long
5	310	0	15	0	8.4±6.5	8.7±4.9	8.5±5.7	
6	310	40	20	200	28.8±18 (n=2)	27.7±13.2	28.1±15.3	
7	320	20	35	200	8.1±0.9	9 (n=1)	8.3±0.9 (n=5)	
8	320	0	15	0	4.3±0.2	4.5±0.1	4.4±0.2	

9	320	40	35	200	14.4±6	14.7±6.2	14.6±6.1	Quite long
					5.2±0.7 (n=2)	3.8±0.3 (n=2)	4.5±0.9 (n=4)	

**Appendix I. P-87 Sutter Instruments glass puller recipes**

TABLE 6. PROGRAM SETTINGS ON THE P-1000 PIPETTE PULLER. THE GLASS PIPETTES HAD A VALUE OF 491 IN THE RAMP TEST.

Program	Heat	Pull	Velocity	Delay (if >1 l is time)	Pressure	Tip diameter (n=2)
1	530/530/530/530	0/0/0/0	25/25/25/25	1/1/1/1	290	15 µm
2	505/505/505	0/0/0	25/25/25	1/1/1	500	16 µm
3	505/505/505	0/0/0	25/25/25	1/1/1	290	3-4 µm
4	500/500/500	0/0/0	25/25/25	1/1/1	290	16 µm
5	500/495/490/485	0/0/0/0	15/20/20/20	1/1/1/1	290	30 µm
6	500/495/490	0/0/0	25/25/25	200/200/200	290	25 µm
7	500/495	10/0	25/0	200/400	290	12 µm
8	493	50	30	200	290	42 µm
9	495/490/490	10/0/0	55/0/30	50/50/200	290	15 µm
10	495/490/490	0/10/15	5/0/15	25/50/200	290	20 µm
11	491/485/485 /491/485	0/10/15 /0/10	15/15/15 /15/15	200/200/200 /200/200	290	100µm

**Appendix J. Table indicating the age of the patients undergoing sex reassignment surgery, body height, weight and the corresponding hormonal data.**

		A	B	C	D	E	F
<b>OP DAY</b>		7-mrt-19	7-5-2019	30-apr-19	7-5-2019	14-5-2019	4-6-2019
<b>Year of Birth</b>				1982	1968	1996	1993
<b>AGE</b>		55yrs	29yrs	37yrs	51yrs	23yrs	26yrs
<b>TESTIS WEIGHT (g)</b>	with capsule	9.56	7.75	9.11	6.15	8.02	7.58
	wo capsule			7.45	4.22	6.09	6
<b>HEIGHT (cm)</b>		180	175	190	176	176	172
<b>BODY WEIGHT (kg)</b>		88	105	86	80	60	62
<b>Hormonal Data</b>	Normal range						
<b>LH</b>	2-10 U/l			<std	0.8	5.1	1.9
<b>FSH</b>	1-7 U/l			0.3	5	3.8	1.1
<b>Testosterone</b>	>12 nmol/l	0.6	10	1.1	1.2	11.9	1.9
<b>SHBG</b>	nmol/l			48	35	33	88
<b>Free Testosterone</b>	pmol/l			16	21	240	17
<b>Östradiol</b>	pmol/l			684	<std	69	<std
<b>DHT</b>	nmol/l			0.14	<std	0.41	0.27
<b>PROLAKTIN</b>	<500 mU/l			871	1942	365	2315

		<b>G</b>	<b>H</b>	<b>I</b>	<b>J</b>
<b>OP DAY</b>		5-6-2019	11-6-2019	18-6-2019	25-06-2019
<b>Year of Birth</b>		1982	1978	1979	1993
<b>AGE</b>		37yrs	41yrs	40yrs	26yrs
<b>TESTIS WEIGHT (g)</b>	with capsule	6.14	10.04	14.73	5.07
	wo capsule	4.41	6.53	12.14	3.65
<b>HEIGHT (cm)</b>		178	172	181	166
<b>BODY WEIGHT (kg)</b>		100	84	107	58
<b>Hormonal Data</b>	Normal range				
<b>LH</b>	2-10 U/l	0.1	4.6	5.6	<std
<b>FSH</b>	1-7 U/l	1.7	15.1	7.3	0.1
<b>Testosterone</b>	>12 nmol/l	0.8	1.4	8.9	0.8
<b>SHBG</b>	nmol/l	42	57	34	51
<b>Free Testosterone</b>	pmol/l	12	18	171	11
<b>Östradiol</b>	pmol/l	<std	40	101	180
<b>DHT</b>	nmol/l	0.2	0.09	0.64	
<b>PROLAKTIN</b>	<500 mU/l	1110	1269	1093	767

### Appendix K. COMSOL Multiphysics simulations microchannel barrier

The microchannels in the barrier have dimensions with a height of 50µm and a width of 125µm. This significantly reduces the flow into the culture chamber. However, the transport of fluid through this microchannels is not solely dependent on diffusion, but also on convection. To determine whether the inflow of fluid generates a shear stresses that could be harmful to the tissue a simulation of the flow is needed.

To run a flow simulation in COMSOL Multiphysics the user must determine the appropriate geometry, mesh size (into how many voxels will the design be cut), materials, the location of the in- and outlets, fluid properties, fluid physics and boundary conditions. Before describing the simulation and its results, the individual decisions that were required to predetermine and initialize the simulation model are discussed and substantiated in subsections.

#### Geometry

The geometry can be imported from a SOLIDWORKS file (AUTOCAD FILE). The geometry resembling the tissue was inserted inside of COMSOL Multiphysics. Essentially shapes were drawn into the culture chamber and extruded from the total design, creating a defect (the tissue) in the culture chamber. This method assumes that the object projecting the presence of a tissue behaves as an object with rigid walls. One can imagine that for a testis tissue it would have absorbing and compressible properties, however this is a more complex operation to simulate.

#### Mesh size and mesh size optimization

For a simulation the mesh size must be optimized, which means finding the right balance between computation time and accuracy of the result. A low mesh size (large voxels and thus calculation) will result in a quick computation but will yield an inaccurate result. The higher the mesh size, meaning smaller voxels, the more detailed and precise the flow is simulated but the higher the computation time. A balance must be determined between the mesh size, computation time and the obtained results. A good indication is to see with what factor the results change in terms of flow upon increasing the mesh size. A large difference (magnitudes) suggests that the element size

should be refined, while a small change (a few percentage) in the outcome suggests that the optimum between results and computation time is reached.

### Materials

The material of the fluid is chosen as water since it has properties that are close to culture media, which is the substance that is aimed to be used during experiments on this chip.

### Fluid flow: properties and assumptions

It was assumed that the fluid flowing through the system had the properties of water at a temperature of 293.15 Kelvin (room temperature). For the simulation of fluid flow, it is important to know the physical behaviour regime a system operates at. This can be determined by calculating the Reynolds number, which is a dimensionless ratio over inertial forces to viscous forces. A flow can be laminar or turbulent. Reynolds numbers below 2000 are considered laminar, between 2000-3000 there is a transition area and above 3000 the flow is considered turbulent. Typically, smaller features in microfluidic devices have higher Reynolds numbers and therefore the smallest element in the system were used to determine the Reynolds number. The smallest feature in the system are the microchannels (see figure K1) with a height of 50 $\mu\text{m}$ , a width of 125 $\mu\text{m}$  and a depth of 250 $\mu\text{m}$ . At a flow of 100 $\mu\text{L}/\text{hour}$  this results in a Reynolds number of 0.32, which is in the laminar regime. Two inlets were chosen, dividing the chosen flow of 100 $\mu\text{L}/\text{hour}$  into two inlets with a flow of 50 $\mu\text{L}/\text{hour}$  and a set entrance length of 1 meter. The outlet was set at a pressure of 0 Pa, which resembles an atmospheric pressure. Furthermore the backflow was suppressed at the outlet. Since there is no change in concentration or flow over time in the simulation, a stationary laminar flow was chosen in terms of physics. When calculating the Mach number inside of the microchannels, a value of 3e-6 was obtained, which indicates that the fluid is incompressible.

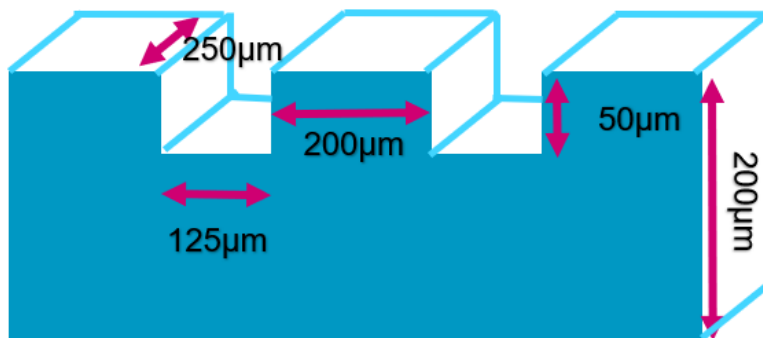


**Figure K1.** Dimensions of the microchannel barrier

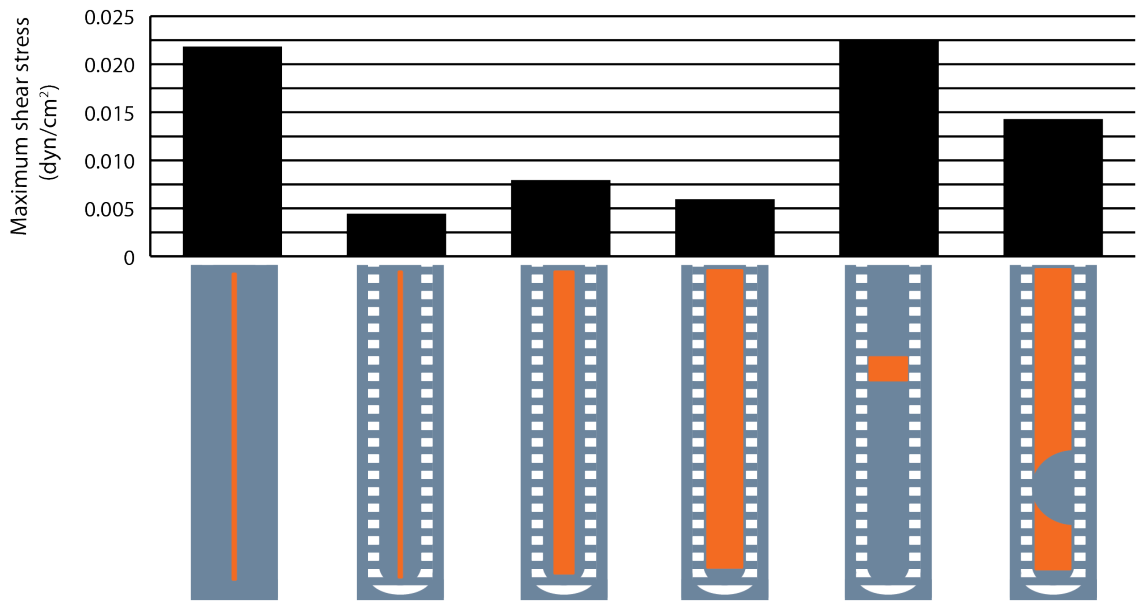
### Running the simulation

From the previous section it can be summarized that for this research a simulation was done under stationary conditions while introducing a laminar incompressible flow of water at 100 $\mu\text{L}/\text{hour}$  into the chip with no-slip boundary conditions and without backflow at a temperature of 293.15 Kelvin. The configurations of the tissue simulated inside the culture chamber were changed according to relevant observations made during the first real experiments with a prototype of the chip. In this section the observations and the obtained results are discussed. To compare the obtained values of maximum shear stress, the statement of McLean *et al.* [83] was used, which states that non-endothelial tissues are subjected to shear stresses up to 0.1 dyn/cm<sup>2</sup>, and they typically become permeable at 2.5 dyn/cm<sup>2</sup>.

For the simulations several configurations of the tissue were recreated. These configurations of the tissue were based on observations of the first few tests with a prototype of the chip. The culture chamber would sometimes be filled and sometimes only partially. To reflect the observations of a low, medium or large amount of tissue in the culture chamber, the tissue was simulated as block of tissue that has the length (4.5mm) of the culture chamber and a percentage of the width (0.8mm). These widths were 0.1, 0.4 and 0.7 mm respectively. Other observations included the presence of a cylindrical defect. In this case the whole culture chamber would be filled with tissue, except for one approximately cylindrical area. In COMSOL these cylindrical shaped defects were

simulated with a radius of 0.2, 0.4 and 0.8mm at different positions along the culture chamber. Lastly, observations showed that the culture chamber would sometimes be only filled at a specific range along the culture chamber. This was simulated by changing the starting location (along the culture chamber) and the end location of the simulated tissue. Figure 2 shows the results for simulated maximum shear stress for the simulated different widths, and the simulations that gave the highest value for the maximum shear stress for the other simulations. Also, the effect of the maximum shear stress was investigated when simulating the tissue without the microchannel barrier.

Maximum shear stress on simulated tissue blocks in COMSOL MULTIPHYSICS



Pillars	✗	✓	✓	✓	✓	✓
Width tissue [mm]	0.1	0.1	0.4	0.7	0.7	0.7
Length tissue [mm]	4.5	4.5	4.5	4.5	0.5	4.5
Starting position [mm]	0	0	0	0	2	0
Cylindrical defect	✗	✗	✗	✗	✗	✓ r=0.8mm

Figure K2. This figure shows the combined results from the COMSOL MULTIPHYSICS simulations. For each simulation the maximum shear stress was determined.

```

c=1481; %[m/s] sound in water speed
w=125e-6;
h=50e-6;
rho=1000; %[kg/m^3]
mu=1e-3; %[Pa*s] OR [kg/(m*s)]
flow=(100*1e-9)/(3600); % uL/hour to m3/s
[Re, Ma]=ReynoldsMach(c,w,h,rho,mu,flow)

% Smallest pores (50mu height, 130mu width)
% 100uL/hour -> Re 0.3
% Ma -> 2.9e-6

% Tissue channel (200mu height, 800mu width)
% 100 uL/hour -> Re 0.06
% Ma -> 1.2e-7
    
```

Figure K3. MATLAB CODE FOR Reynolds number calculations & Mach number

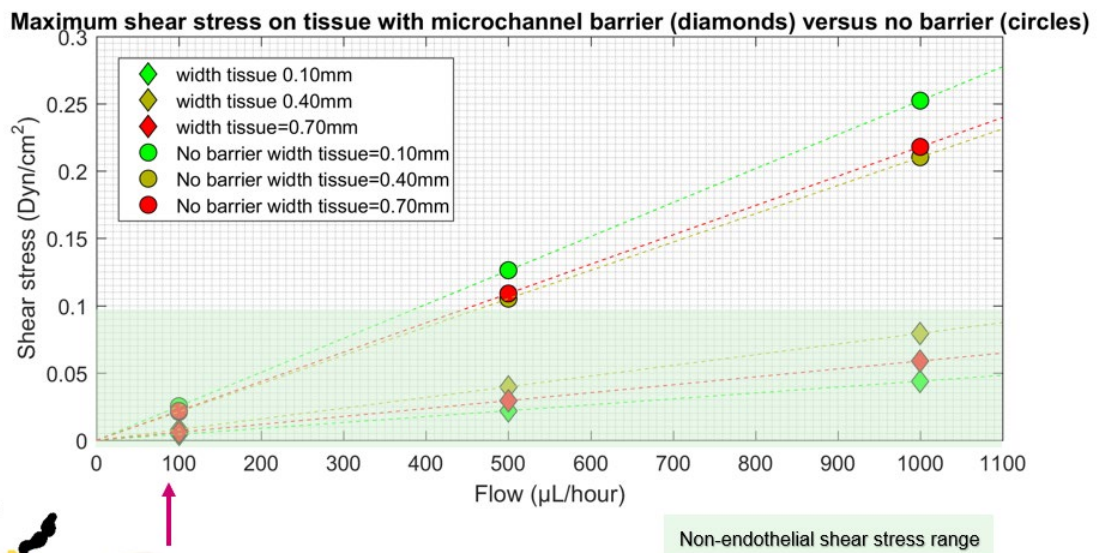
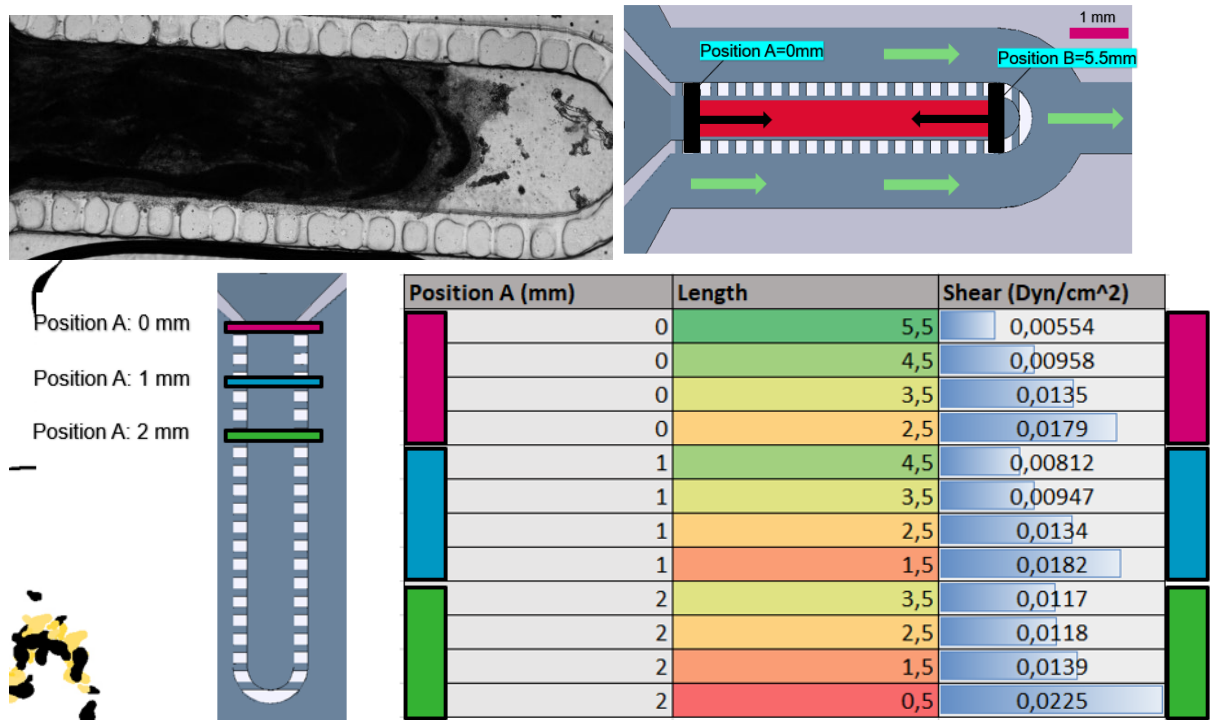
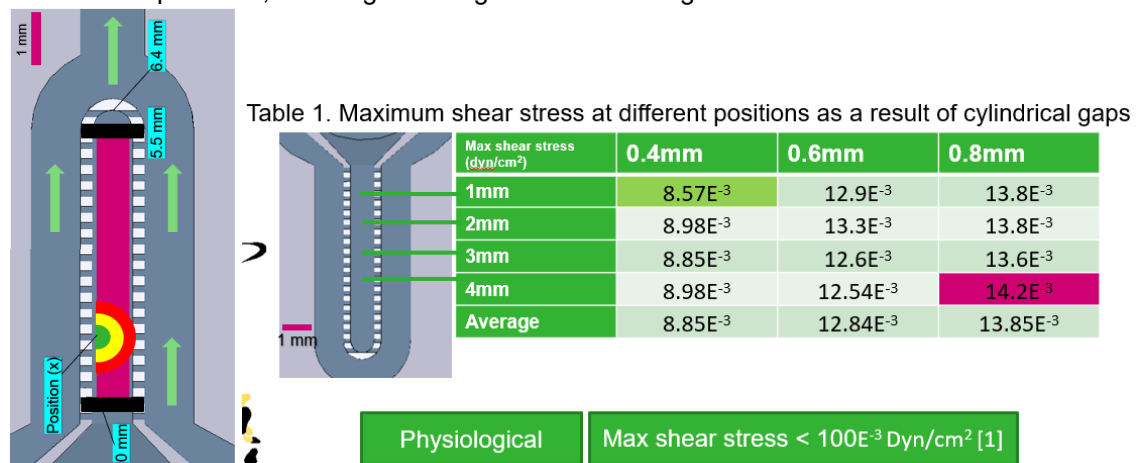


Figure K4. Shows the proportional increase in maximum shear stress simulated with the increase of the flow.



**Figure K5.** A) Shows an image of an observation of the filling of the tissue in a real live experiment on which the simulations were based. B) Principle of the simulations, position A and B are changed, creating a large set of different simulations for different lengths and locations of the tissue in the chip. C) Results from the simulation. Three different starting positions were compared along with different end positions, resulting in a range of different lengths of tissue as well.



**Figure K6.** A) Design of the chip, showing an example of the dimensions and the sizes of different cylindrical defects in different colours. (green=0.4mm, yellow=0.6mm, red=0.8mm) B) This table shows the maximum shear stress simulated as a result of the different cylindrical defect radius size and the position of the defect along the culture chamber. The lowest value is depicted in green and the highest maximum shear stress is depicted in purple.

### Appendix L. PCR tape detachment

During the experiment about 3 out of the 4 chips did not have the PCR tape attached anymore, it was floating inside the well plate. Hypothesis were made that the detachment of the tape was caused by proteins in the serum that get sandwiched between the PCR tape and the PDMS chip and thereby interfere with the bonding. To check this hypothesis a design was created (see Figure 40) to check the delamination pressure and the delamination upon incubation at 37 °C, 5% CO<sub>2</sub>

of a PCR-PDMS chip in different media. Considered conditions were air, deionized water, PBS, culture media (DMEM, 1% pen/strep) and culture media with 10% FBS added.

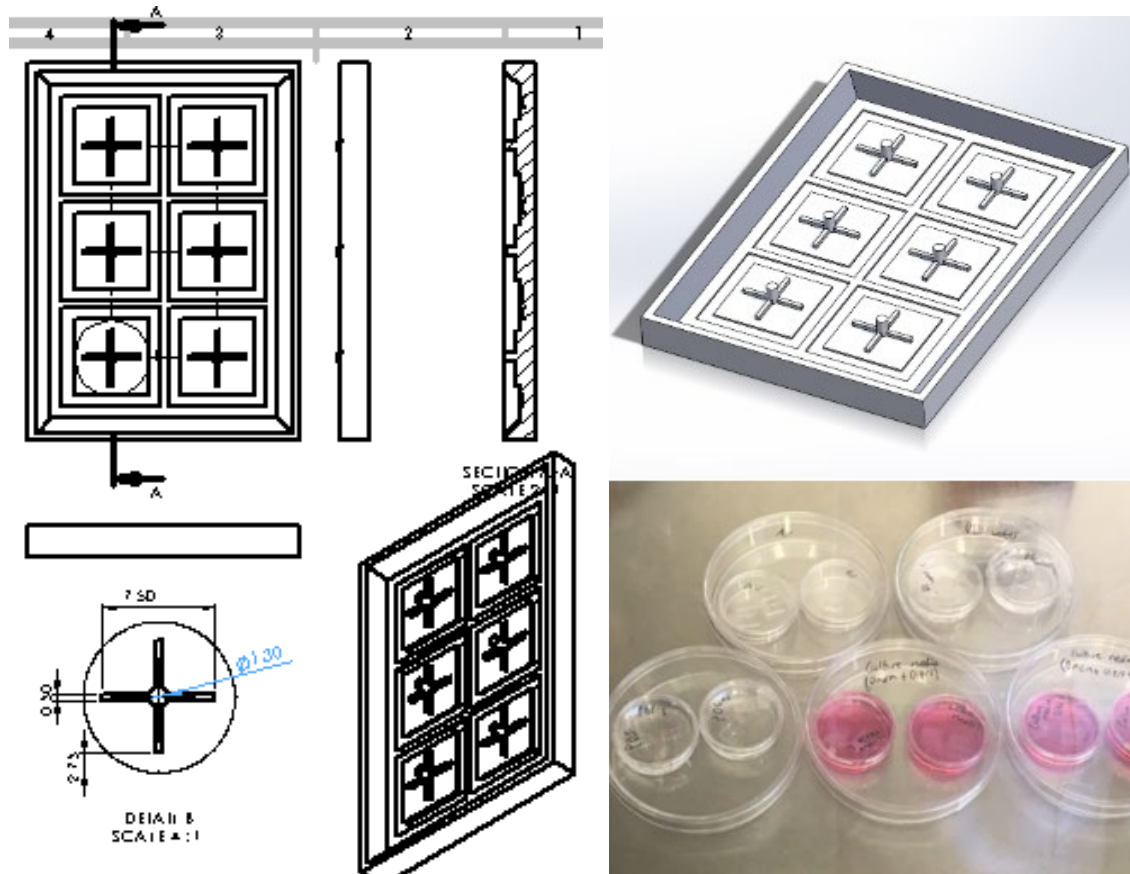


FIGURE 40. TAPE DETACHMENT DESIGN, SHOWING 3D PRINTED MOLD DESIGN (A/B) AND THE SETUP OF THE PDMS CHIPS SEALED WITH PCR TAPE AND DIFFERENT MEDIA (C)

Table 7 shows the delamination of the tape occurred after 69 hours of incubation at 37 °C at 5% CO<sub>2</sub>.

TABLE 7. DELAMINATION OF THE PCR TAPE 69 HOURS OF INCUBATION AT 37 °C AT 5% CO<sub>2</sub>.

PDMS/	Air	DI water	PBS	Culture media (DMEM, 1% pen/strep)	Culture media (DMEM, 10% FBS, 1% pen/strep)
Detached tape	0% (n=3)	25% (n=4)	25% (n=4)	25% (n=4)	100% (n=4)

### Appendix M. Glass-syringe connector design

Penetrating the barrier of the epididymal tubes while keeping the tube intact is one of the main goals of the project. This experiment required designing and fabricating new interfacing solutions to allow to connect the glass needle to a syringe.

Tips with a diameter larger than approximately 75µm were aspirating fluid through capillary forces. However, for tips with a smaller diameter these forces did not allow for enough fluid to be collected in the glass needle. Therefore, a syringe-needle connector was designed in Solidworks and 3D printed. Figure 41 and Figure 42 show two of the glass-syringe connector designs. Both were able to connect to a syringe although some of the liquid was leaking through the connector, which could

explain why aspirating below 75 $\mu\text{m}$  was difficult and aspirating was also possible due to the help of capillary forces.

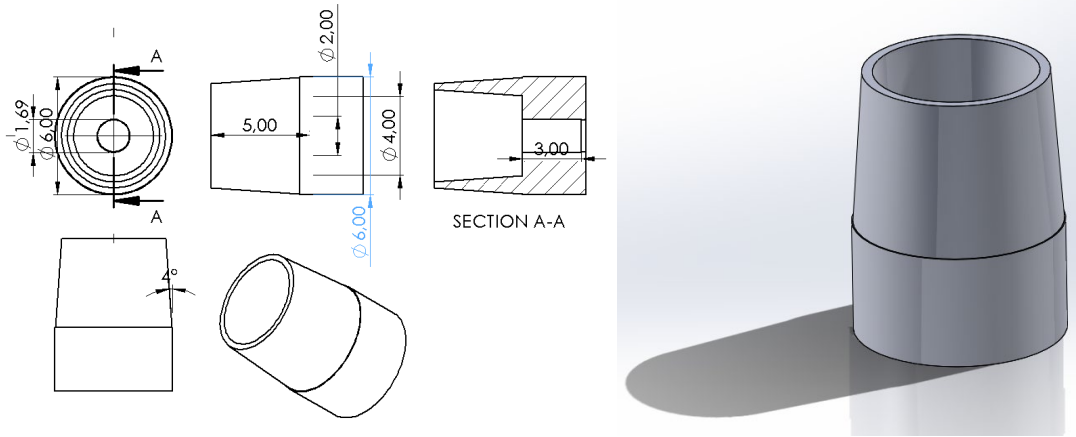


FIGURE 41. IMAGE SHOWING THE V1 NEEDLE-SYRINGE CONNECTOR. THE CONICAL TOP SHAPE FITS AROUND THE TIP OF A STANDARDIZED SYRINGE. THE BOTTOM PART WITH THE 1.69 MILLIMETER DIAMETER ALLOWS THE INSERTION OF THE GLASS CAPILLARY.

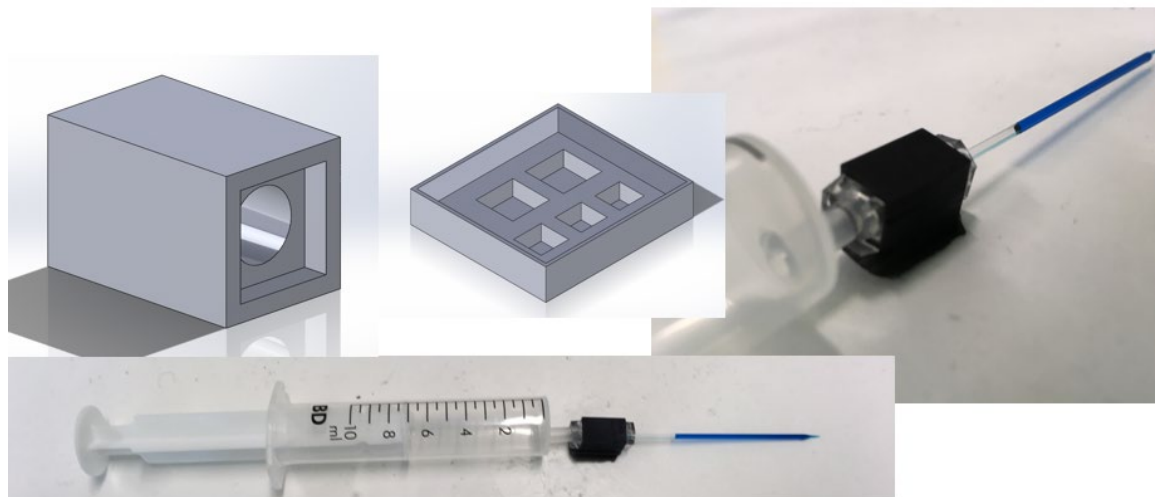


FIGURE 42. IMAGE SHOWING THE FINAL NEEDLE-SYRINGE CONNECTOR. THIS DESIGN ATTEMPTED TO CREATE A LEAKAGE FREE CONNECTION BY HAVING A LEAKAGE FREE PDMS SEAL BETWEEN THE SYRINGE-GLASS CONNECTOR AND THE GLASS CAPILLARY. HOWEVER, THE FITTING STILL LEAD TO SUBOPTIMAL CONNECTION. AN ATTEMPT TO USE PDMS TO GLUE THE PARTS TOGETHER DID ALSO NOT WORK SINCE THE CONNECTOR CRACKED IN THE OVEN AT 60 DEGREES CELSIUS IN THE OVEN.

The glass-syringe connector did work for needles with a diameter of about 50 $\mu\text{m}$ . But for those smaller than that it did not. The main reason for this would be the fact that the connector is not a tight sealing and the resistance of tips below 50 $\mu\text{m}$  is too small.

## 17 CV OUTPUT

### **Paper**

Epididymis-on-a-chip: a bottom-up approach to study tight physiological barriers', **T.C.Q. Burgers**, B. Venzac, A. Jafek, S. Sharma, S. Schlatt, S. Le Gac, under preparation

'Microfluidics in male reproduction: Is *ex vivo* culture of primate testis tissue a future strategy for assisted reproductive technologies or toxicology research?' - S. Sharma\*, B. Venzac\*, **T.C.Q. Burgers**, S. Le Gac\*, S. Schlatt\*, Molecular Human Reproduction, invited review paper, under review.

### **Conference contributions**

'Epididymis-on-a-chip: a valuable research tool to study tight barriers, sperm maturation and to screen endocrine disruptors', **T.C.Q. Burgers**, B. Venzac, S. Sharma, S. Schlatt, S. Le Gac, NanoBioTech Montreux, Montreux, 18-20 November 2019, poster, submitted

'Developing microfluidic platforms for culturing primate seminiferous and epididymal tubules' – B. Venzac, T.C.Q. Burgers, A. Jafek, S. Sharma, S. Schlatt and S. Le Gac, Int. Conf. Biomed. Eng. (ICBME), Singapore, 15-19 Dec. 2019, submitted.

'Testes-on-chip model for in vitro primate spermatogenesis' – S. Sharma, B. Venzac, **T.C.Q. Burgers**, S. Le Gac, S. Schlatt, Gordon Research Conf. in Germinal Stem Cell Biology, Hong-Kong, 19-24 May 2019, poster; contribution selected for a short oral presentation by S. Sharma.

'Developing testes-on-chip model for in vitro primate spermatogenesis' – S. Sharma, B. Venzac, T.C.Q. Burgers, S. Le Gac, S. Schlatt, 6<sup>th</sup> international Workshop on mol. Andrology and 12<sup>th</sup> NYRA meeting, Giesen, 23-24 September 2019, submitted